Capacity and Spectral Efficiency of Multihop Radio Networks

Koji YAMAMOTO

Capacity and Spectral Efficiency of Multihop Radio Networks

Koji YAMAMOTO

Capacity and Spectral Efficiency of Multihop Radio Networks

by

Koji YAMAMOTO

The Graduate School of Informatics

Kyoto University

Kyoto, Japan

June 2005

Preface

The purpose of this thesis is to evaluate the performance of multihop-type radio networks such as wireless ad hoc networks and multihop cellular systems, and to make it clear what conditions will lead to large performance benefits from multihop relaying. In these networks, the initial motivation for introducing multihop relaying is the expansion of system coverage. In our evaluation, we explicitly take into account the opposite effects of multihop relaying on the spectral efficiency. We first establish the achievable end-to-end throughput of a single isolated multihop route assuming symbol rate and modulation level control, and indicate that by controlling symbol rate or using multihop relaying, the end-to-end communication range can be extended at the cost of end-to-end throughput. We then found a tradeoff between the end-to-end throughput and the area spectral efficiency of interference-limited multihop radio networks. Numerical results reveal that the resulting area spectral efficiency depends on the specific circumstances, which, however, can be increased only by using multihop relaying.

We next consider multihop cellular systems. We formulate the spectral efficiency and outage probability of multihop TDMA cellular systems under single-cell environment and indicate that multihop relaying is superior to symbol rate control in terms of both coverage and spectral efficiency. We also evaluate the capacity of two-hop CDMA cellular systems under multi-cell environment, in which tight power control is essential. We propose an efficient routing algorithm for two-hop CDMA cellular systems. Simulation results reveal that by using the proposed routing algorithm in combination with a call admission control, the capacity can be increased even under heavy traffic load conditions.

Finally, we apply a game-theoretic analysis to the evaluation of capacity and stability of wireless ad hoc networks, in which each source node independently chooses a route to the destination node so as to enhance throughput. We define the decentralized adaptive route selection problem in which each source node competes for resources over arbitrary topologies as a game and reveal that in some cases this game has no Nash equilibria; i.e., each rational source node cannot determine a unique route. The occurrence of such cases depends on both the transmit power and spatial arrangement of the nodes. Then, the obtained network throughput under the equilibrium conditions is compared to the capacity under centralized scheduling. Numerical results also reveal that when the transmit power is low, decentralized adaptive route selection may attain throughput near the capacity.

Acknowledgments

I would like to thank my supervisor Professor Susumu Yoshida for giving helpful suggestions based on a long-term perspective and keeping freedom for my research activities. Without his continuous encouragement and careful review, this work would not have been completed.

I wish to thank Professors Tatsuro Takahashi and Yutaka Takahashi for many important advices in performing the present work.

I wish to thank Dr. Hidekazu Murata, an Associate Professor of Tokyo Institute of Technology, for his encouragement to pursue this work.

I wish to express my gratitude to Dr. Shoichi Hirose, an Associate Professor of the University of Fukui, for helpful suggestions in carrying out this work. My thanks are also due to the staffs of laboratory, Ms. Tomoko Ono and Ms. Ami Akino.

I benefited from my discussions with Kazuto Yano regarding the design of wireless networks. I wish to thank my colleague Toshiaki Koike for his intuitive discussions and suggestions. My colleague Atsushi Kusuda helped me some evaluations in a certain chapter of this paper. I also appreciate my group members, Hua Xu, Keisuke Ozaki, Masahiro Fujii, Liang Xu, and Tsuyoshi Nakano, for their various advices.

We appreciate the benefits received in fruitful discussions with Dr. Yasushi Yamao, Dr. Toru Otsu, Dr. Narumi Umeda, Mr. Atsushi Fujiwara, Mr. Shinji Takeda, and Mr. Akira Yamada of NTT DoCoMo Inc.

The writing of this paper was made possible largely through grants from Research Fellowships of the JSPS for Young Scientists, NTT DoCoMo Scholarship, and the 21st Century COE Program of Kyoto University, and I would like to acknowledge here the generosity of these organizations.

Contents

List of Figures

List of Tables

Notations

Roman Symbols

ℓ	Number of channels
C	Capacity
d	Distance
F	Ratio of inter-cell interference power and intra-cell interference power
f	Function of bandwidth efficiency on CINR and BER
G	Power gain
g	Geometry
L_{s}	Path loss
m	Number of nodes
n	Number of hops
p	Probability density function
r	Data rate
t	Bandwidth efficiency, end-to-end throughput
u	Payoff function
W	Bandwidth
x	Horizontal distance between the mobile and the diffracting edges
x	Random variable

Greek Symbols

α	Path loss exponent
η	Area spectral efficiency
μ	Mean
ν	Noise power spectral density
ρ	Density of nodes
σ	Standard deviation

γ	CINR
λ	Wavelength

Subscripts

$f_n, t_n, \beta_n, \eta_n, \rho_n,$	Number of hops
p_b	BER
P_r	Received power
P_t	Transmit power

Acronyms

M-QAM	M-ary Quadrature Amplitude Modulation
ASE	Area Spectral Efficiency
AWGN	Additive White Gaussian Noise
BE	Bandwidth Efficiency
BER	Bit Error Rate
BS	Base Station
CDMA	Code Division Multiple Access
CINR	Carrier-to-Interference plus Noise ratio
CIR	Carrier-to-Interference Ratio
CNR	Carrier-to-Noise Ratio
DARS	Decentralized Adaptive Route Selection
FDD	Frequency Division Duplex
GSM	Global System for Mobile Communications
IEEE	Institute of Electrical and Electronic Engineers
MAC	Medium Access Control
MS	Mobile Station
ODMA	Opportunity Driven Multiple Access
PDF	Probability Density Function
QAM	Quadrature Amplitude Modulation
QPSK	Quadrature Phase Shift Keying
RS	Relaying Station
TCP	Transmission Control Protocol
TDMA	Time Division Multiple Access

Chapter 1

Introduction

1.1 Background

Recent advancements in radio technologies and the success of the Internet have shown the potential of information systems as ubiquitous networks accessible from anywhere, at any time, and with any device [1]. A key enabling technology for such networks is wireless ad hoc networking.

Wireless ad hoc networks are self-configuring systems formed by co-operating nodes without any established infrastructure or centralized administration. A key assumption is that any two nodes can communicate directly if there is an adequate radio propagation path between them subject to the maximum transmit power constraints of the nodes. Otherwise, packets are relayed from the source to the final destination, which can be relatively far apart, by multihop relaying [2].

The characteristics of ad hoc networks, including possible node mobility, lack of centralized control, constraints on energy consumption, and bandwidth-constrained wireless links, have led to the creation of widespread research fields [3]. Research in the area of ad hoc networks has been concentrated on the network layer [4–6], the medium access control (MAC) layer, and the physical layer. Cross-layer design that takes into account the characteristics of the underlying layers can provide optimizations across multiple layers [7, 8].

Wireless ad hoc networks can become an information infrastructure formed by co-operating wireless nodes without centralized administration [9]. For this type of wide area radio networks, referred to as multihop radio networks, high system spectral efficiency is required since the amount of spectrum available for wireless systems is limited. This type of spectral efficiency, referred to as area spectral efficiency (ASE), is defined to be the maximum end-to-end bit rate through multiple hops per unit bandwidth per unit area as that defined in cellular networks [10–12]. Mukai et al. demonstrated that the ASE of multihop radio networks does not experience significant degradation compared with that of cellular networks [13].

The ASE of multihop radio networks is sensitive to many factors, such as fairness of nodes [14–16], possible node mobility [17], and lack of centralized control [18,19]. Gupta et al. estimated the throughput per source-destination pair in multihop radio networks with optimal routing and scheduling, and found that the smallest possible transmit power that still ensures connectivity may be most effective in terms of the ASE [20].

In recent years, there has been lots of interest in applying a relaying function to conventional wireless cellular systems, in which all mobile stations (MS's) are directly connected to base stations (BS's), because of its various advantages. For example, the transmit power of an MS can be reduced or the coverage area in cellular systems can be enhanced with the same transmit power. There are some works related to cellular systems with multihop relaying, referred to as multihop cellular systems. For example, in [21], Aggélou et al. proposed to integrate relaying functions with GSM (Global System for Mobile Communications) cellular systems. In [22], Wu et al. introduced stations dedicated to relaying for high bandwidth usage. In [23], opportunity driven multiple access (ODMA) is proposed to enhance the coverage by allowing MS's beyond the reach of the cell coverage to reach the BS. Moreover in [24,25], multihop CDMA (code division multiple access) cellular systems have been analyzed.

1.2 Current Research

1.2.1 Network Capacity

Gupta et al. estimated per node throughput in a large scale ad hoc network. It is reported that in a network with m nodes distributed uniformly and independently, the throughput obtainable by each node is of order $O\left(\frac{1}{\sqrt{m \log m}}\right)$ bits per second. Even under optimal routing and scheduling, the throughput for each node is only $O\left(\frac{1}{\sqrt{m}}\right)$. This result implies that the throughput per node approaches to zero as the number of node increases [20]. Therefore, in a large scale ad hoc network, each node should not communicate with any other nodes, and some distributed controls may be required to establish communications only within local neighborhood [3].

1.2.2 Capacity Region

Toumpis et al. defined "capacity region" as the achievable capacity of a wireless ad hoc network and evaluated various transmit schemes including routing, scheduling, and power control. Optimal routing and scheduling require coordination among all the nodes in the network. They showed that if the data rate is adjusted to the received power, additional power control leads to negligible capacity gains in a wireless ad hoc network [26].

1.2.3 Game-Theoretic Analysis

Power Control Games

Consider a system where nodes interfere with each other. For the purpose of adjusting the transmit power of all nodes such that the received carrier-to-interference plus noise ratio (CINR) of each node meets a given required value, power control is applied.

Bambos illustrated the conditions that a feasible set of transmit powers for all nodes exists and the Pareto optimal set of transmit powers [27]. In addition, he proposed a distributed power control algorithm by which the iteration converges to the Pareto optimal set of transmit powers [27].

Goodman et al. developed power control game. Let r be the information bit rate, let γ be the received CINR, and let M be the symbol size of each packet. It is assumed in this game that the set of transmit power levels P is a strategy and the ratio of the number of bits transferred to the energy cost,

$$u = \frac{r}{P}[1 - \exp(-\gamma/2)]^M \tag{1.1}$$

is the payoff function of the packet transmission. They prove that this one-shot power control game has a unique Nash equilibrium, however, this equilibrium point is not Pareto optimal [28, 29]. An introduction of a price function [28] or repetition of this game [30] are reasonable to increase the payoff.

Random Access Games

MacKenzie et al. developed a game-theoretic model of slotted Aloha named Aloha game. This game is a stochastic game [31] in which each player has two strategies: transmit or wait. It is assumed that nodes know the number of active nodes m who currently have packets to transmit. If and only if one node transmits in a given time slot, each of other $m-1$ active nodes continue to play the game in the next time slot. They showed that this Aloha game has a Nash equilibrium [32, 33].

1.2.4 Cross-Layer Evaluation

Typical characteristics of radio channel are multipath fading, shadowing, path loss, interference, and shared medium. Layering approach may not work well especially under tight performance requirements. For example, power control has an impact on the topology of the radio network as well as the performance of link layer such as received CINR.

For another example, in wireless networks in which IEEE 802.11 is used, packets may be dropped due to either buffer overflow or contention at link layer. These packet losses affect TCP window adaptation. Fu et al. evaluated TCP performance over multihop

networks in which IEEE 802.11 was used. It is shown in this study that packet loss due to buffer overflow is rare and packet drops due to contention at link layer dominate the performance [34].

1.2.5 Cooperative Diversity and Multihop Diversity

Cooperative diversity and multihop diversity are new forms of spatial diversity for mitigating the effects of fading. Conventional spatial diversity is obtained using multiple antennas spaced appropriately so that the received signals are not correlated. However, multiple antennas are not necessarily mounted on small nodes. The user cooperation diversity is achieved by using the other nodes' antennas [35–37].

Sendonaris et al. considered both additional power requirement for relaying and power reduction because of the diversity gains, and revealed that user cooperation can result in an increased data rate and a decreased sensitivity [38,39]. The referenced cooperative schemes consider two-hop relaying between the source and destination nodes. Boyer et al. evaluated the physical layer of multihop relaying channels. The performances of two types of relaying such as decoded and amplified relaying are estimated in both multihop channel and multihop diversity channel [40].

1.3 Overview of Contributions

One of the advantages of multihop transmission over single-hop transmission is a larger end-to-end communication range. However, the spectral efficiency of multihop transmission is not necessarily the same as that of single-hop transmission. Therefore, to consider in what situation multihop transmission results in higher spectral efficiency may be of interest in system design. This type of spectral efficiency, referred to as bandwidth efficiency, is defined to be the maximum end-to-end bit rate through multiple hops per unit bandwidth.

In Chapter 3, we provide a simple yet meaningful theoretical framework for analyzing the bandwidth efficiency of multihop transmission and the area spectral efficiency of interference-limited multihop radio networks. In our argument, we assume that the networks have controls for symbol rate and modulation level. We first consider a single isolated multihop route and show that the end-to-end communication range can be extended at the cost of end-to-end throughput of multihop transmission. We also evaluate the effects of the transmit power reduction and spatial channel reuse on the end-to-end throughput of a single isolated multihop route. We then consider the area spectral efficiency under interference-limited situation. We establish a relationship between area spectral efficiency and bandwidth efficiency, and show that there is a tradeoff between them. We also attempt to relax the assumption that co-channel interference dominates the thermal noise.

In Chapter 4, we formulate the performance of rate adaptation in TDMA (time division multiple access) cellular systems as described in [41]. Next, as the formulation of the performance of rate adaptation, we formulate spectral efficiency and outage probability of multihop transmission in TDMA cellular systems, assuming two scenarios. First scenario is a situation where relaying stations are on a straight line segment between a calling station and the base station. Second scenario is a situation where relaying stations are uniformly and independently distributed in each cell.

In most of studies on multihop cellular systems [21,23–25], the main purpose of using multihop relaying for uplink transmission is the coverage enhancement rather than the capacity improvement. As an example, the routing algorithms that choose the route with the minimum total path loss [23] or the minimum total transmit power [42] have been adopted. These routing algorithms may decrease the radiated power, however, the interference power at BS's, which limits the user capacity, does not necessarily decrease.

In Chapter 5, we consider the introduction of two-hop relaying in CDMA cellular systems such as W-CDMA [43, 44]. Particularly, we study the uplink capacity in two-hop CDMA cellular systems. We show that as a result of power control, which is essential for CDMA cellular systems, the introduction of two-hop relaying does not decrease the intra-cell interference, however, can reduce the inter-cell interference. We propose an interference evaluation method using downlink geometry [45]. We then reveal the condition for the interference of uplink to be reduced by changing some single-hop transmissions to two-hop transmissions, and propose to use the route with the maximum amount of interference reduction as a route selection criterion. By using this criterion, we also propose an effective routing algorithm for two-hop CDMA cellular systems with the aim of enhancing the system capacity.

On the basis of these observations, we will next consider decentralized control to achieve high throughput. The decentralization and distribution of control in ad hoc networks mean that such networks are inherently scalable. However, the natural conflict among nodes in a network due to selfishness cannot always attain throughput near the capacity. A promising approach to analyzing decentralized control and node selfishness is game theory, which deals with how individuals interact and compete for resources. The effect of "selfish" random access has been evaluated using game-theoretic analysis [32,33]; an algorithm has been proposed for deciding whether to accept or reject a relay request for multihop transmission [46]; and studies have been made of decentralized power control problems in which each node chooses its power level for establishing connectivity between the source and destination [47].

In Chapter 6, we report a game-theoretic analysis of a decentralized adaptive route selection (DARS) problem in a wireless ad hoc network, in which multiple decision-making nodes select a route to the destination so as to enhance their own throughput. This problem is similar to that defined by Eidenbenz et al. [47]. However, the focus

here is not connectivity but the capacity of bandwidth-constrained wireless networks. We first define a DARS game and apply equilibrium analysis to study the behavior of this game. We categorize many possible node arrangements according to the number of Nash equilibria and show that in some cases the DARS game has no Nash equilibria; i.e., even with perfect knowledge except for information of the other nodes' decisions, each rational selfish node cannot determine a unique route. We then compare the obtained network throughput under the equilibrium conditions to the capacity under centralized scheduling. We also attempt to evaluate the joint effect of DARS and transmit power control on the capacity.

Chapter 2

Wireless Networks

2.1 Wireless Radio Channel

Prediction of propagation characteristics is essential for designing and installing a radio communication system. The signals propagating through the radio channel will experience path loss, shadowing, and multipath fading.

Multipath fading is caused by multiple receptions of the original signal. The transmitted signal travels along multiple paths with different delays and gains varying over time. The variation of the multipath fading occurs over several hundred wavelengths. Shadowing is caused by terrain configuration or obstacles between the transmitter and receiver. The power fluctuation due to shadowing occurs over several ten meters. Path loss is affected by the distance between the transmitter and receiver. In this section, we describe the models for signal propagation.

2.1.1 Path Loss

The path loss is defined as the ratio of the transmit power P_{t} to the average received power P_{r}.

$$L_{\mathrm{s}} = \frac{P_{\mathrm{t}}}{P_{\mathrm{r}}} \tag{2.1}$$

Free Space Path Loss

Let d denote the distance between the transmitter and receiver. A signal traveled through free space, i.e. with no obstructions or reflection, follows the free space path loss:

$$L_{\mathrm{s}} = -10\log_{10}\left(\frac{\lambda}{4\pi d}\right)^2 \ [\mathrm{dB}] \tag{2.2}$$

where λ is the wavelength.

Xia's Path Loss Model for Vehicular Environment

Xia developed an analytical path loss model applicable for the situation in urban and suburban areas where the buildings are of nearly uniform height and the base station is above rooftop level [48–50] .

$$L_{\mathrm{s}} = -10\log_{10}\left(\frac{\lambda}{4\pi d}\right)^2 - 10\log_{10}\left[\frac{\lambda}{2\pi^2 r}\left(\frac{1}{\theta} - \frac{1}{2\pi+\theta}\right)^2\right] - 10\log_{10}\left[(2.35)^2\left(\frac{\Delta h_{\mathrm{b}}}{d}\sqrt{\frac{d'}{\lambda}}\right)^{1.8}\right] \ [\mathrm{dB}] \tag{2.3}$$

$$r = \sqrt{(\Delta h_{\mathrm{m}})^2 + x^2} \qquad \theta = \tan^{-1}\left(\frac{|\Delta h_{\mathrm{m}}|}{x}\right)$$

$$\Delta h_{\mathrm{b}} = h_{\mathrm{b}} - h_{\mathrm{roof}} \qquad \Delta h_{\mathrm{m}} = h_{\mathrm{roof}} - h_{\mathrm{m}}$$

where x is the horizontal distance between the mobile and the diffracting edges, d' is the average separation distance between the rows of buildings, h_{b}, h_{m}, and h_{roof} represent the base station antenna height, the mobile antenna height, and the mean building height, respectively. In the above expressions, the path loss has a $d^{3.8}$ distance dependence.

Milstein's Path Loss Model for Microcell Environment

Milstein et al. measured the path loss between a mobile station and a base station whose antenna height was relatively low (5~13.1 m) by several field tests. In these experiments,

center frequency was set to about 2 GHz. Under line-of-sight conditions, it is confirmed that the distance dependence of the variation of path loss is described by a piecewise linear curve with a single breakpoint. The distance of the breakpoint is approximately given by

$$D_{\mathrm{bk}} = \frac{4h_{\mathrm{m}}h_{\mathrm{b}}}{\lambda}.$$

In the absence of blockage, the loss is given by

$$L_{\mathrm{s}} = \left|20\log_{10}\left(\frac{\lambda^2}{8\pi h_{\mathrm{b}}h_{\mathrm{m}}}\right)\right| + \begin{cases} 20\log_{10}(d/D_{\mathrm{bk}}) & [\mathrm{dB}] \quad (d < D_{\mathrm{bk}}) \\ 40\log_{10}(d/D_{\mathrm{bk}}) & [\mathrm{dB}] \quad (d > D_{\mathrm{bk}}) \end{cases}. \tag{2.4}$$

In the above expressions, the path loss has a d^2 distance dependence before the breakpoint and a d^4 distance dependence after the break point. This model is calculated by using the two-ray model that consists of a direct and a single reflected ray from the ground [51].

Simplified Path Loss Model

As described earlier, path loss is approximately inversely proportional to the α-th power of the distance

$$P_{\mathrm{r}}(d) \propto P_{\mathrm{t}}d^{-\alpha} \tag{2.5}$$

where α is called as path loss exponent.

When the transmit power is the same, at locations where the distances to a certain transmitter are d and d_0, the mean received powers $P_{\mathrm{r}}(d)$ and $d_{\mathrm{r}}(d_0)$ satisfy the following relationship:

$$P_{\mathrm{r}}(d) = P_{\mathrm{r}}(d_0)\left(\frac{d}{d_0}\right)^{-\alpha}. \tag{2.6}$$

Accurate path loss models are essential for tight system specifications. However, this relationship is sufficient for general tradeoff analysis to capture the path loss [52].

2.1.2 Shadowing

Shadowing is modeled as a log-normal distributed random variable with a standard deviation of 6 dB to 10 dB [53]. This model has been validated to be accurate by measurements. We assume x is a random variable with a log-normal distribution. Then, the distribution of $x_{\mathrm{dB}} = 10 \log_{10} x$ becomes a normal distribution.

$$p_{\mathrm{nor}}(x_{\mathrm{dB}}) = \frac{1}{\sqrt{2\pi}\sigma_{x_{\mathrm{dB}}}} \exp\left[-\frac{(x_{\mathrm{dB}} - \mu_{x_{\mathrm{dB}}})^2}{2{\sigma_{x_{\mathrm{dB}}}}^2}\right] \tag{2.7}$$

where $\mu_{x_{\mathrm{dB}}}$ is a mean of x_{dB} and $\sigma_{x_{\mathrm{dB}}}$ is a standard deviation of x_{dB}. Let $\phi_{\text{log-nor}}(x)$ be the probability density function (PDF) of x and we get

$$\int_0^x \psi(x')\,\mathrm{d}x' = \int_{-\infty}^{x_{\mathrm{dB}}} p(x'_{\mathrm{dB}})\,\mathrm{d}x'_{\mathrm{dB}}. \tag{2.8}$$

We obtain the PDF of x by differentiating Eq. (2.8) relative to x.

$$\psi(x) = p(x_{\mathrm{dB}})\frac{\mathrm{d}x_{\mathrm{dB}}}{\mathrm{d}x} \tag{2.9}$$

$$= \frac{\xi}{\sqrt{2\pi}\sigma_{x_{\mathrm{dB}}} x} \exp\left[-\frac{(10\log_{10} x - \mu_{x_{\mathrm{dB}}})^2}{2{\sigma_{x_{\mathrm{dB}}}}^2}\right] \tag{2.10}$$

where $\xi = 10/\ln 10$. Note that the mean of x is not $10^{\mu_{x_{\mathrm{dB}}}/10}$ but

$$\mu_x = E[x] = \exp\left[\frac{\mu_{x_{\mathrm{dB}}}}{\xi} + \frac{{\sigma_{x_{\mathrm{dB}}}}^2}{2\xi^2}\right]. \tag{2.11}$$

2.1.3 Multipath Fading

When a direct path is not present between the transmitter and receiver, the received signal consists of reflected, refracted, and scattered copies of the transmitted signal, it can be shown that the signal envelope is Rayleigh-distributed. Therefore, non-line of sight multipath fading is called Rayleigh fading. The CNR is then exponentially distributed with mean γ_0.

$$p_{\mathrm{Rayleigh}}(\gamma) = \frac{1}{\gamma_0} \exp\left(-\frac{\gamma}{\gamma_0}\right). \tag{2.12}$$

2.2 Symbol Rate and Modulation Level Control

We assume that the transmitting node adjusts the data rate r based on the average received carrier-to-interference plus noise ratio (CINR) γ for a given required bit error rate (BER) p_b as

$$r = f_1(\gamma, p_b). \tag{2.13}$$

Shannon capacity, which is the maximum of the information rates without error,

$$f_1(\gamma, p_b) = \log_2(1 + \gamma), \tag{2.14}$$

has been used to obtain the specific dependence of r on γ [19,26,54]. One of the problems of multihop transmission is accumulation of bit errors or packet errors over multihop relaying [55]; however, the bit error probability cannot be evaluated with Shannon capacity. Using results presented in [56, 57], we derived a specific dependence of r on both γ and p_b considering symbol rate control and modulation level control with M-ary quadrature amplitude modulation (M-QAM).

Let γ_{QPSK} denote the required CINR for QPSK (4QAM). When the received CINR is higher than γ_{QPSK}, variable-rate M-QAM [56] ($4 \leq M \leq 64$) is used for modulation level control. As described in [56], the bandwidth efficiency (BE) of this modulation level control in the additive white Gaussian noise channel is approximated by

$$f_1(\gamma, p_b) = \log_2(1 + \beta_1 \gamma), \qquad \beta_1 = -1.5/\ln(5p_b), \tag{2.15}$$

where the subscript of the BE f and that of the constant β denote the number of hops. Since the BE of QPSK is 2, we have the required CINR for QPSK

$$\gamma_{QPSK} = 3/\beta_1. \tag{2.16}$$

When the received CINR is lower than γ_{QPSK}, the symbol rate is reduced to decrease the required CINR. Lower symbol rate transmission is equivalently obtained from consecutive transmission of the identical symbols [57]. When the symbol rate of QPSK is reduced to $1/K$ $(1 < K \leq 4)$, the required CINR can be lowered by $10\log_{10} K\,\mathrm{dB}$ at the cost of BE as

$$f_1(\gamma, p_{\mathrm{b}}) = 2/K. \tag{2.17}$$

When K is controlled to meet the received CINR γ, we have

$$\gamma = \gamma_{\mathrm{QPSK}}/K. \tag{2.18}$$

The approximated model for BE of symbol rate and modulation level control may be expressed by using Eqs. (2.15), (2.17), and (2.18),

$$f_1(\gamma, p_{\mathrm{b}}) = \begin{cases} 2\beta_1\gamma/3 & 3/4\beta_1 \leq \gamma < 3/\beta_1 \\ \log_2(1+\beta_1\gamma) & 3/\beta_1 \leq \gamma \leq 63/\beta_1. \end{cases} \tag{2.19}$$

We compare the CINR dependence of the BE (2.19) at BER's of 10^{-3} and 10^{-6} in Figure 2.1. Figure 2.1 also shows the bit error probability for coherent detection of 1/4-rate QPSK, 1/2-rate QPSK, QPSK, 16QAM, and 64QAM [41]. The required CINR of M-QAM is 5.5 dB ($p_{\mathrm{b}} = 10^{-3}$) and 9.1 dB ($p_{\mathrm{b}} = 10^{-6}$) larger than that of Shannon capacity. When the symbol rate is reduced, the difference between the required CINR of this model and that of Shannon capacity becomes larger.

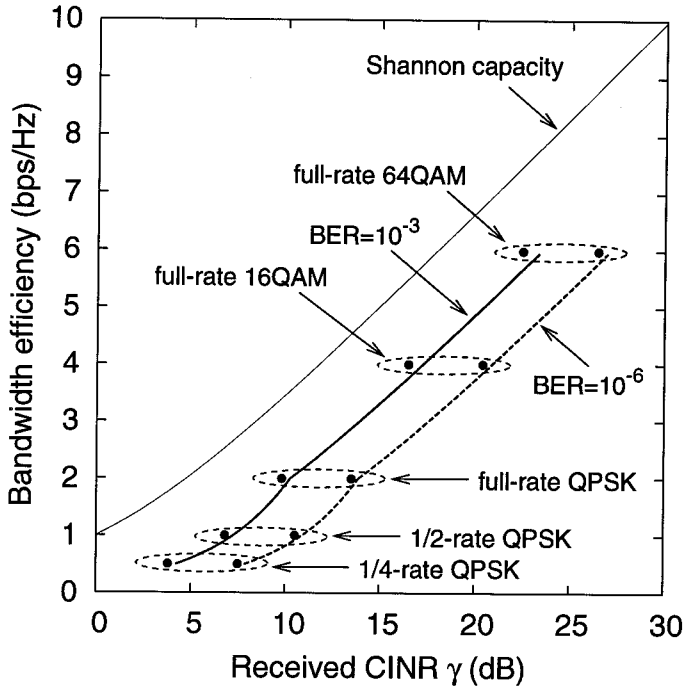

Figure 2.1: Bandwidth efficiency of symbol rate and modulation level control.

Chapter 3

Area Spectral Efficiency of Rate-Adaptive Multihop Radio Networks

In this chapter, we present a simple yet meaningful theoretical framework for analyzing the bandwidth efficiency (BE) of multihop transmission, which is defined to be the maximum end-to-end bit rate through multiple hops per unit bandwidth, and the area spectral efficiency (ASE) of interference-limited multihop radio networks, which is defined to be the maximum end-to-end bit rate through multiple hops per unit bandwidth per unit area. In particular, we assume that the networks have controls for symbol rate and modulation level.

The remainder of this chapter is organized as follows. In Section 3.1, we discuss a system model. In Section 3.2, we consider a single isolated multihop route and evaluate the BE considering error accumulation over multihop relaying. In addition, we evaluate the effect of power control and spatial channel reuse on the BE of multihop transmission in Section 3.3. In Section 3.4, we investigate the ASE of interference-limited multihop radio networks. Section 3.5 concludes this chapter with a summary and some final remarks.

3.1 System Model

We assume that each node can either transmit or receive at a given time, and omnidirectional antennas are used for the nodes. We assume simplified path loss model, i.e. propagation loss with the path loss exponent α. The effects of shadowing and multipath fading are not considered for the sake of simplicity, as has been done in [7]. All interference signals are assumed to be equivalent to additive white Gaussian noise over the channel (which is discussed in more detail in [11]). We assume symbol rate and modulation level control as described in Section 2.2

3.2 Bandwidth Efficiency of Multihop Transmission without Spatial Channel Reuse

One of the prominent advantages of multihop transmission over single-hop transmission is a larger end-to-end communication range. However, the BE of multihop transmission is not necessarily the same as that of single-hop transmission. In order to perform a fair comparison between transmission range of multihop transmission and that of single-hop transmission, we evaluate the tradeoff between the BE and the number of hops.

3.2.1 Analysis

Consider a single isolated source-destination pair. Under this environment, the CINR reduces to the carrier-to-noise ratio (CNR). Let the received CNR at the destination node be γ as shown in Figure 3.1(a), regardless of whether these two nodes can communicate directly (hereinafter referred to as "end-to-end CNR"). End-to-end CNR is considered to be an appropriate parameter to reflect both the transmit power per node and the end-to-end distance since the absolute values of the transmit power and the distance do not have meaning in our simple model.

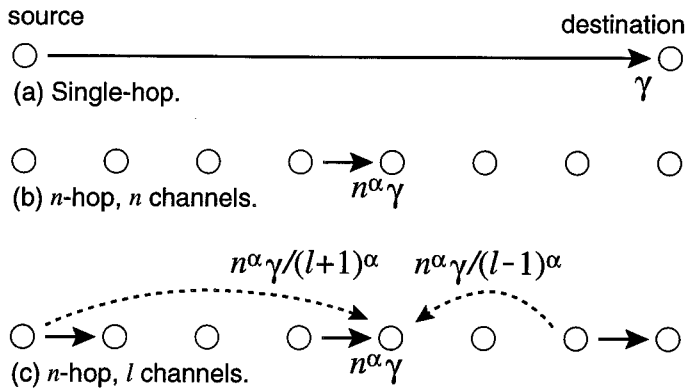

Figure 3.1: Models of single-hop and multihop transmission ($n=7$, $\ell=3$). Solid arrows represent desired signals and dashed arrows represent co-channel interference.

We assume regenerative relaying (sometimes referred to as digital relaying) such that relaying nodes decode and re-encode before retransmission. As shown in Figure 3.1(b), we model the topology of n-hop transmission as equally spaced $(n-1)$ relaying nodes on a straight line segment from the source node to the destination node, and assume that spatial channel reuse is not allowed. While these assumptions are not necessarily realistic, they do enable us to gain insight into the design of multihop radio networks. We can switch from this single-hop transmission to n-hop transmission with the same transmit power and the same required end-to-end BER p_{b} by allowing only one node at a time to transmit. Whether frequency division is used is immaterial to our results since time division and frequency division are equivalent in that they both divide up the spectrum orthogonally, and this orthogonal division results in the same number of channels [3, 58].

This switching has three effects. First, the per-hop distance is reduced to $1/n$ of the end-to-end distance. Therefore, the per-hop CNR can be expressed as $n^{\alpha}\gamma$. This is one of the advantages of multihop transmission over single-hop transmission. Second, the required per-hop BER for n-hop transmission over an additive white Gaussian noise (AWGN) channel for a given required end-to-end BER p_{b} becomes p_{b}/n. This is because

Table 3.1: Parameters used in evaluations.

Parameters	Values
Path loss exponent α	2, 3.5
Required end-to-end BER p_{b}	10^{-3}

when the required BER of every hop is p_{hop}, the end-to-end BER p_{b} becomes

$$\begin{aligned} p_{\mathrm{b}} &= 1-(1-p_{\mathrm{hop}})^n \\ &\simeq np_{\mathrm{hop}} \qquad\qquad (p_{\mathrm{hop}} \ll 1). \end{aligned}$$

Finally, the percentage of time a node can transmit a signal becomes approximately $1/n$. Consequently, the BE of n-hop transmission at given end-to-end CNR γ and required end-to-end BER p_{b} can be expressed as

$$f_n(\gamma, p_{\mathrm{b}}) = \frac{1}{n} f_1(n^\alpha \gamma, p_{\mathrm{b}}/n) \tag{3.1}$$

where f_1 is the bandwidth efficiency of single-hop transmission (2.19). Therefore, this relationship between the BE of n-hop and that of single-hop is extendable when using other modulation schemes. The BE of n-hop transmission assuming symbol rate and modulation level control may be expressed by substituting the expression for the BE of single-hop transmission f_1 in Eq. (2.19) into Eq. (3.1),

$$f_n(\gamma, p_{\mathrm{b}}) = \begin{cases} 2\beta_n n^\alpha \gamma/3n & 3/4\beta_n \le n^\alpha\gamma < 3/\beta_n \\ \log_2(1+\beta_n n^\alpha \gamma)/n & 3/\beta_n \le n^\alpha\gamma \le 63/\beta_n \end{cases} \tag{3.2}$$

where $\beta_n = -1.5/\ln(5p_{\mathrm{b}}/n)$.

3.2.2 Numerical Results

Table 3.1 summarizes the parameters we used in our evaluation. When the number of hops is assumed to be fixed to n ($n=1,2,4,8,16$), the end-to-end CNR dependence of the BE (3.2) for the two different path loss exponent α is as shown in Figure 3.2. The figure

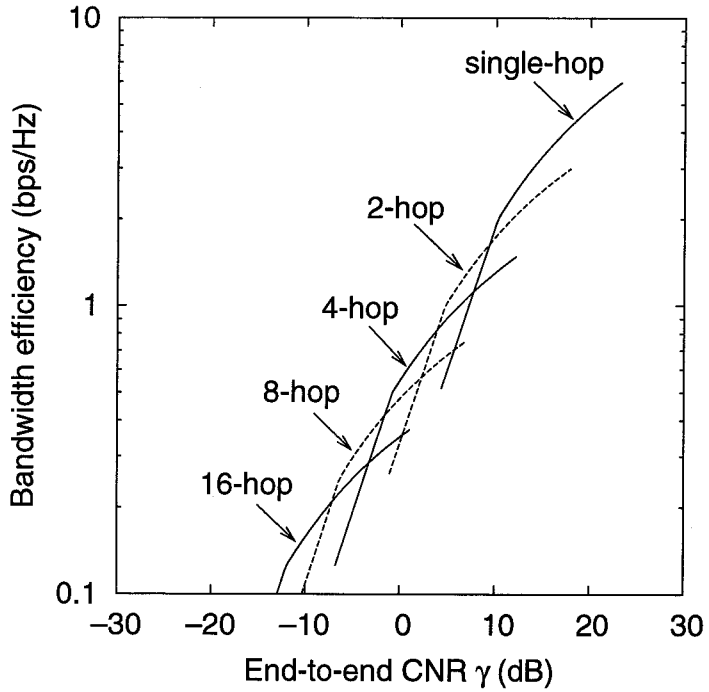

(a) $\alpha=2$.

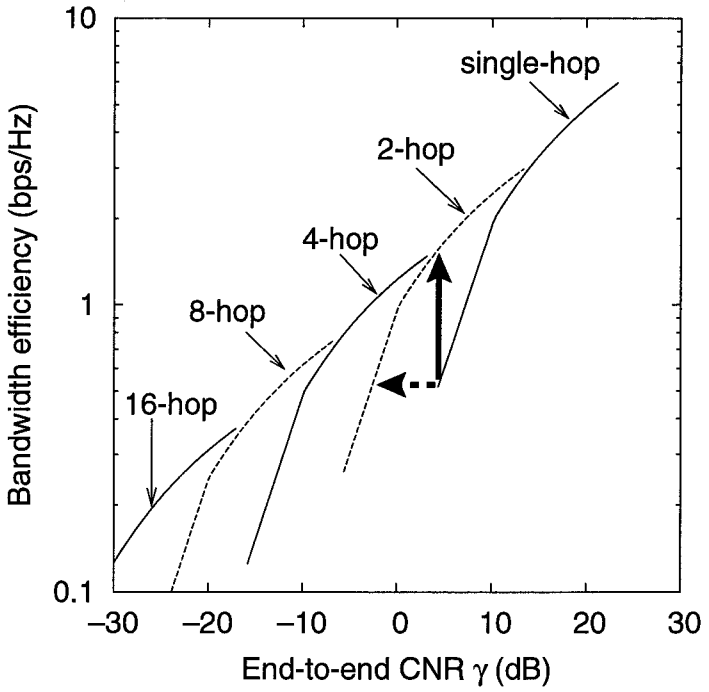

(b) $\alpha=3.5$.

Figure 3.2: Dependence of end-to-end throughput of multihop transmission on CNR between source and destination nodes. Bold and dashed arrows correspond to those in Figure 3.9(b).

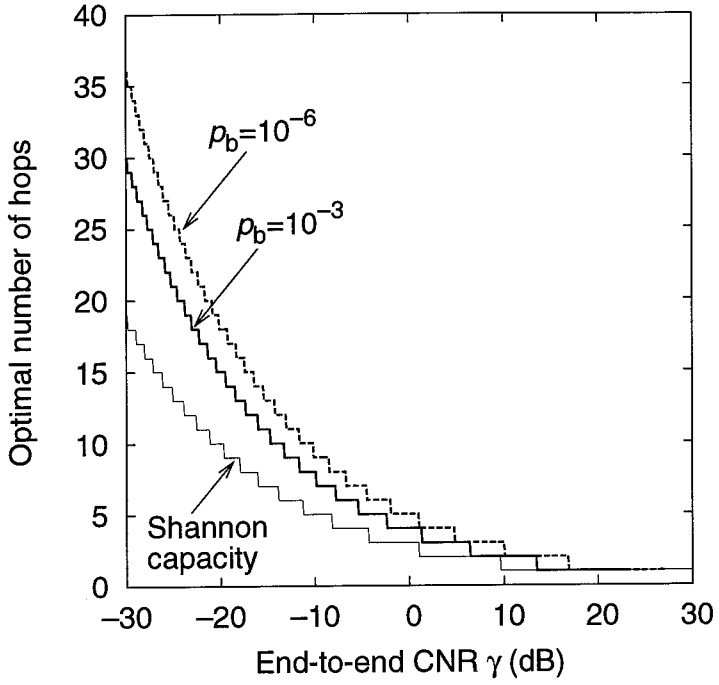

Figure 3.3: Effect of accumulated bit error on optimal number of hops (α=3.5).

shows that under low end-to-end CNR conditions introducing multihop transmission may be more effective in terms of the BE; however, the absolute value of the BE may be small. Therefore, symbol rate control and multihop transmission have the same ability to decrease the required end-to-end CNR at the cost of BE.

Next, we consider adaptive route selection by which the route with an optimal number of hops attaining the maximum BE is chosen. Compared to single-hop transmission, the required per-hop BER of n-hop transmission is reduced to $1/n$, and thus the required CNR is increased. Figure 3.3 shows the optimal number of hops for the different required end-to-end BER ($p_b = 10^{-3}, 10^{-6}$). Figure 3.3 also shows the optimal number of hops when Shannon capacity is used. We see that along with the reduction of end-to-end CNR, the amount of difference between the optimal number of hops with symbol rate and modulation level control and that with Shannon capacity increases.

Figure 3.4 shows the end-to-end CNR dependence of the BE through the use of

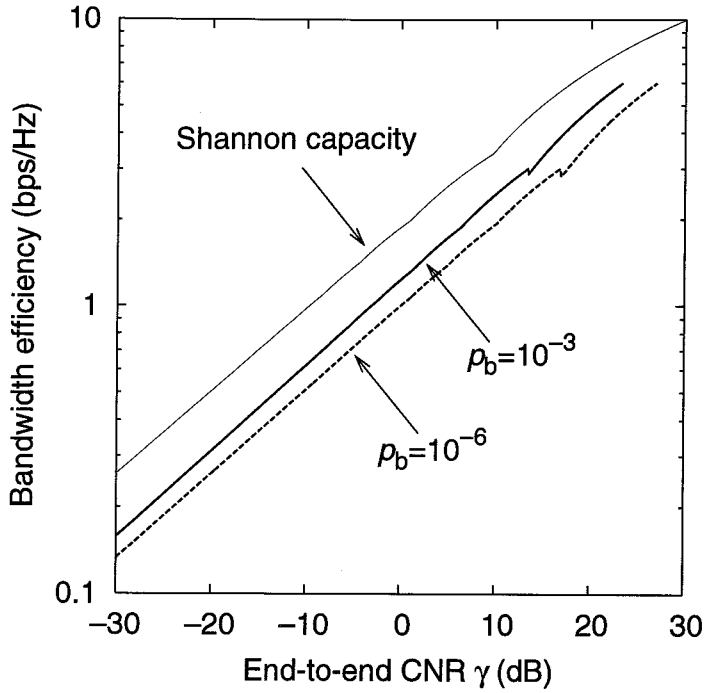

Figure 3.4: Effect of accumulated bit error on bandwidth efficiency ($\alpha=3.5$).

adaptive route selection. We see that the difference between the BE with symbol rate and modulation level control and that with Shannon capacity is relatively small. Thus, in this situation, error accumulation does not necessarily become the main factor in capacity degradation.

Thus far, we have assumed the same transmit power irrespective of the number of hops. This assumption provides a fair comparison between single-hop transmission and multihop transmission in terms of energy efficiency because the total transmit energy of all transmitting nodes is the same regardless of the number of hops.

Here, we consider the scenario where the transmit power is reduced with the number of hops. The BE of this scenario can be derived from the same Figure 3.4 since the end-to-end CNR is increased or decreased in proportion to the transmit power. When the number of hops is optimally selected in terms of the BE, an increase in the end-to-end CNR implies an increase in the BE. Thus, the BE is a monotonically increasing function

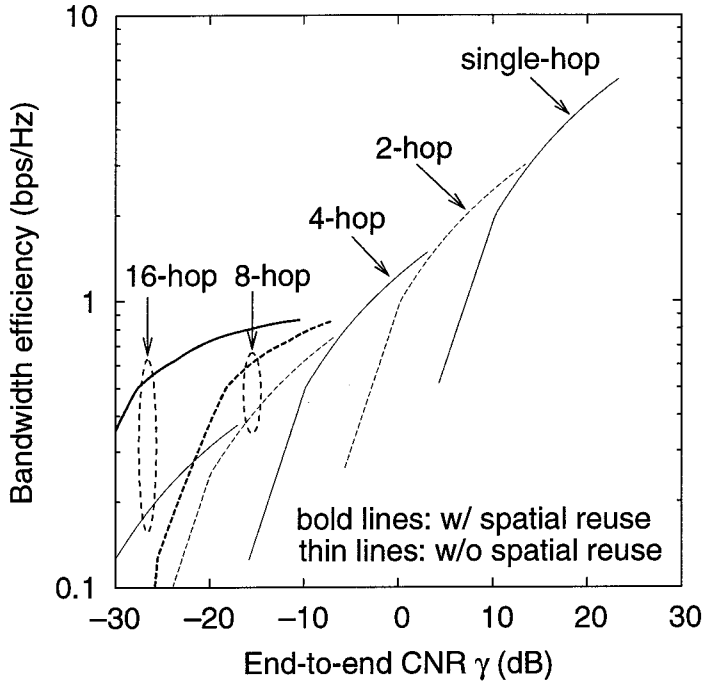

Figure 3.5: Bandwidth efficiency with optimal number of channels ($\alpha=3.5$).

of the end-to-end CNR or the transmit power per node. Therefore, when the spatial channel reuse is not allowed, transmission at the maximum power is effective from the viewpoint of the BE.

3.3 Bandwidth Efficiency of Multihop Transmission with Spatial Channel Reuse

3.3.1 Analysis

In this section, we investigate in what situation the BE of multihop transmission may increase through spatial channel reuse. Through the use of symbol rate and modulation level control, the required CINR is adjusted to meet the received CINR. In addition to this, varying the numbers of hops and channels can control the received CINR. Therefore, the numbers of hops and channels are the variables to be optimized.

Until now, we have assumed n different channels for n-hop transmission. Now, we

assume ℓ ($< n$) different channels so that the percentage of time a node can transmit a signal becomes $1/\ell$. Consider the node receiving the largest interference in a single isolated n-hop transmission using ℓ channels as shown in Figure 3.1(c). Co-channel interference signals come from those nodes separated by the following number of hops, i.e., $\ell-1, \ell+1, 2\ell-1, \ldots, \lceil(\lceil n/\ell\rceil-1)/2\rceil\ell+(-1)^{\lceil n/\ell\rceil-1}$. Let $P_{n,\ell}$ denote the received power level from the desired node, and let $I_{n,\ell}$ denote the total interference power at the receiving node. Then, the received carrier-to-interference ratio (CIR) $P_{n,\ell}/I_{n,\ell}$ can be written as

$$\frac{P_{n,\ell}}{I_{n,\ell}} = \left\{ \sum_{i=1}^{\lceil n/\ell\rceil-1} \left[\lceil i/2\rceil\ell+(-1)^i\right]^{-\alpha} \right\}^{-1} \equiv \gamma_{\mathrm{i}}.$$

Let N be the noise power level. The per-hop CNR is then expressed as $P_{n,\ell}/N = n^{\alpha}\gamma$. Therefore, per-hop CINR can be expressed as

$$\begin{aligned}\frac{P_{n,\ell}}{N+I_{n,\ell}} &= \frac{1}{(P_{n,\ell}/N)^{-1}+(P_{n,\ell}/I_{n,\ell})^{-1}} \\ &= (1/n^{\alpha}\gamma+1/\gamma_{\mathrm{i}})^{-1}.\end{aligned}$$

Assuming every node adjusts its data rate based on $P_{n,\ell}/(N+I_{n,\ell})$, we get the BE of n-hop transmission over ℓ channels as

$$f_{n,\ell}(\gamma, p_{\mathrm{b}}) = \frac{1}{\ell} f_1((1/n^{\alpha}\gamma+1/\gamma_{\mathrm{i}})^{-1}, p_{\mathrm{b}}/n). \tag{3.3}$$

3.3.2 Numerical Results

When we assume the number of hops is fixed to n ($n = 1, 2, 4, 8, 16$) and the number of channels ℓ is a variable to be optimized, the end-to-end CNR dependence of the BE (3.3) is as shown in Figure 3.5. The BE can increase through spatial channel reuse under low end-to-end CNR conditions.

Then, we assume the numbers of hops and channels are variables to be chosen optimally in terms of the BE. Figure 3.6 shows the optimal numbers of hops and channels

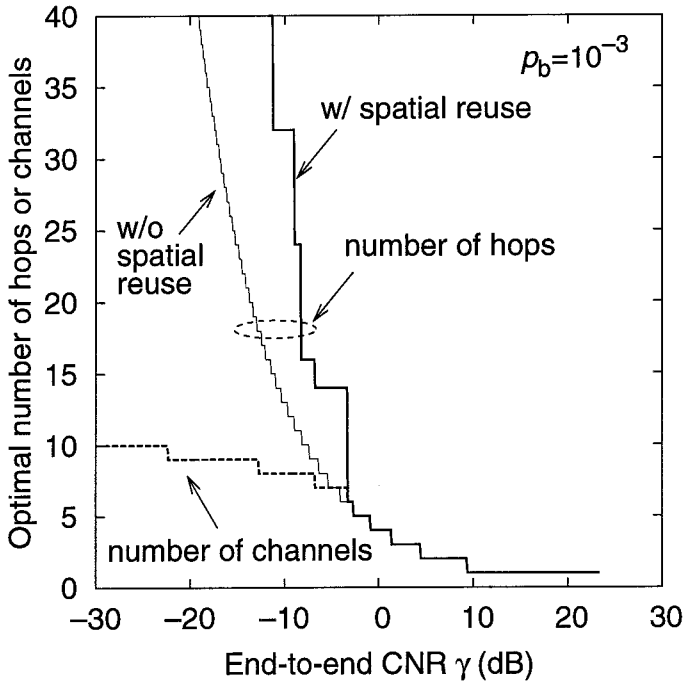

(a) $\alpha = 2$.

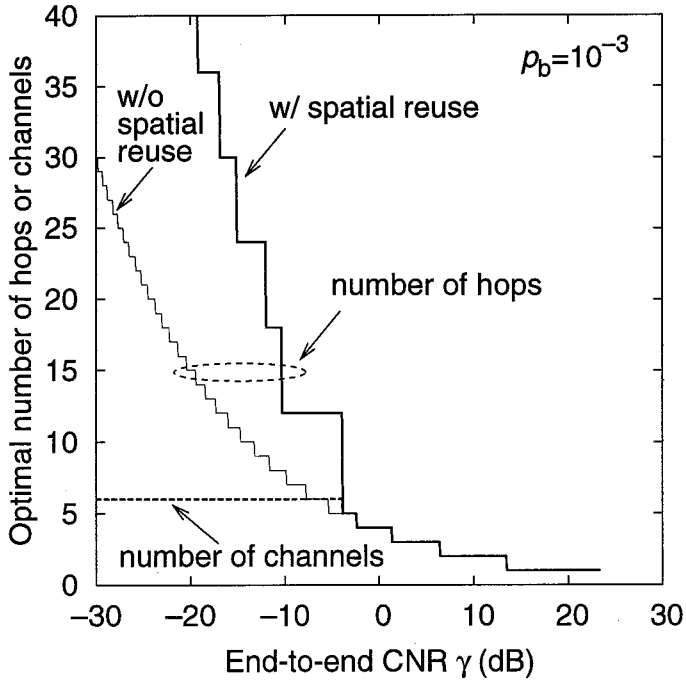

(b) $\alpha = 3.5$.

Figure 3.6: Optimal numbers of hops and channels for bandwidth efficiency.

for different values of the path loss exponent α. Multihop transmission outperforms single-hop transmission in terms of the BE below the end-to-end CNR of 9 dB and 13 dB for $\alpha = 2$ and 3.5, respectively. In addition to this, multihop transmission with spatial channel reuse outperforms that without spatial channel reuse below the end-to-end CNR of -3 dB and -4 dB for $\alpha = 2$ and 3.5, respectively. The optimal number of hops increases rapidly with reduction in the end-to-end CNR compared to multihop transmission without spatial channel reuse.

Figure 3.7 shows the BE with the optimal numbers of hops and channels for different values of the path loss exponent α. When the path loss exponent is relatively small, nodes will receive larger interference from simultaneous transmissions. To mitigate the interference, a large number of channels are required, and consequently, the BE will be small.

In contrast to the case without spatial channel reuse, the loss of BE along with the reduction of end-to-end CNR is relatively small especially when the path loss exponent is large ($\alpha = 3.5$). Therefore, under the condition that the spatial channel reuse is effective, energy efficiency can be increased by reducing the transmit power per node at the cost of a slight decrease in the BE.

3.4 Area Spectral Efficiency of Multihop Radio Networks

In the previous section, we assume that channels are spatially reused in a single isolated multihop route. On the contrary, in this section, we assume that channels are spatially reused only among multihop routes.

We consider the interference-limited situation where co-channel interference totally dominates the thermal noise. Under this environment, the CINR reduces to the CIR. In a single-hop transmission scenario, the decrease of the required CIR allows more simultaneous transmissions in a given area but each node should transmit at a lower

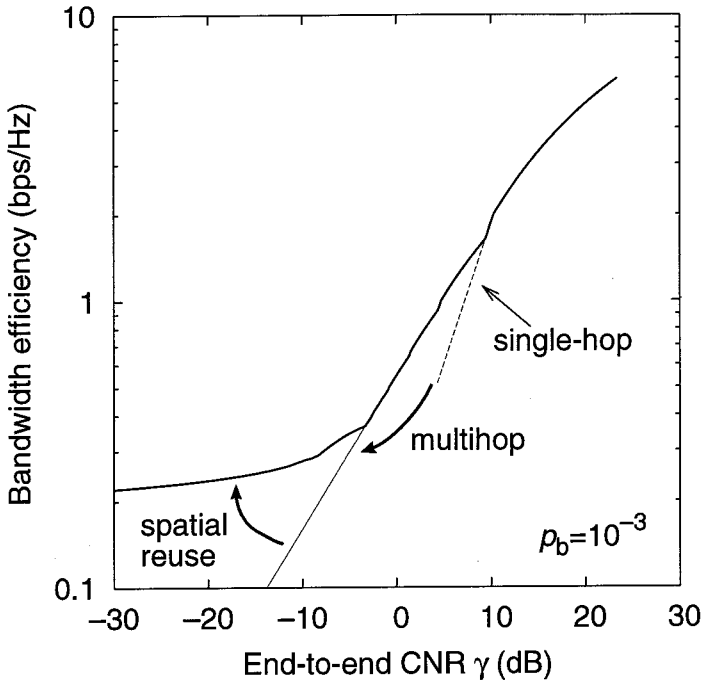

(a) $\alpha = 2$.

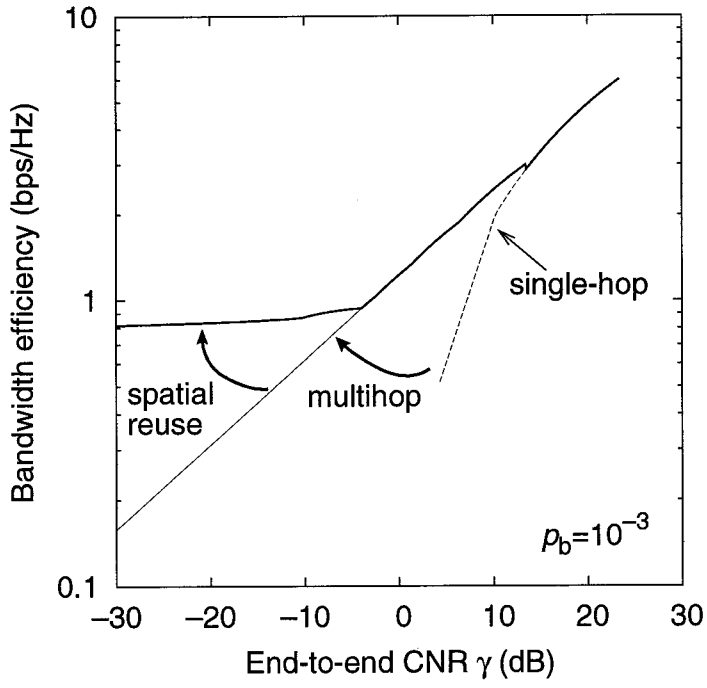

(b) $\alpha = 3.5$.

Figure 3.7: Bandwidth efficiency with optimal numbers of hops and channels.

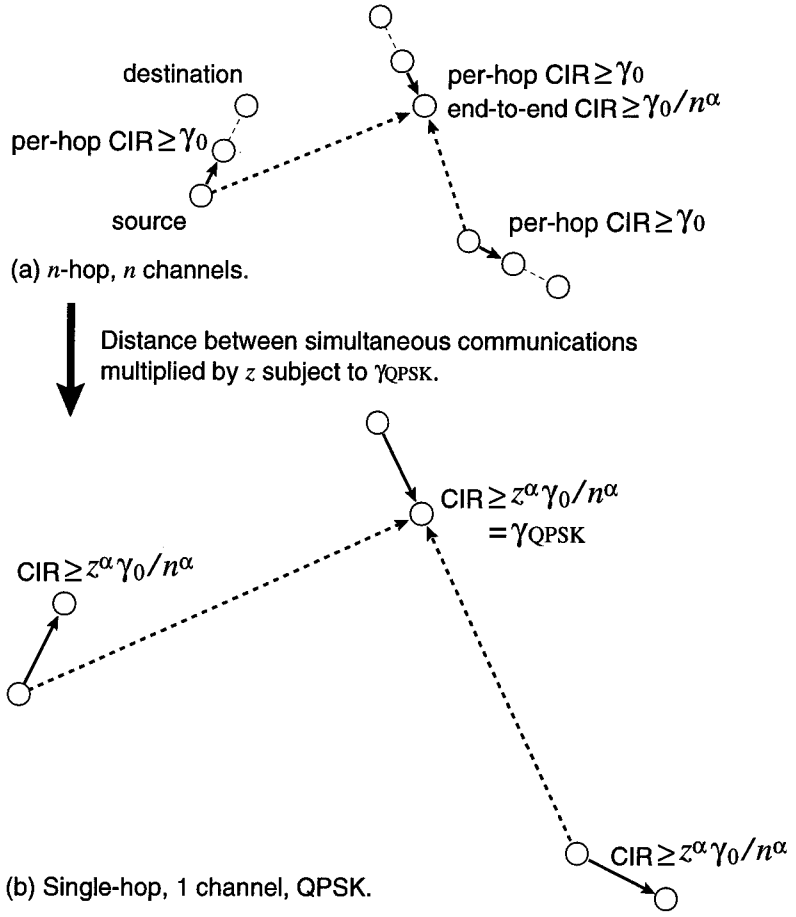

Figure 3.8: Models of single-hop and multihop transmissions ($n = 2$). Solid arrows represent desired signals and dashed arrows represent co-channel interference.

rate. In a multihop transmission scenario, the increased number of hops allows more simultaneous transmissions in a given area because adaptive route selection has the same ability as symbol rate control to decrease required end-to-end CINR at the cost of lower end-to-end throughput, as was presented in Section 3.2.2. Therefore, we evaluate the resulting ASE of multihop radio networks, which is defined as the maximum end-to-end bit rate through multiple hops per unit bandwidth per unit area.

3.4.1 Analysis

The ASE of multihop radio networks is sensitive to lots of factors, particularly fairness, as mentioned in Section 1.1. Since the main purpose of this investigation is to examine the impact of symbol rate and modulation level control and adaptive route selection on the ASE, we must set aside the fairness problem and investigate the ASE under the condition that the number of hops for all transmissions is the same and the per-hop CIR of all transmissions is greater than a given value γ_0 as shown in Figure 3.8(a). In addition to this, we model the topology of n-hop transmission as equally spaced $(n-1)$ relaying nodes as shown in Section 3.2.

Consider the situation where every source node transmits directly to its destination regardless of whether every source-destination pair can communicate directly, and we designate the received CIR as being the end-to-end CIR. Similar to the end-to-end CNR, the end-to-end CIR is considered to be an appropriate parameter to reflect the density of simultaneous communications since the absolute value of this density does not have meaning in our simple model. Therefore, the BE in an interference-limited situation can also be expressed by replacing end-to-end CNR with end-to-end CIR in Eq. (3.2).

Let t_n be the BE of n-hop transmission. Under the assumption above, the end-to-end CIR of all simultaneous communications are greater than γ_0/n^α. We assume that every node adjusts its data rate based on γ_0. Thus, the BE of each n-hop transmission may be expressed by using the end-to-end CIR γ_0/n^α as

$$t_n = f_n(\gamma_0/n^\alpha, p_\mathrm{b}). \tag{3.4}$$

Let ρ_n be the density of source-destination pair achieving the given per-hop CIR γ_0 when transmitting simultaneously. Then, defining the ASE of n-hop transmission as

$$\eta_n = t_n \cdot \rho_n \tag{3.5}$$

naturally follows. The goal of this section is to approximate the ASE of multihop radio networks. Through the use of rate adaptation, the required CIR is adjusted to meet the received CIR. In addition to this, changing the distance between simultaneous communications and the number of hops can control the received CIR.

For comparison, we also consider single-hop radio networks with QPSK. We assume the distance between source and destination nodes is the same as that in multihop radio networks. We then consider multiplying the distances between simultaneous communications by z subject to the required CIR of QPSK, γ_{QPSK}, as shown in Figure 3.8(b). The interference power is then reduced to roughly $1/z^{\alpha}$ of that with n-hop transmission, so that the end-to-end CIR of all transmissions satisfy the following condition:

$$\text{end-to-end CIR} \geq z^{\alpha}\frac{\gamma_0}{n^{\alpha}} = \gamma_{\mathrm{QPSK}}. \tag{3.6}$$

Let $t_{1,\mathrm{QPSK}}=2$ represent the BE; let $\rho_{1,\mathrm{QPSK}}$ be the density of simultaneous communications, and let $\eta_{1,\mathrm{QPSK}}$ be the ASE of single-hop transmission with QPSK. The density of simultaneous communications is reduced to roughly $1/z^2$ of that with n-hop transmission

$$\rho_{1,\mathrm{QPSK}} = \frac{\rho_n}{z^2} = \frac{\eta_n}{z^2 t_n}.$$

The ASE of single-hop transmission with QPSK is therefore expressed as

$$\eta_{1,\mathrm{QPSK}} = t_{1,\mathrm{QPSK}} \cdot \rho_{1,\mathrm{QPSK}} = \frac{2\eta_n}{z^2 t_n}. \tag{3.7}$$

Substituting Eqs. (2.16) and (3.6) into Eq. (3.4), we get

$$t_n = f_n(3/z^{\alpha}\beta_1, p_{\mathrm{b}}).$$

Combining the above equation with Eq. (3.2) and solving for z, we get

$$z = \begin{cases} n\left(\dfrac{2}{nt_n}\dfrac{\beta_n}{\beta_1}\right)^{1/\alpha} & \dfrac{1}{2n} \leq t_n < \dfrac{2}{n} \\ n\left(\dfrac{3}{2^{nt_n}-1}\dfrac{\beta_n}{\beta_1}\right)^{1/\alpha} & \dfrac{2}{n} \leq t_n \leq \dfrac{6}{n}. \end{cases} \tag{3.8}$$

The ASE of n-hop transmission is approximated by substituting Eq. (3.8) into Eq. (3.7):

$$\begin{aligned}\eta_n &= \frac{z^2 t_n}{2}\eta_{1,\mathrm{QPSK}} \\ &= \begin{cases} \dfrac{n^2 t_n}{2}\left(\dfrac{2}{nt_n}\dfrac{\beta_n}{\beta_1}\right)^{2/\alpha}\eta_{1,\mathrm{QPSK}} & \dfrac{1}{2n} \le t_n < \dfrac{2}{n} \\ \dfrac{n^2 t_n}{2}\left(\dfrac{3}{2^{nt_n}-1}\dfrac{\beta_n}{\beta_1}\right)^{2/\alpha}\eta_{1,\mathrm{QPSK}} & \dfrac{2}{n} \le t_n \le \dfrac{6}{n}. \end{cases}\end{aligned} \tag{3.9}$$

3.4.2 Numerical Results

The combined effect of symbol rate control, modulation level control, and the number of hops on the ASE for the two different path loss exponent α is shown in Figure 3.9. The absolute value of $\eta_{1,\mathrm{QPSK}}$ depends on the specific value of the path loss exponent α; therefore, there is no way to conduct a direct comparison between Figures 3.9(a) and 3.9(b).

When the nodes are only allowed n-hop transmission, the ASE decreases with the increase of the BE from $2/n$ (QPSK) to $6/n$ (64QAM). In addition to this, the ASE can decrease with the reduction of the BE from $2/n$ (QPSK) to $0.5/n$ (1/4-rate QPSK). This result is consistent with other results on multilevel modulation in cellular networks, and it indicates that QPSK rather than 16QAM is the optimal modulation scheme to obtain high ASE [59].

When the nodes are allowed to select the number of hops, as expected, the ASE increases with the number of hops at the cost of BE. Recall the results in Figure 3.2 where symbol rate control and adaptive route selection have the same tradeoff between the BE and the end-to-end CNR. However, only adaptive route selection has a tradeoff between the ASE and the BE. This result is also consistent with other results reported in investigations of cellular networks that show a tradeoff between the ASE and the BE of single-hop transmission [10].

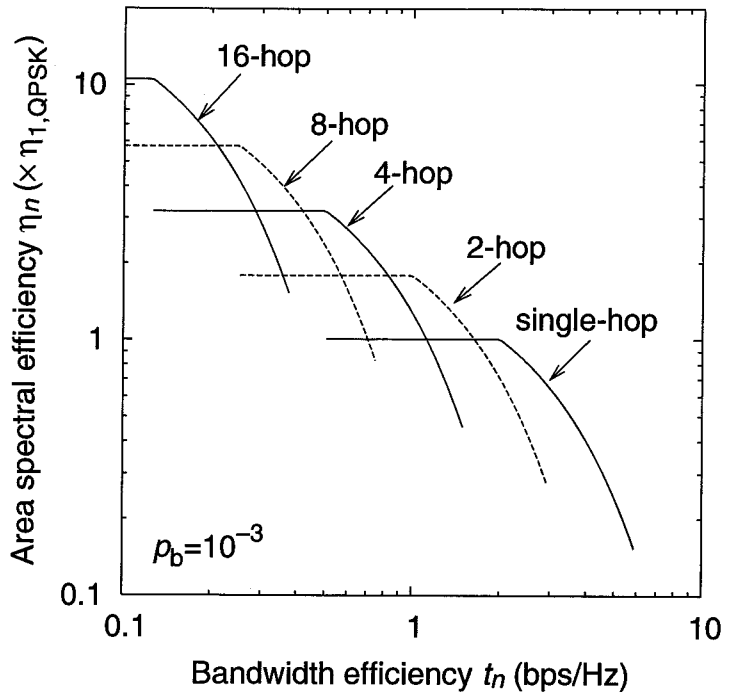

(a) $\alpha=2$.

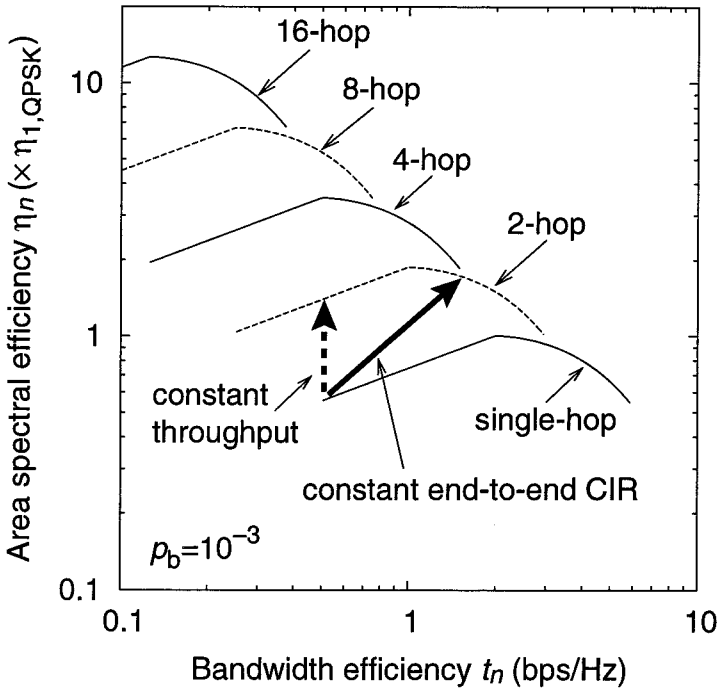

(b) $\alpha=3.5$.

Figure 3.9: Area spectral efficiency η_n vs. bandwidth efficiency t_n. Bold and dashed arrows correspond to those in Figure 3.2(b).

By comparing Figures 3.2(b) and 3.9(b), one can see that increase of the BE resulting from varying the number of hops (as shown by the bold arrow in Figure 3.2(b)) corresponds to the enhancement of the ASE by fixing the density of simultaneous communications (as shown by the bold arrow in Figure 3.9(b)). One can also see that decreasing the required end-to-end CIR through the use of multihop transmission (as shown by the dashed arrow in Figure 3.2(b)) corresponds to the enhancement of the ASE by varying the number of hops and the density of simultaneous communications and fixing the BE (as shown by the dashed arrow in Figure 3.9(b)).

Suppose now that we relax our assumption that co-channel interference totally dominates the thermal noise, i.e. the end-to-end CNR is infinite, and instead the end-to-end CNR γ_n is finite. In this case, the ASE is expressed as

$$\eta_n = \begin{cases} \dfrac{t_n}{2}\left(\dfrac{\dfrac{2n^\alpha\beta_n}{3nt_n} - \dfrac{1}{\gamma_n}}{\dfrac{\beta_1}{3} - \dfrac{1}{\gamma_n}}\right)^{2/\alpha} \eta_{1,\mathrm{QPSK}} & \dfrac{1}{2n} \le t_n < \dfrac{2}{n} \\ \dfrac{t_n}{2}\left(\dfrac{\dfrac{n^\alpha\beta_n}{2^{nt_n}-1} - \dfrac{1}{\gamma_n}}{\dfrac{\beta_1}{3} - \dfrac{1}{\gamma_n}}\right)^{2/\alpha} \eta_{1,\mathrm{QPSK}} & \dfrac{2}{n} \le t_n \le \dfrac{6}{n}. \end{cases} \tag{3.10}$$

When the end-to-end CNR γ_n is infinite, the above equation becomes Eq. (3.9). Figure 3.10 shows the BE dependence of the ASE. We choose 15 dB and 20 dB for the example values of γ_n. One can see that smaller end-to-end CNR γ_n leads to smaller ASE, particularly under condition that the number of hops is small. That is because under the same end-to-end CNR condition, the per hop CNR of multihop transmission becomes higher than that of single-hop transmission.

3.5 Summary

Assuming symbol rate and modulation level control, we have considered two types of spectral efficiency for multihop radio networks. First, we examined the spectral efficiency

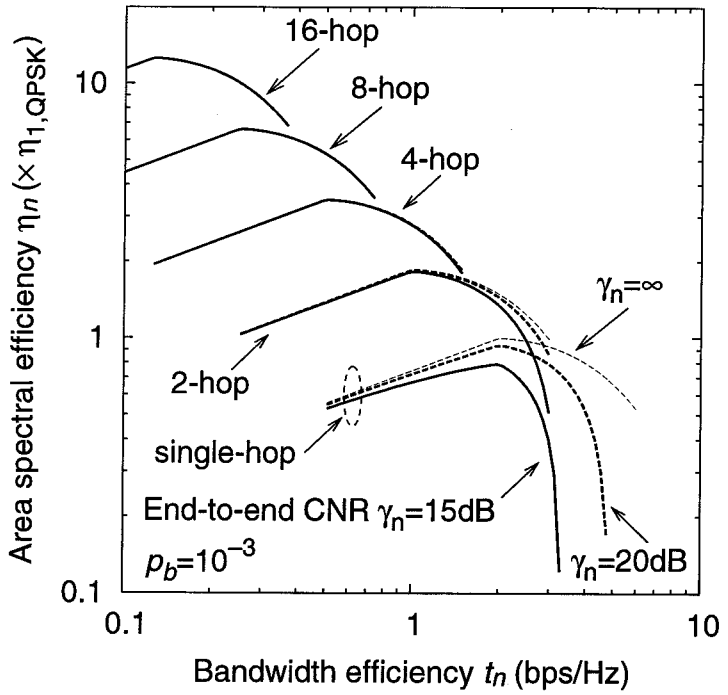

Figure 3.10: Area spectral efficiency η_n vs. bandwidth efficiency t_n assuming finite end-to-end CNR γ_n ($\alpha = 3.5$).

of a single isolated multihop route, named as bandwidth efficiency, which is defined as the maximum end-to-end bit rate through multiple hops per unit bandwidth. We have taken into account the effect of bit error accumulation over multihop transmission. We found a relationship between the bandwidth efficiency of n-hop transmission and that of single-hop transmission. Numerical results revealed that symbol rate control and adaptive route selection have the same ability to enhance the end-to-end communication range at a loss of bandwidth efficiency.

Next, we also investigated the overall spectral efficiency of multihop radio networks, named as area spectral efficiency, which is defined as the maximum end-to-end bit rate through multiple hops per unit bandwidth per unit area. We derived an expression for area spectral efficiency as a function of end-to-end throughput and the number of hops. Numerical results revealed a significant difference between symbol rate control

and adaptive route selection. The use of symbol rate control can decrease area spectral efficiency. On the other hand, a tradeoff between the area spectral efficiency and the end-to-end throughput of multihop transmission is such that the use of multihop transmission can increase the area spectral efficiency. Note that these results are consistent with those of other research on the area spectral efficiency of cellular networks with modulation level control.

Chapter 4

Multihop and Rate-Adaptive TDMA Cellular Systems in Single-Cell Environments

In Chapter 3, we established a fundamental relationship between the area spectral efficiency and bandwidth efficiency of multihop radio networks in which every communication pair has nearly the same performance. However, in a real system, the wireless channel of each communication pair is different. In this chapter, we attempt to theoretically estimate the spectral efficiency and outage probability of multihop TDMA cellular systems in which mobile stations are distributed randomly in a cell. In addition to the path loss, the effects of shadowing is considered. Since multihop transmission and symbol rate control have the same ability to enhance the end-to-end communication range at the loss of bandwidth efficiency as shown in Chapter 3, we formulate the cell-radius dependence of spectral efficiency and outage probability of multihop cellular systems by using the similar methodology that is used for performance formulation of rate-adaptive cellular systems.

The remainder of this chapter is organized as follows. In Section 4.1, we describe the system model of TDMA cellular systems. In Section 4.2, we describe the formulation of spectral efficiency and outage probability in rate-adaptive cellular systems as shown

in [41]. In Sections 4.3 and 4.4, we present the formulation of performances in multihop cellular systems for two different scenarios. In the first scenario, we consider lots of candidate for relaying stations in the cell and assume that relaying stations are located on a straight line segment between the mobile station and the base station. In the second scenario, we consider some relaying stations are uniformly and independently distributed in the cell and assume that the selection of the relaying station is determined in terms of the bandwidth efficiency and the required BER.

4.1 System Model

We consider a single isolated cell and assume that signals are multiplexed by the TDMA, i.e. there is no co-channel interference. All stations can either transmit or receive at a given time and use omnidirectional antennas with the same transmit power.

We take into account the log-normal shadowing as well as the propagation loss with the path loss exponent α as follows. First, at locations where the distances to a certain station are r and r_0, the mean received CNR's $\gamma_{\mathrm{m}}(r)$ and $\gamma_{\mathrm{m}}(r_0)$ satisfy the following relationship:

$$\gamma_{\mathrm{m}}(r) = \gamma_{\mathrm{m}}(r_0)\left(\frac{r}{r_0}\right)^{-\alpha}. \tag{4.1}$$

Second, the probability density function (PDF) of the local mean received CNR γ is given by

$$f_r(\gamma) = \frac{1}{\sqrt{2\pi}\sigma\gamma}\exp\left[-\frac{1}{2\sigma^2}\left(\ln\frac{\gamma}{\gamma_{\mathrm{m}}(r)}\right)^2\right], \tag{4.2}$$

where $\sigma = (\ln 10)\sigma_0/10$.

We assume that the symbol rate and the multihop route are determined by the local mean received CNR (hereinafter referred to as "the received CNR").

4.2 Rate-Adaptive Cellular Systems

In this section, we formulate outage probability and spectral efficiency of TDMA cellular systems with rate adaptation (hereinafter referred to as "rate-adaptive cellular systems") as described in [41]. When QPSK modulation is used, $1/2^k$-rate QPSK transmission is equivalently obtained from consecutive transmission of the 2^k identical symbols, and the required CNR can be decreased by $10(\log_{10} 2)k$ dB, where k represents an integer of zero or more. Let $K\ (\geq 1)$ denote the upper limit of k [57]. We assume that the symbol rate is set as high as possible while maintaining the required BER. We assume that when the BER for the $1/2^{K-1}$-rate does not satisfy the required BER, the $1/2^K$-rate is used.

4.2.1 Outage Probability

First, we formulate the outage probability. The outage probability of rate-adaptive cellular systems is defined as the probability that the BER for the minimal rate, i.e. the $1/2^K$-rate, does not satisfy the required BER.

Let γ denote the received CNR, and $\beta_{\text{A-}k}(\gamma)$ denote the CNR dependence of BER for $1/2^k$-rate QPSK. The subscript "A" of the BER β denotes "adaptive-rate". When the distance between a calling station and the base station is r, the probability that $\beta_{\text{A-}k}$ does not satisfy the required BER β_{req} can be expressed as

$$p_{\text{A-}k}(r) = \int_{D_{\text{A-}k}} f_r(\gamma)\, \mathrm{d}\gamma\,, \tag{4.3}$$

where

$$D_{\text{A-}k} = \{\gamma\ ;\ \gamma > 0\ ,\ \beta_{\text{A-}k}(\gamma) > \beta_{\text{req}}\}. \tag{4.4}$$

Note that when the BER for the $1/2^k$-rate, $\beta_{\text{A-}k}$, satisfies the required BER, $\beta_{\text{A-}(k+1)}$ also satisfies the required BER and therefore, the following relationship holds:

$$D_{\text{A-}(k+1)} \subset D_{\text{A-}k}\,. \tag{4.5}$$

Assuming that calling stations are uniformly distributed in the cell, we get the outage probability of rate-adaptive cellular systems as follows:

$$\begin{aligned} P_{\mathrm{A}}(R) &= \int_0^R \frac{2\pi r}{\pi R^2} p_{\mathrm{A}\text{-}K}(r)\,\mathrm{d}r \\ &= \frac{2}{R^2}\int_0^R r\, p_{\mathrm{A}\text{-}K}(r)\,\mathrm{d}r\,. \end{aligned} \tag{4.6}$$

4.2.2 Spectral Efficiency

Next, we formulate the spectral efficiency. We define the bandwidth efficiency (BE) as the end-to-end bit rates per unit bandwidth. When the distance between a calling station and the base station is r, the average BE can be expressed as

$$t_{\mathrm{A}}(r) = \frac{2R_{\mathrm{smax}}F_{\mathrm{eff}}}{B_{\mathrm{ch}}}\left[1 - \sum_{k=0}^{K-1}\frac{p_{\mathrm{A}\text{-}k}(r)}{2^{k+1}}\right], \tag{4.7}$$

where R_{smax} is the QPSK symbol rate, F_{eff} is the TDMA frame efficiency, and B_{ch} is the channel bandwidth. We define the spectral efficiency of rate-adaptive cellular systems as the average of bandwidth efficiency in the cell as follows:

$$\eta_{\mathrm{A}}(R) = \frac{2}{R^2}\int_0^R r\, t_{\mathrm{A}}(r)\,\mathrm{d}r. \tag{4.8}$$

4.3 Multihop Cellular Systems with Equally Spaced Relaying Stations

Multihop relaying enables communications between the base station and calling stations that are relatively far apart. In this section, we formulate the outage probability and the spectral efficiency of TDMA cellular systems with multihop transmission (hereinafter referred to as "multihop cellular systems") in a similar way to our derivation of single-hop rate-adaptive cellular systems in the previous section. First, we assume the simple situation where relaying stations are located on a straight line segment between a calling

station and the base station. In this case, the number of hops is the variable to be optimized in terms of the required BER and the BE. Next, we assume the general situation that relaying stations are uniformly and independently distributed in each cell. In this case, we use the required BER and the BE for the route selection criteria.

We assume only full-rate QPSK modulation. Let $N\,(\geq 2)$ denote the upper limit of the number of hops n. We assume that a calling station selects as small number of hops as possible while maintaining the required BER and N-hop transmission is used when for all $1 \leq n \leq N-1$, the end-to-end BER of n-hop transmission does not satisfy the requirement.

4.3.1 Analysis

We define the outage probability of multihop cellular systems as the probability that the end-to-end BER does not satisfy the required BER.

For the i-th $(1 \leq i \leq n)$ hop of n-hop transmission, let r_{ni}, γ_{ni}, and $\beta_{\text{M-}ni}$, denote the per-hop distance, the per-hop CNR, and the per-hop BER. The subscript "M" of the BER β denotes multihop relaying. Let $\beta_{\text{M-}n}$ denote the end-to-end BER for n-hop transmission. When the BER per hop is very low, it is approximated by

$$\beta_{\text{M-}n} = \sum_{i=1}^{n} \beta_{\text{M-}ni}\,. \tag{4.9}$$

Therefore, the probability that the end-to-end BER for n-hop transmission does not satisfy the required BER β_{req} can be expressed as

$$p_{\text{M-}n}(r_{n1},\ldots,r_{nn}) = \int_{D_{\text{M-}n}} \left[\prod_{i=1}^{n} f_{r_{ni}}(\gamma_{ni})\,\mathrm{d}\gamma_{ni}\right], \tag{4.10}$$

where

$$D_{\text{M-}n} = \left\{(\gamma_{n1},\ldots,\gamma_{nn})\ ;\ \gamma_{n1}>0,\ldots,\gamma_{nn}>0, \beta_{\text{M-}n} = \sum_{i=1}^{n} \beta_{\text{A-0}}(\gamma_{ni}) > \beta_{\text{req}}\right\}. \tag{4.11}$$

To simplify the evaluation, we first model the topology of n-hop transmission as equally spaced $(n-1)$ relaying stations on a straight line segment from a calling station to the base station. This gives

$$r_{n1} = \cdots = r_{nn} = r/n, \tag{4.12}$$

where r represents the distance between a calling station and the base station. Therefore, the probability that the end-to-end BER for n-hop transmission does not satisfy the required BER β_{req} can be expressed as

$$p_{\text{M-}n}(r/n, \dots) = \int_{D_{\text{M-}n}} \left[\prod_{i=1}^{n} f_{r/n}(\gamma_{ni})\, \mathrm{d}\gamma_{ni} \right]. \tag{4.13}$$

Assuming that calling stations are uniformly distributed in the cell, we get the outage probability of multihop cellular systems:

$$P_{\text{M}}(R) = \frac{2}{R^2} \int_0^R r \left[\prod_{n=1}^{N} p_{\text{M-}n}(r/n, \dots) \right] \mathrm{d}r\,. \tag{4.14}$$

Next, the average BE can be expressed as

$$t_{\text{M}}(r) = \frac{2R_{\text{smax}}F_{\text{eff}}}{B_{\text{ch}}} \left\{ \frac{1}{N} \prod_{n'=0}^{N-1} p_{\text{M-}n'}(r/n', \dots) + \sum_{n=1}^{N-1} \left[\frac{1 - p_{\text{M-}n}(r/n, \dots)}{n} \prod_{n'=0}^{n-1} p_{\text{M-}n'}(r/n', \dots) \right] \right\}, \tag{4.15}$$

where $p_{\text{M-}0} = 1$. Assuming that calling stations are uniformly distributed in the cell, we get the spectral efficiency of multihop cellular systems:

$$\eta_{\text{M}}(R) = \frac{2}{R^2} \int_0^R r\, t_{\text{M}}(r)\, \mathrm{d}r\,. \tag{4.16}$$

4.3.2 Numerical Results

Table 4.1 summarizes the parameters we used in our evaluation. We assume Rayleigh fading channels and two-branch maximal ratio combining diversity reception. Figure 4.1

Table 4.1: Parameters used in evaluations.

Parameters	Values
Path loss exponent α	2, 3.5
Shadowing	Log-normal distribution
	$\sigma_0 = 4\,\mathrm{dB}, 8\,\mathrm{dB}$
Channel	Rayleigh fading
Required end-to-end BER β_{req}	10^{-2}

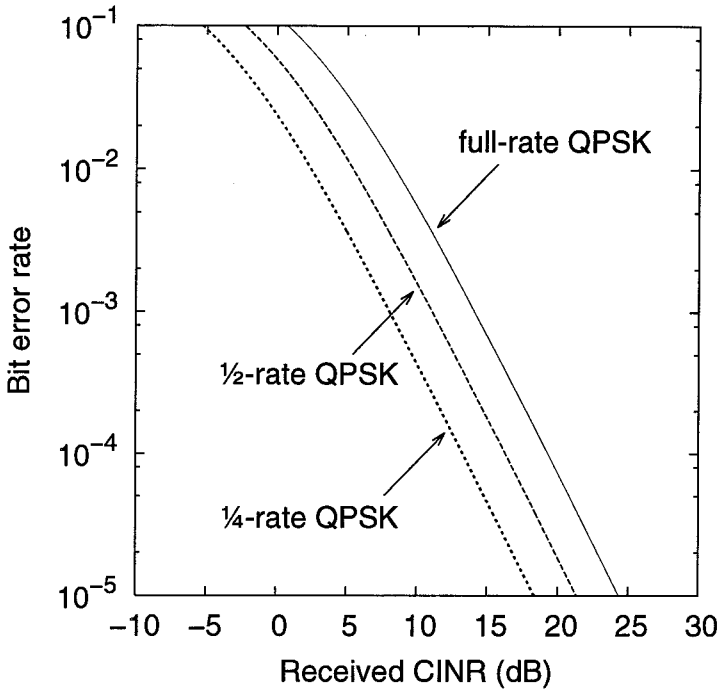

Figure 4.1: BER for $1/2^k$-rate QPSK on the received CNR ($k = 0, 1, 2$).

shows the dependence of the BER for $1/2^k$-rate QPSK (k = 0, 1, and 2) on the received CNR. The curves for full-rate, 1/2-rate, and 1/4-rate QPSK correspond to $\beta_{\text{A-0}}(\gamma)$, $\beta_{\text{A-1}}(\gamma)$, and $\beta_{\text{A-2}}(\gamma)$.

Figure 4.2(a) shows the cell-radius dependence of the spectral efficiency of the rate-adaptive system (4.8) and the multihop system (4.16) for $\alpha = 3.5$ and $\sigma = 8\,\mathrm{dB}$. We define the coverage of cellular systems to be the distance from the BS at which the outage probability $P_{\mathrm{A}}(R)$ or $P_{\mathrm{M}}(R)$ equal a certain required outage probability P_{req}. In

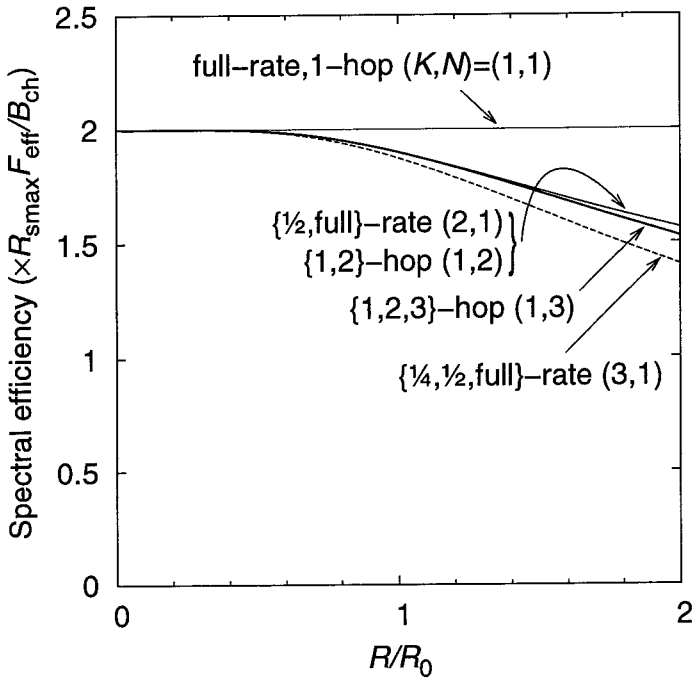

(a) Spectral efficiency.

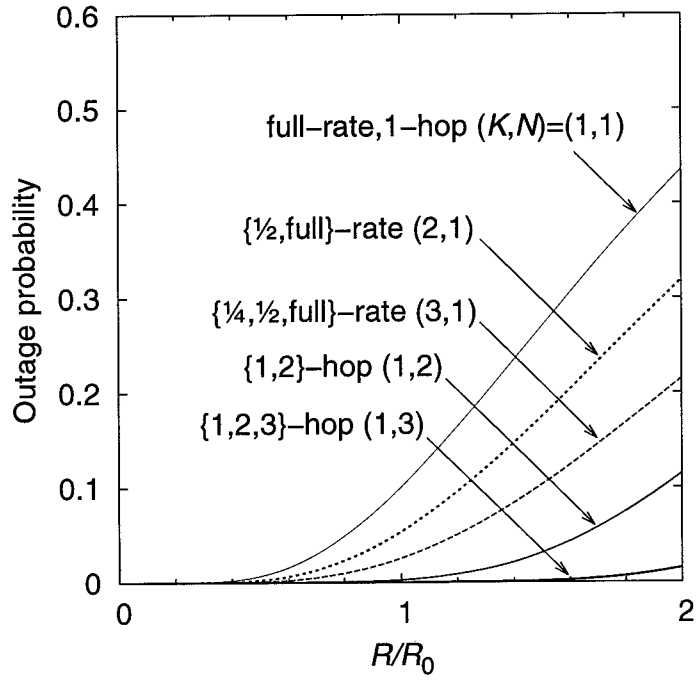

(b) Outage probability.

Figure 4.2: Comparison between rate-adaptive cellular and multihop cellular systems ($\alpha = 3.5, \sigma = 8\,\mathrm{dB}$).

this figure, R_0 is the coverage of full-rate single-hop cellular systems associated with the outage probability of 10%, which is shown in Figure 4.2(b). As shown in Figure 4.2(a), the spectral efficiencies of the half-rate system ($K = 2$) and the two-hop system ($N = 2$) are the same because of their definitions.

Figure 4.2(b) shows the outage probabilities of the rate-adaptive system (4.6) and the multihop system (4.14). We see that the outage probability of the two-hop system ($N = 2$) is less than that of the half-rate system ($K = 2$) while the spectral efficiencies of these systems are the same. Therefore, under these conditions, two-hop relaying is superior to rate adaptation in terms of coverage.

In order to explore the impact of the shadowing on the superiority of multihop relaying over rate adaptation, we show the spectral efficiency and outage probability for $\alpha = 3.5$ and $\sigma = 4\,\mathrm{dB}$ in Figure 4.3. Note that the absolute value of R_0 depends on the specific values of α and σ; therefore, there is no way to conduct a direct comparison between Figures 4.2 and 4.3.

We then show the relationships between spectral efficiency and coverage associated with the required outage probability of 5% and 10% in Figures 4.4 and 4.5. These figures indicate that the multihop relaying and rate adaptation have the same ability to increase the coverage at a loss of spectral efficiency in cellular systems. In addition, we see that the superiority of multihop relaying over rate adaptation still holds.

Next, in order to explore the impact of the path loss exponent on the superiority of multihop relaying, we show the coverage dependence of the spectral efficiency for $\alpha = 2$ and $\sigma = 8\,\mathrm{dB}$ in Figure 4.6. We see that the superiority of multihop relaying still holds.

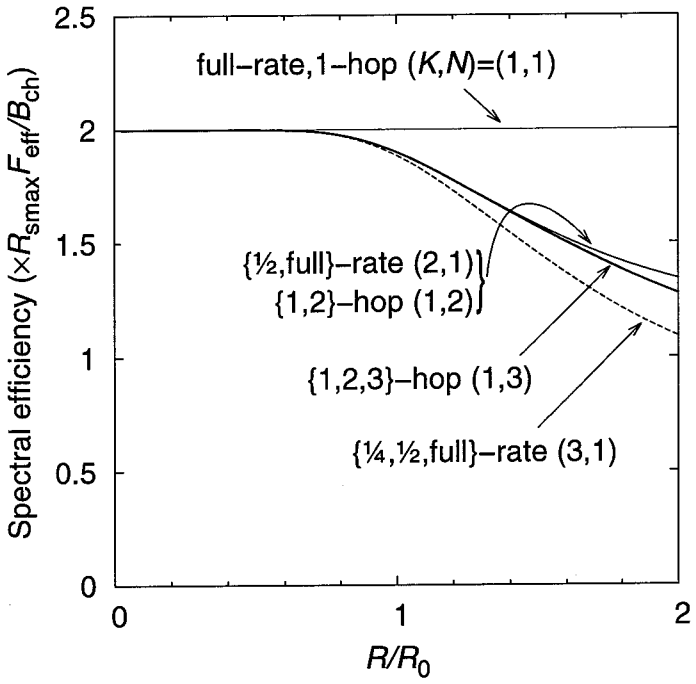

(a) Spectral efficiency.

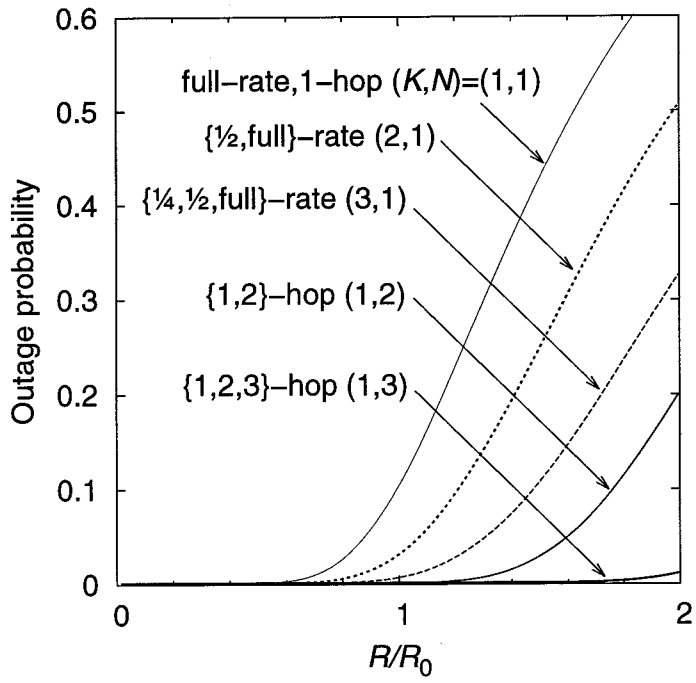

(b) Outage probability.

Figure 4.3: Comparison between rate-adaptive cellular and multihop cellular systems ($\alpha = 3.5, \sigma = 4\,\mathrm{dB}$).

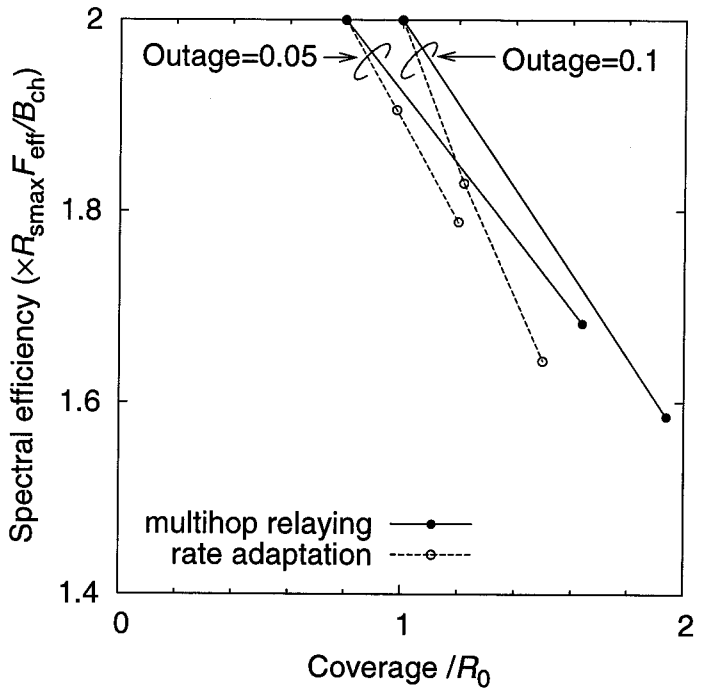

Figure 4.4: Spectral efficiency as a function of coverage ($\alpha = 3.5, \sigma = 8\,\text{dB}$).

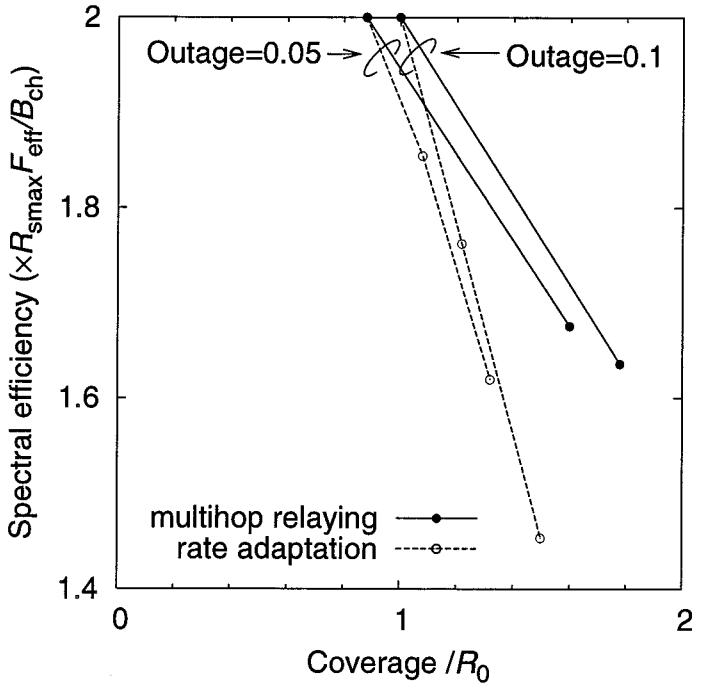

Figure 4.5: Spectral efficiency as a function of coverage ($\alpha = 3.5, \sigma = 4\,\text{dB}$).

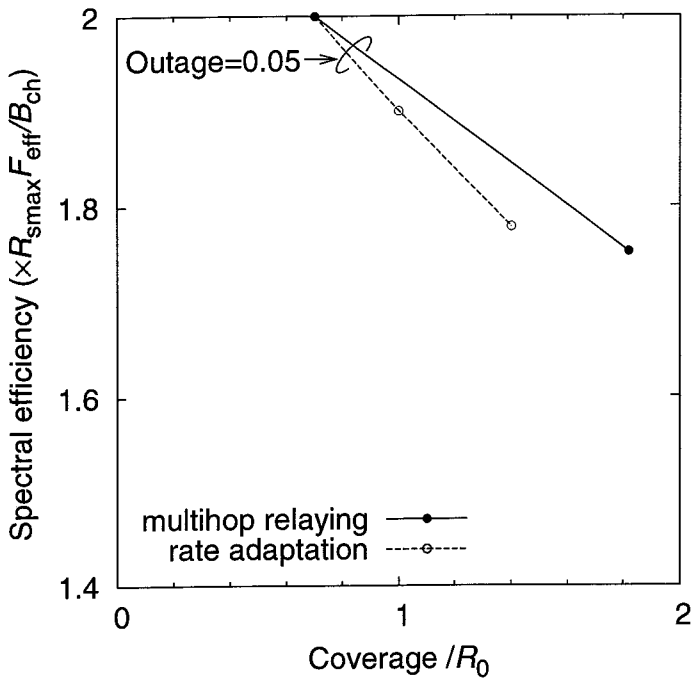

Figure 4.6: Spectral efficiency as a function of coverage. ($\alpha = 2, \sigma = 8\,\mathrm{dB}$)

4.4 Multihop Cellular Systems with Uniformly Distributed Relaying Stations

Next, we consider the situation where relaying stations are uniformly and independently distributed in the cell and assume that the maximum number of hops is limited up to two ($N = 2$).

4.4.1 Analysis

As shown in Figure 4.7, let (r, θ) and $(r_{21}, \alpha+\theta)$ denote the polar coordinates of a calling station and a relaying station relative to the base station. The probability that the BER for single-hop transmission does not satisfy the required BER β_{req} can be written as

$$p_{\text{1-hop}}(r) = p_{\text{M-1}}(r)\,. \tag{4.17}$$

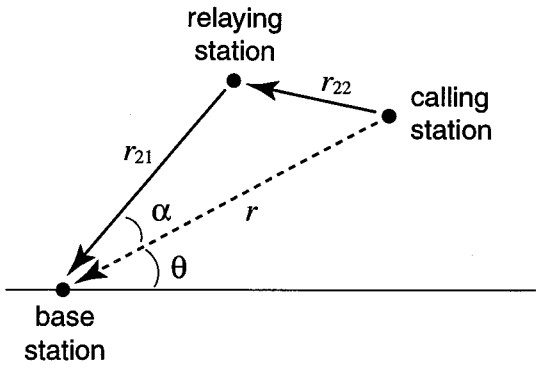

Figure 4.7: Positions of base station, calling station, and relaying station. Dashed arrow and solid arrows represent single-hop transmission and 2-hop transmission.

We assume that relaying stations are uniformly distributed in each cell. For the first hop of 2-hop transmission, the propagation distance of the desired signal can be written as

$$r_{22} = (r_{21}^2 + r^2 - 2r_{21}r\cos\alpha)^{\frac{1}{2}} . \tag{4.18}$$

Note that $p_{\text{M-2}}(r_{21}, r_{22})$ is a function of r, r_{21}, and α. Therefore, when the distance between a calling station and the base station is r, the probability that the end-to-end BER for 2-hop transmission does not satisfy the required BER β_{req} can be expressed as

$$\begin{aligned} p_{\text{2-hop}}(r) &= \int_0^R \frac{2\pi r_{21}}{\pi R^2} \left[\int_0^{2\pi} \frac{1}{2\pi} p_{\text{M-2}}(r_{21}, r_{22}) \mathrm{d}\alpha \right] \mathrm{d}r_{21} \\ &= \frac{1}{\pi R^2} \int_0^R \int_0^{2\pi} r_{21}\, p_{\text{M-2}}(r_{21}, r_{22})\, \mathrm{d}r_{21} \mathrm{d}\alpha . \end{aligned} \tag{4.19}$$

We assume that a relaying station can be selected so that the end-to-end BER satisfies the required BER β_{req}. Let m denote the number of relaying stations per cell. The probability that the end-to-end BER does not satisfy β_{req} can be expressed as

$$p_{\text{1,2-hop}}(r) = p_{\text{1-hop}}(r)\, (p_{\text{2-hop}}(r))^m . \tag{4.20}$$

Finally, we get the outage probability of multihop cellular systems ($N = 2$):

$$P_{\text{M}}(R) = \frac{2}{R^2} \int_0^R r\, p_{\text{1,2-hop}}(r)\, \mathrm{d}r . \tag{4.21}$$

The spectral efficiency η_{M} can be expressed as (16) only when $N = 2$.

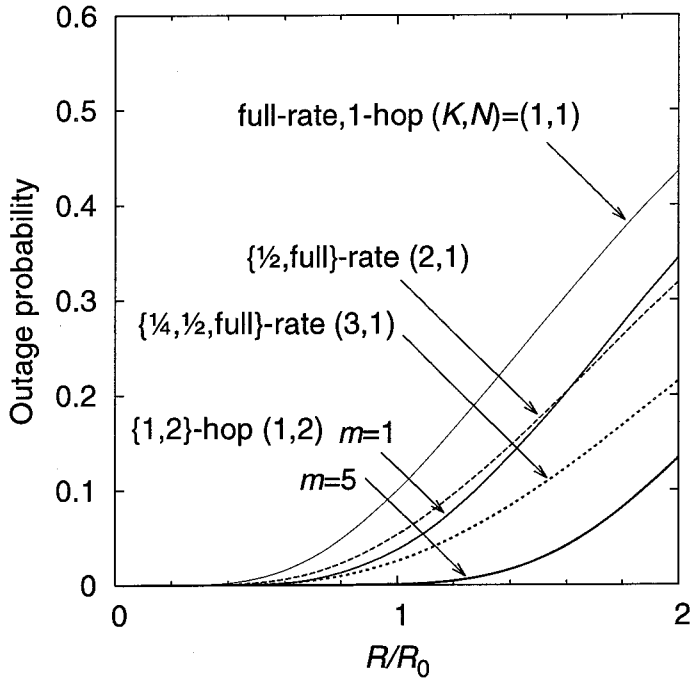

Figure 4.8: Outage probability with uniformly distributed relaying stations ($\alpha = 3.5, \sigma =$ 8 dB).

4.4.2 Numerical Results

Figure 4.8 shows the cell-radius dependence of the outage probability. We see that the outage probability can be decreased along with the number of relaying stations m. By comparing Figures 4.2(b) and 4.8, two-hop relaying under the situation that there are 5 relaying stations is superior to equally spaced three-hop relaying in terms of the outage probability. We next show the station density dependence of the cell-radius in Figure 4.9.

4.5 Summary

Assuming shadowing effects as well as the path loss, we have theoretically estimated the spectral efficiency and outage probability of multihop TDMA cellular systems in which mobile stations are randomly distributed in a single-cell. First, we formulated the cell-radius dependence of spectral efficiency and outage probability of multihop TDMA

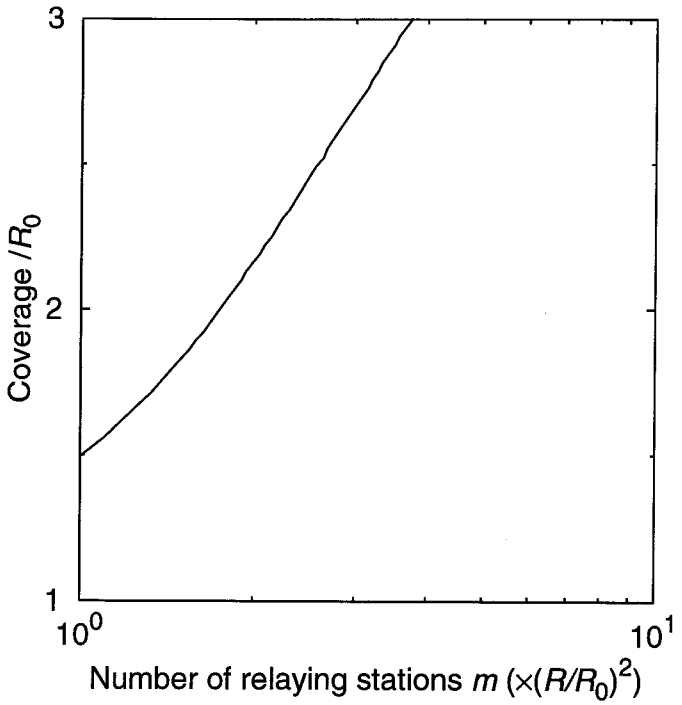

Figure 4.9: Coverage of multihop cellular systems with uniformly distributed relaying stations ($P_{\mathrm{req}} = 0.1, \alpha = 3.5, \sigma = 8\,\mathrm{dB}$).

cellular systems, in which relaying stations located on a straight line between the mobile station and the base station are selected. Numerical results revealed that symbol rate control and multihop transmission have the same ability to enhance the capacity at a loss of spectral efficiency as well as in the multihop radio networks as has been shown in Chapter 3. In addition, multihop transmission is superior to symbol rate control in terms of both coverage and spectral efficiency.

Second, we formulated the performances of multihop TDMA cellular systems, in which relaying stations are uniformly distributed in the cell and the selection of relaying stations is based on the bandwidth efficiency. Numerical results also revealed that the coverage area of multihop TDMA cellular systems can be increased along with the number of relaying stations in the cell.

Chapter 5

Capacity Enhancement for CDMA Cellular Systems Using Two-Hop Relaying

In this chapter, we pay attention to the uplink capacity enhancement in CDMA cellular systems as a result of interference reduction by introducing two-hop relaying. We propose an interference evaluation method using downlink geometry [45]. We then analyze the condition for the interference of uplink to be reduced by changing some single-hop transmissions to two-hop transmissions and propose to use the route with the maximum amount of interference reduction as a route selection criterion. By using this criterion, we also propose an effective routing algorithm for two-hop CDMA cellular systems with the aim of enhancing the system capacity.

The remainder of this chapter is organized as follows. In Section 5.1, we describe the system design of CDMA cellular systems. In Section 5.2, we analyze the condition for the interference to be reduced by introducing two-hop relaying. In Section 5.3, we describe the proposed two-hop relaying method. In Section 5.4, we report the performance of two-hop cellular systems. Section 5.5 concludes this chapter.

5.1 CDMA Cellular System

In this section, we describe design issues in CDMA/FDD single-hop cellular systems.

We describe the design method of the uplink and downlink separately because in CDMA cellular systems, the uplink and downlink have different characteristics. In uplink, BS receives signals transmitted from lots of MS's simultaneously. On the contrary in downlink, many MS's receive orthogonally coded signals transmitted from BS.

5.1.1 Near-Far Problem and Transmit Power Control

We now consider applying CDMA techniques in cellular systems. In uplink, the signals transmitted from each MS propagate through different channels. When multiple MS's transmit with the same power, the performance of CDMA systems suffers from the near-far problem, where MS's that are closed to the BS can cause a significant interference to the reception from MS's located far away from the BS.

To overcome the near-far problem, transmit power control is required to keep all MS's signals at the same level at the BS. It has been reported that the distribution of power control error can be approximated by log-normal distribution, and power control error with a standard deviation of 1 dB can reduce the capacity of the system to about half [60, 61]. Therefore, tight transmit power control is essential in CDMA cellular systems in order to optimize the bandwidth utilization.

5.1.2 Capacity in Uplink

In uplink, the capacity depends on the received power at BS, which is controlled to maintain a certain level of quality through transmit power control by MS's. Consider a single isolated cell, i.e. there is no inter-cell interference. We assume that there are N users using the same services. Let $(E_b/I_0)_{req}$ denote the received E_b/I_0 required to achieve the quality of service, let R_b (bps) denote the bit rate of information, let

R_c denote the chip rate, let N_0 (W/Hz) denote the thermal noise density taking into account the noise factor of the receiver. To maintain the required quality, the received E_b/I_0 should satisfy the following equation.

$$\frac{E_b R_b G_p}{E_b R_b (N-1) + N_0 R_c} = (E_b/I_0)_{req}$$

where $G_p = R_c/R_b$. Solving the above equation for N, we get

$$N = \frac{G_p}{(E_b/I_0)_{req}} + 1 - \frac{N_0 G_p}{E_b}. \tag{5.1}$$

We consider the extreme case where the transmit power is unlimited.

$$C_0 = \lim_{E_b \to \infty} N = \lim_{E_b \to \infty} \left(\frac{G_p}{(E_b/I_0)_{req}} + 1 - \frac{N_0 G_p}{E_b} \right) \tag{5.2}$$

$$= \frac{G_p}{(E_b/I_0)_{req}} + 1 \tag{5.3}$$

where marginal capacity C_0 is called as pole capacity.

Now we introduce interference margin η to evaluate the capacity under the condition that the transmit power is limited. Interference margin η is defined as

$$\eta = \frac{E_b R_b N + N_0 R_c}{N_0 R_c} \tag{5.4}$$

and it indicates the total amount of interference power compared to the thermal noise. Substituting the above equation into Eq. (5.1), we get

$$C = N|_\eta = \left(\frac{G_p}{(E_b/I_0)_{req}} + 1 \right) \left(1 - \eta^{-1}\right) = C_0 \left(1 - \eta^{-1}\right). \tag{5.5}$$

We can understand from the above relationship, a larger η leads to a larger capacity C. However, this implies that MS's require large transmit power. Therefore, there is a tradeoff between the capacity and the transmit power of MS's.

Next, we evaluate the capacity under multi-cell environment. Let F denote the ratio of inter-cell interference power and intra-cell interference power. The capacity can be

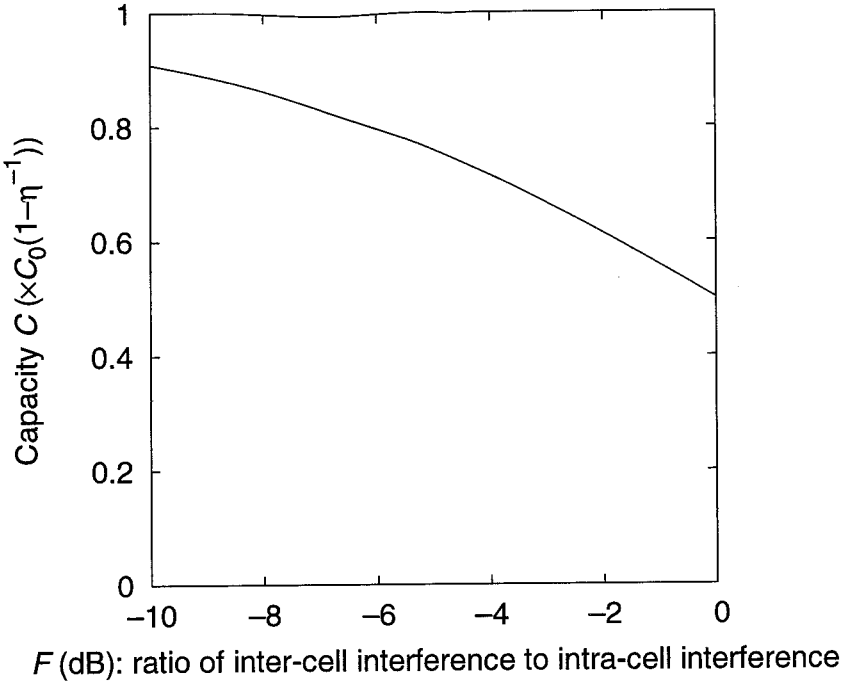

Figure 5.1: Dependence of capacity on ratio of inter-cell interference to intra-cell interference.

evaluated in the same way as in a single-cell environment.

$$C = \left[\frac{G_{\mathrm{p}}}{(E_{\mathrm{b}}/I_0)_{\mathrm{req}}} + 1\right] \frac{1}{1+F}\left(1-\eta^{-1}\right) = C_0 \frac{1-\eta^{-1}}{1+F}. \tag{5.6}$$

The value of the parameter F is affected by many factors such as the path loss model, the standard deviation of shadowing, and so on. Assuming the standard conditions in urban districts, it is reported that the value of F is around 0.7 [44]. Figure 5.1 shows the dependence of the capacity on the parameter F. We see that if the parameter F is reduced, the capacity C can be increased.

5.1.3 Capacity in Downlink

In downlink, the total transmit power of BS is a resource to be shared among all MS's. Consider the situation where a certain MS receives a channel transmitted from J BS's. We assume that every BS transmits the channel with the same unit power (1 W). Let

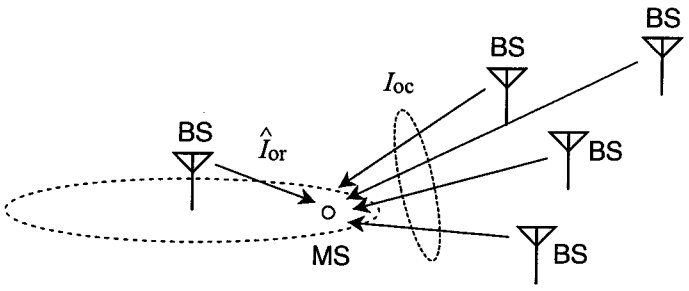

Figure 5.2: Downlink interference from the BS communicating with the MS, $\widehat{I}_{\text{or}}$, and from the other BS's, I_{oc}.

$r_1, r_2, \ldots, r_J$ represent the received power at the MS in descending order. Let P_{total} be the total transmit power of each BS and let ξ be the proportion of power allocated to the subject channel in the total transmit power P_{total}. To maintain the required quality, the received E_{b}/I_0 should satisfy the following equation.

$$r_1 \xi P_{\text{total}} \left[\frac{1}{G_{\text{p}}} \left(r_1 P_{\text{total}} \gamma + \sum_{j=2}^{J} r_j P_{\text{total}} \right) + N_0 R_{\text{b}} \right]^{-1} = (E_{\text{b}}/I_0)_{\text{req}} \tag{5.7}$$

where γ is an orthogonality factor ($0 \leq \gamma \leq 1$) to reflect the reduction of intra-cell interference by using the orthogonal codes.

Now we introduce geometry g [45] to represent location-dependent interference. Geometry is defined as

$$g = \frac{\widehat{I}_{\text{or}}}{I_{\text{oc}} + N_0} \tag{5.8}$$

where $\widehat{I}_{\text{or}}$ is the total received power density at MS in all code channels from the BS to which the MS belongs, and I_{oc} is the total received power density at MS from all other BS's as shown in Figure 5.2. The value of geometry g is used to express the difference in the amount of interference, which depends on the location of the MS and g increases as the MS comes closer to the BS. Substituting Eq. (5.8) into Eq. (5.7) and solving for ξ, we get

$$\xi = \frac{(E_{\text{b}}/I_0)_{\text{req}}}{G_{\text{p}}} \left(\gamma + \frac{1}{g} \right). \tag{5.9}$$

Assuming that βP_{total} $(0 \leq \beta \leq 1)$ is shared by each MS except for the control channels, such as broad cast information, paging information and so on. The capacity C can be approximated by

$$C = \beta / E[\xi] \tag{5.10}$$

where $E[\cdot]$ represents the ensemble mean [44].

5.1.4 Admission Control in Uplink

In CDMA cellular systems, multiple MS's share the same frequency band and each signal is multiplexed statistically. As described in Section 5.1.2, the user capacity of CDMA is essentially limited by the total level of co-channel interference arising from the simultaneous utilization of the radio channel by several users. A call admission control thus plays a very important role in CDMA cellular systems to guarantee a certain level of the QoS because it directly controls the number of active users. In this scheme, a new call is accepted so long as the total interference observed by the BS does not exceed a preset interference threshold, η, where η is defined as $\eta = I_{0,\text{req}}/N_0$, and $I_{0,\text{req}}$ is the maximum total acceptable interference density [62, 63].

5.2 Analysis of Uplink Interference Reduction by Introducing Two-hop Relaying

In this section, we analyze the condition for the interference to be reduced by changing some single-hop transmissions to two-hop transmissions. Figure 5.3(a) shows the total received power in uplink of CDMA single-hop cellular systems. Introduction of two-hop transmission with minimum total transmit power criterion [42] can reduce the total received power as shown in Figure 5.3(b). However, this interference reduction does not necessarily enhance the capacity because these figures are calculated based on the

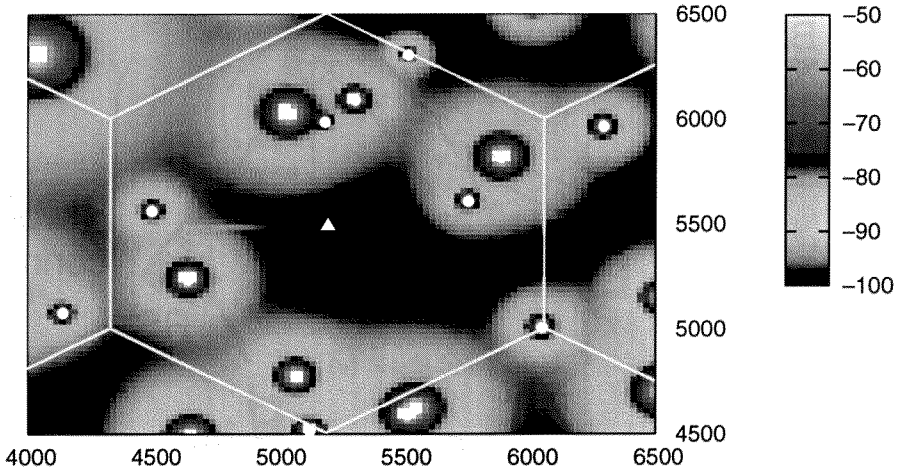

(a) Single-hop systems.

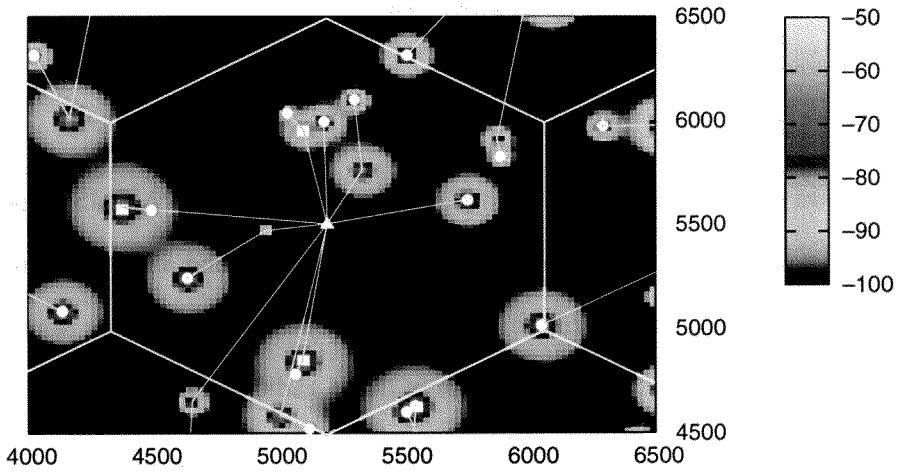

(b) Two-hop systems (minimum total power criterion).

Figure 5.3: Total received power in uplink of CDMA cellular systems.

same number of MS's and additional call can increase the interference. In addition, the set of active MS's can change as time passes. Therefore, the best route at the start of transmission may cause excessive interference to new active MS's.

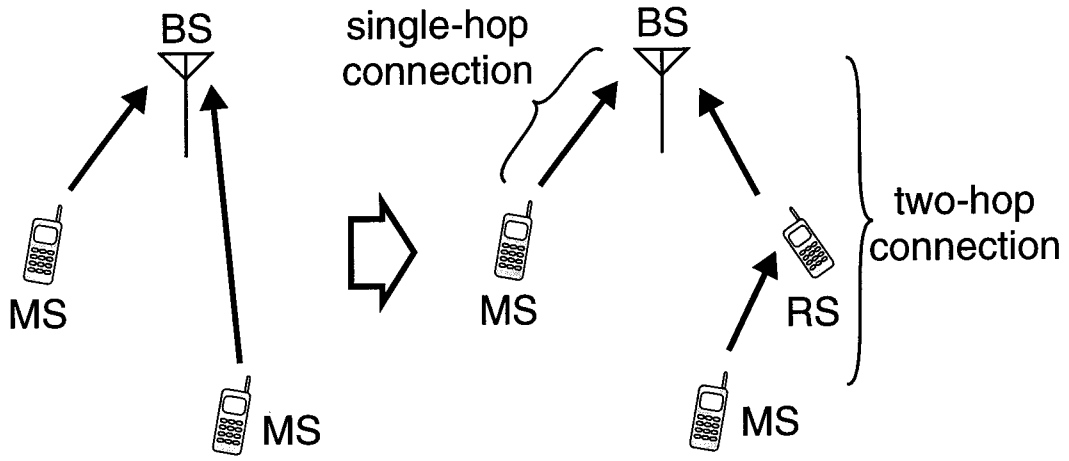

(a) Single-hop system.

(b) Two-hop system.

Figure 5.4: Single-hop and two-hop CDMA cellular systems.

5.2.1 Underlying Assumptions

Figure 5.4 shows single-hop and two-hop CDMA cellular systems. All MS's are assumed to communicate with BS. In two-hop cellular systems, an MS and a BS can communicate with each other by using an intermediate MS as a repeater. An MS is assumed to be able to relay only one signal. An MS that acts like a radio repeater is called a relaying station (RS).

In this chapter, we deal with uplink capacity of CDMA/FDD (frequency division duplex) systems. In order to enhance spectrum efficiency, the same frequency band that is pre-allocated is reused for relaying. In this section, an RS is assumed to be able to receive a signal from an MS and relay it to the BS simultaneously for the ease of analysis. More details and implementations are discussed in Section 5.3.1.

5.2.2 Intra-cell Interference in Two-hop Cellular Systems

First, we consider single-hop cellular systems as shown in Figure 5.5(a); there are N MS's (MS 1 to MS N) transmitting a signal to BS i. The interference power at BS i,

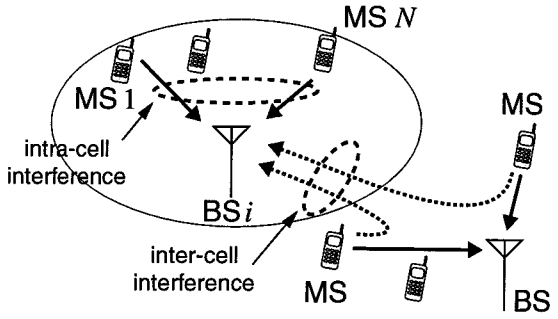

(a) Single-hop system.

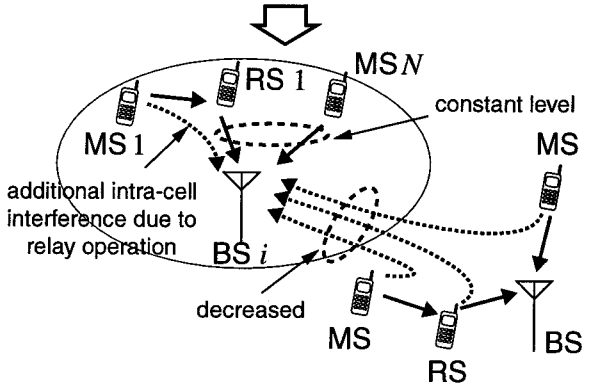

(b) Two-hop system.

Figure 5.5: Interference in uplink frequency.

$I_{1\text{hop}}$, can be expressed as follows:

$$I_{1\text{hop}} = I_{\text{intra},1\text{hop}} + I_{\text{inter},1\text{hop}} \tag{5.11}$$

$$I_{\text{intra},1\text{hop}} = \sum_{m=1}^{N} P_{\text{M}m} \tag{5.12}$$

where $I_{\text{intra},1\text{hop}}$ and $I_{\text{inter},1\text{hop}}$ are intra-cell interference and inter-cell interference, respectively. $P_{\text{M}m}$ denotes the received power at BS i from MS m. In CDMA systems, transmit power control is inevitable because of the well-known near-far problem. Therefore, we assume perfect power control from the MS's, i.e., all signals arrive at the BS with equal power S. For this reason, the interference power received by the BS from

each MS is fixed. In this case, Eq. (5.12) is reduced to:

$$I_{\text{intra,1hop}} = \sum_{m=1}^{N} P_{\text{M}m} = NS. \tag{5.13}$$

Second, we consider two-hop cellular systems as shown in Figure 5.5(b), where M MS's in the cell (MS 1 to MS M) have two-hop links. In case RS m relays a signal from MS m, the interference level at BS i, I_{2hop}, can be written as:

$$I_{\text{2hop}} = I_{\text{intra,2hop}} + I_{\text{inter,2hop}} \tag{5.14}$$

$$I_{\text{intra,2hop}} = \sum_{m=1}^{M} (P'_{\text{M}m} + P'_{\text{R}m}) + \sum_{m=M+1}^{N} P_{\text{M}m} \tag{5.15}$$

where $P'_{\text{R}m}$ and $P'_{\text{M}m}$ are the received power at BS i from RS m and MS m, respectively. In case that MS m communicates with BS i via RS m, the interference power at BS i caused by RS m is the same as that caused by MS m in single-hop cellular systems as a result of power control, i.e., $P'_{\text{R}m} = P_{\text{M}m} = S$. Substituting this relationship into Eq. (5.15) yields:

$$I_{\text{intra,2hop}} = NS + \sum_{m=1}^{M} P'_{\text{M}m} > I_{\text{intra,1hop}}. \tag{5.16}$$

Therefore, the total intra-cell interference increases by introducing relaying. Consequently, in the single-cell environment, the two-hop relaying may not be helpful for capacity enhancement.

5.2.3 Inter-cell Interference in Single-hop Cellular Systems

Next, we evaluate interference at the BS taking into consideration inter-cell interference. When MS m transmits a signal to BS i as shown in Figure 5.6(a), the received power at BS i from MS m is expressed as:

$$P_{\text{M}m} = G_{mi} T_{\text{M}m} \tag{5.17}$$

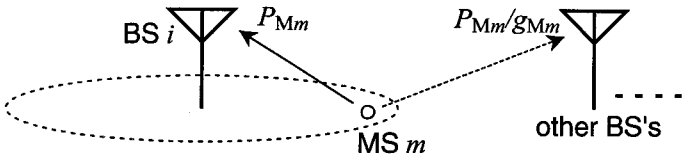

(a) Single-hop case.

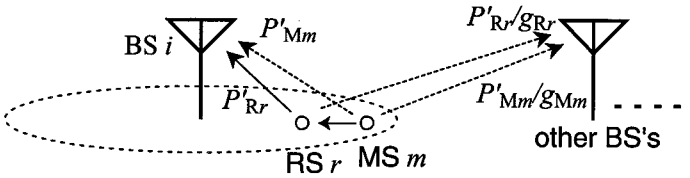

(b) Two-hop case.

Figure 5.6: Analysis of interference with geometry. P_{Mm}, P'_{Mm}, and P'_{Rr} represent the received power at the BS. As a result of power control, $P_{Mm} = P'_{Rr}$.

where G_{mi} is the power gain from MS m to BS i and T_{Mm} is the transmit power of MS m. In order to evaluate the interference power at the other BS's from MS m, it is necessary to measure the power gain from MS m to each BS.

On the contrary, the total inter-cell interference power received by all the other BS's is given by:

$$\sum_{j \neq i} G_{mj} T_{Mm} = P_{Mm} \Big/ \frac{G_{mi}}{\sum_{j \neq i} G_{mj}}. \tag{5.18}$$

To simplify this equation, we introduce downlink "geometry" [45] defined by

$$g = \widehat{I}_{or}/(I_{oc} + N_0) \tag{5.19}$$

In the following, we assume that the noise power density N_0 is small enough in comparison to I_{oc}. When MS m communicates with BS i, geometry of MS m can be approximately written as:

$$\begin{aligned} g_{Mm} &\simeq \widehat{I}_{or}/I_{oc} \\ &= \frac{G_{im} T_{Bi}}{\sum_{j \neq i} G_{jm} T_{Bj}} \end{aligned} \tag{5.20}$$

where $T_{\mathrm{B}i}$ is the total transmit power of BS i. We assume that the total transmit power of all BS's is kept constant, i.e., $T_{\mathrm{B}i} = T_{\mathrm{B}j}$, and we also assume that the difference between the power gain of uplink and downlink is negligible, i.e., $G_{mj} = G_{jm}$. Using these assumptions, Eq. (5.20) can be simplified as:

$$g_{\mathrm{M}m} = \frac{G_{mi}}{\sum_{j \neq i} G_{mj}}. \tag{5.21}$$

Substitution of this relationship into Eq. (5.18) yields:

$$\sum_{j \neq i} G_{mj} T_{\mathrm{M}m} = \frac{P_{\mathrm{M}m}}{g_{\mathrm{M}m}}. \tag{5.22}$$

Accordingly, the total interference power at all the other BS's can be expressed by fixed received power and geometry of the MS.

5.2.4 Inter-cell Interference in Two-hop Cellular Systems

Interference power of the two-hop case is considered as shown in Figure 5.6(b). In case RS r whose geometry is $g_{\mathrm{R}r}$ relays a signal from MS m, the total inter-cell interference power at all the other BS's from MS m and RS r is expressed as follows:

$$\frac{P'_{\mathrm{R}r}}{g_{\mathrm{R}r}} + \frac{P'_{\mathrm{M}m}}{g_{\mathrm{M}m}}. \tag{5.23}$$

Since intra-cell interference is increased by $P'_{\mathrm{M}m}$ as shown in Section 5.2.2, the total interference power at all the other BS's is expressed as follows:

$$\frac{P'_{\mathrm{R}r}}{g_{\mathrm{R}r}} + P'_{\mathrm{M}m}\left(1 + \frac{1}{g_{\mathrm{M}m}}\right). \tag{5.24}$$

Consequently, the condition for the interference to be reduced can be expressed as follows:

$$\frac{P_{\mathrm{M}m}}{g_{\mathrm{M}m}} > \frac{P'_{\mathrm{R}r}}{g_{\mathrm{R}r}} + P'_{\mathrm{M}m}\left(1 + \frac{1}{g_{\mathrm{M}m}}\right). \tag{5.25}$$

Therefore, in case an MS transmits via such an RS that satisfies the condition of (5.25), the total interference power at BS's is decreased compared to the case of using a single-hop transmission.

5.3 System Model

In this section, we describe features of two-hop cellular systems. First, in order to realize the assumptions in Section 5.2.1, frequency division is used. Next, a call admission control, which plays a very important role to guarantee a certain level of the QoS, is described. Next, on the basis of the above-mentioned analysis, a new route selection criterion is proposed to decrease interference. Finally, by using the call admission control and the proposed route selection criterion, a new routing algorithm with the aim of enhancing the capacity is proposed.

5.3.1 Frequency Division Relaying

In case the RS receives a signal from an MS and relays it to the BS at the same time by using the same frequency band, a part of the radio wave radiated from the transmitting antenna of the RS might be fed back to the antenna receiving the MS's signal. This might cause signal degradation. One of the solutions of this problem is to introduce an interference canceller in a portable radio station. However, it is difficult to realize it with a small-sized radio equipment. For this reason, to avoid the interference between first-hop (from MS to RS) transmission and second-hop (from RS to BS) transmission, a pair of frequency bands is assumed to be used for the uplink transmission.

In this case, a frequency band assigned to the first-hop transmission should be different from that assigned to the second-hop transmission. However, when one frequency band is always assigned to the first-hop transmissions and the other frequency band is always assigned to the second-hop transmissions, the interference may be concentrated on the latter frequency band. To solve this problem, upon each new admission request, the frequency whose co-channel interference level at the BS is smaller than the other frequency is assigned to the single-hop or the second-hop transmission and the other

frequency band is assigned to the first-hop transmission. RS is assumed to be able to transmit and receive signals simultaneously. In this case, the same end-to-end throughput is achieved for both single-hop and two-hop transmission.

5.3.2 Route Selection Criterion

Most of the routing protocols for the multihop cellular systems consider the shortest-path with the minimum total path loss [23] or the minimum total transmit power [42] as a route selection criterion. These route selection criteria are not necessarily appropriate for capacity enhancement because the interference at the BS's, which limits the user capacity, is not taken into consideration. In order to enhance the capacity, we propose to use the route with the maximum amount of total interference reduction at the other BS's as a route selection criterion.

If MS m transmits a signal via RS r, the amount of interference reduction can be written as:

$$\Delta I = \frac{P_{\mathrm{M}m}}{g_{\mathrm{M}m}} - \left[\frac{P'_{\mathrm{R}r}}{g_{\mathrm{R}r}} + P'_{\mathrm{M}m}\left(1 + \frac{1}{g_{\mathrm{M}m}}\right)\right]. \tag{5.26}$$

As a result of power control, the received power at BS i from RS r is almost the same as that from MS m in single-hop systems. This relationship can be written as: $P_{\mathrm{M}m} = P'_{\mathrm{R}r} = S$. In this case, Eq. (5.26) can be written as:

$$\begin{aligned}\frac{\Delta I}{S} &= \frac{1}{g_{\mathrm{M}m}} - \left[\frac{1}{g_{\mathrm{R}r}} + \frac{P'_{\mathrm{M}m}}{P_{\mathrm{M}m}}\left(1 + \frac{1}{g_{\mathrm{M}m}}\right)\right] \\ &= \frac{1}{g_{\mathrm{M}m}} - \left[\frac{1}{g_{\mathrm{R}r}} + \frac{T'_{\mathrm{M}m}}{T_{\mathrm{M}m}}\left(1 + \frac{1}{g_{\mathrm{M}m}}\right)\right]\end{aligned} \tag{5.27}$$

where $T'_{\mathrm{M}m}$ is the required transmit power of MS m in a two-hop case. In order that BS can centrally evaluate the amount of interference reduction to select a route, each MS sends its geometry in addition to its transmit power to the BS to which the MS belongs.

5.3.3 Routing Algorithm

Under light traffic load conditions, it is not necessary to decrease interference at the sacrifice of consuming the power of RS's. Therefore, at the start of the transmission, a single-hop transmission is used. When the traffic increases and, consequently, a new call request is blocked as a result of the admission control, the BS informs the BS's in the adjacent cells of the call blocking. Then, in order to decrease interference, each BS independently searches for a pair of one MS whose call is in progress and another MS that is neither transmitting nor relaying, and thus is able to play a role of an RS by finding such a pair maximizing Eq. (5.27). By this scheme, interference power at BS's may be decreased and more calls can be admitted.

In case all call requests can be admitted, the BS informs the BS's of the adjacent cells of no further necessity of two-hop relaying. Until the reception of this information, BS's repeat asking MS's to switch from single-hop to two-hop transmissions. An MS is assumed to be able to serve as an RS for only one MS and BS removes such an MS that is transmitting or relaying from the candidates of an RS. When an RS originates a new call, the two-hop transmission is returned to a single-hop transmission.

The interference power at nearby BS's can be decreased by this route selection criterion. However, in case frequency assignment described in Section 5.3.1 is adopted, MS's and RS's that share the same frequency channels interfere with each other. Particularly, when a new transmission severely interferes with the RS, the transmit power of the MS increases as a result of power control. This might cause serious interference to BS's. In order to avoid serious interference to BS's, when the amount of interference reduction expressed by Eq. (5.27) turns to negative, the MS selects the single-hop transmission to prevent excessive interference at BS's.

5.4 Computer Simulations

5.4.1 Simulation Parameters

The performances of the proposed route selection criterion and routing algorithm are evaluated using computer simulations assuming 7 hexagonal cells layout. Each cell is split into six sectors. The parameters assumed in computer simulations are listed in Table 5.1. BS's are arranged at the center of each cell and assumed to be equipped with sectorized directional antennas. MS's are assumed to be uniformly distributed in the cell and to be stationary throughout the simulation. Omnidirectional antennas are used for MS's. Interference is assumed to be equivalent to Gaussian noise over the signal bandwidth. Thermal noise is also considered at the receiver, which has a noise figure of 5 dB. The routing is assumed to be completed in advance of a transmission.

In order to implement frequency division relaying described in Section 5.3.1, two frequency bands are necessary. To make a fair comparison, two frequency bands are used for both the single-hop system and the two-hop system, and throughput of these systems are compared in terms of spectral efficiency (bit/sec/Hz).

The data are assumed to be generated according to an exponential distribution for interarrival-time and a log-normal distribution for data size, and divided into packets. The average data size is set to 4,400 bytes and the average interarrival-time is used to change the system load. The packet length is fixed to 80 bits.

In CDMA systems, tight transmit power control is inevitable to keep all MS's signals at the same level at the BS receiver because of the well-known near-far problem. In addition to this, by reducing transmit power from an MS to an RS while maintaining the E_b/I_0 requirements at the BS, the interference at the BS can be further reduced, where E_b/I_0 is signal energy per bit-to-interference and noise power spectral density ratio. Therefore, transmit power control is applied to all the packets to satisfy the E_b/I_0

Table 5.1: Parameters assumed in computer simulations.

Parameters	Values
Number of cells	7
Cell radius	1000 m
Number of MS's	200 /cell
BS total Tx power	30 dBm
MS max Tx power	20 dBm
Antenna gain	16 dBi (BS), 0 dBi (MS)
Thermal noise density	−174 dBm/Hz
Noise figure	5 dB
Path loss (BS-MS)	Xia's vehicular model [48]
(MS-MS)	Milstein's microcell model [51]
Shadowing	Log-normal distribution (σ_0 =8 dB)
Packet length	80 bits
Carrier frequency	2 GHz
Bandwidth	3.84 MHz × 2
Spreading factor	32
Required E_b/I_0	5 dB
Interference margin η	6 dB

target at the start of each packet transmission. Receiving a packet will fail if the received power is below the required E_b/I_0. In this case, the lost packet is retransmitted after the power is controlled unless the amount of interference reduction ΔI becomes negative.

Wireless communication links are severely influenced by various radio propagation effects. Therefore, prediction of radio signal propagation in each of the specific radio environments is essential to design the system. Propagation between BS and MS is assumed to be modeled by Walfisch-Ikegami model [48]. Propagation between RS and MS is assumed to be modeled by a two-ray model, which consists of a direct path and single ground bounce [51]. The MS is connected at all times to the best BS, i.e. the one that gives the least attenuation due to propagation loss.

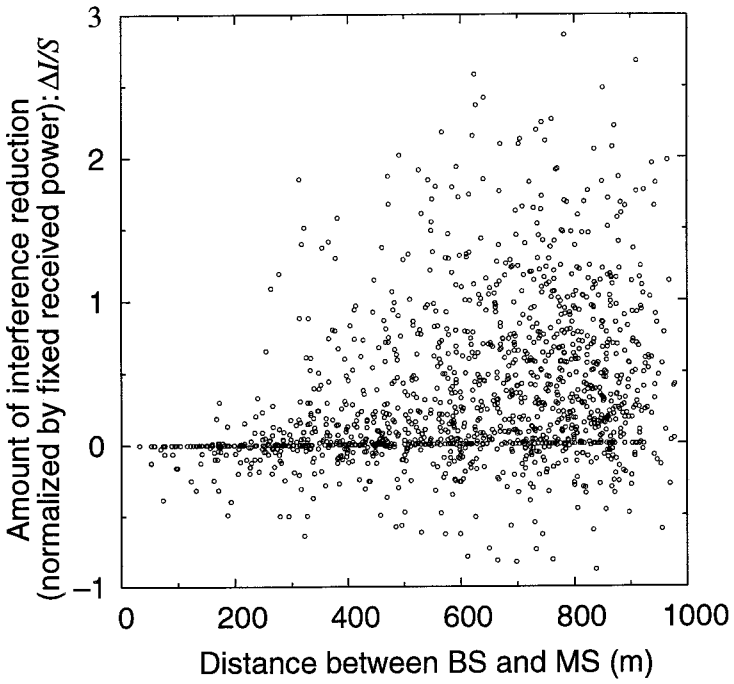

Figure 5.7: Amount of interference reduction by using minimum power criterion.

5.4.2 Simulation Results

Interference Reduction under Low Traffic Load Conditions

In this section, we evaluate the interference reduction ability of the minimum total transmit power criterion (hereinafter referred to as "minimum power criterion") and the proposed interference reduction criterion. For the ease of analysis, only one MS is assumed to be transmitting, i.e., there is no co-channel interference.

Figures 5.7 and 5.8 show the amount of interference reduction $\Delta I/S$ of each MS versus the distance between BS and MS using the minimum power criterion and the proposed interference reduction criterion, respectively. Figure 5.7 shows that some MS's have negative $\Delta I/S$, and it means that these MS's increase interference though the total radiated power is decreased by changing a single-hop transmission to a two-hop transmission. Therefore, the minimum power criterion does not always lead to interference

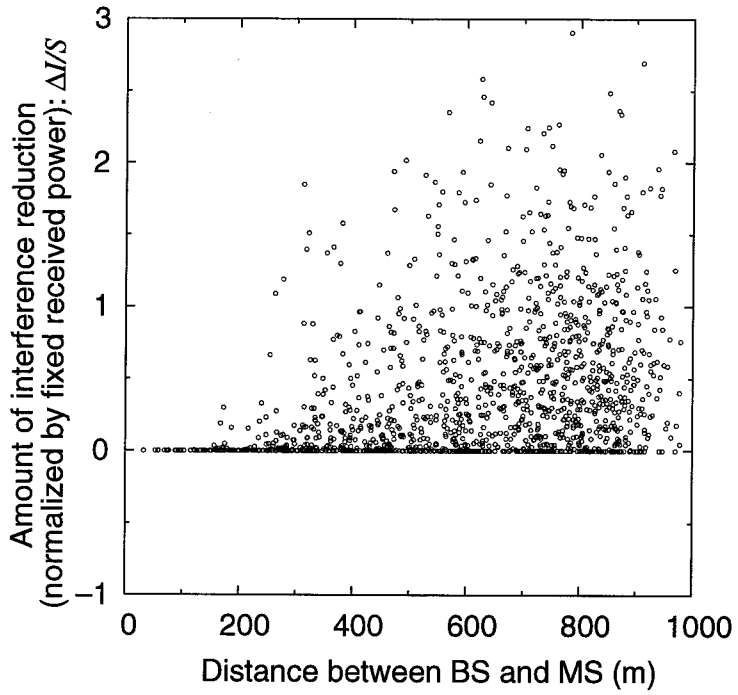

Figure 5.8: Amount of interference reduction by using proposed interference reduction criterion.

reduction. On the other hand, Figure 5.8 shows that no MS has negative $\Delta I/S$ according to the proposed criterion.

Figure 5.9 shows the average interference power at the other BS's versus the distance between BS and MS for the two route selection criteria. The interference power at the other BS's of the single-hop transmission and the two-hop transmission are described in Eqs. (5.22) and (5.24), respectively. In case that MS is located near BS, the minimum power criterion increases interference despite of using a two-hop transmission. This is because of the additional intra-cell interference due to relay operation described in Section 5.2.2 since these MS's are far from the other BS's.

Increase of interference by the minimum power criterion can be explained by Eq. (5.26) as follows. One case is that an MS is located near the BS, and such an RS that is located also near the BS will be selected. It means that geometry of both the MS and the RS is

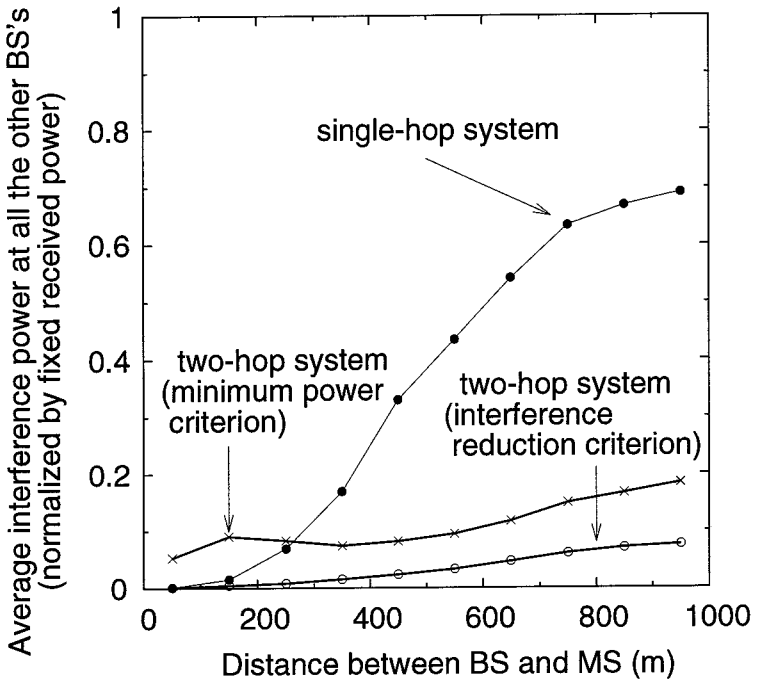

Figure 5.9: Average interference of two route selection criteria as a function of the distance.

large. In this case, Eq. (5.26) can be written as:

$$\lim_{g_{\mathrm{M}m}, g_{\mathrm{R}r} \to \infty} \Delta I = -P'_{\mathrm{M}m} < 0. \tag{5.28}$$

Therefore, interference is increased by two-hop relaying. However, since the MS that increases interference exists throughout a cell as shown in Figure 5.7, the reason why interference increases is not unique. In order to explore another reason, the case that the MS is located on the fringe of its cell is considered. In this case, large transmit power reduction might be achieved according to the minimum power criterion, i.e. $T'_{\mathrm{M}m}/T_{\mathrm{M}m} \ll 1$, and Eq. (5.27) can be written as:

$$\lim_{T'_{\mathrm{M}m}/T_{\mathrm{M}m} \to 0} \Delta I/S = \frac{1}{g_{\mathrm{M}m}} - \frac{1}{g_{\mathrm{R}r}}. \tag{5.29}$$

Therefore, selecting an RS whose geometry is smaller than that of the MS increases interference.

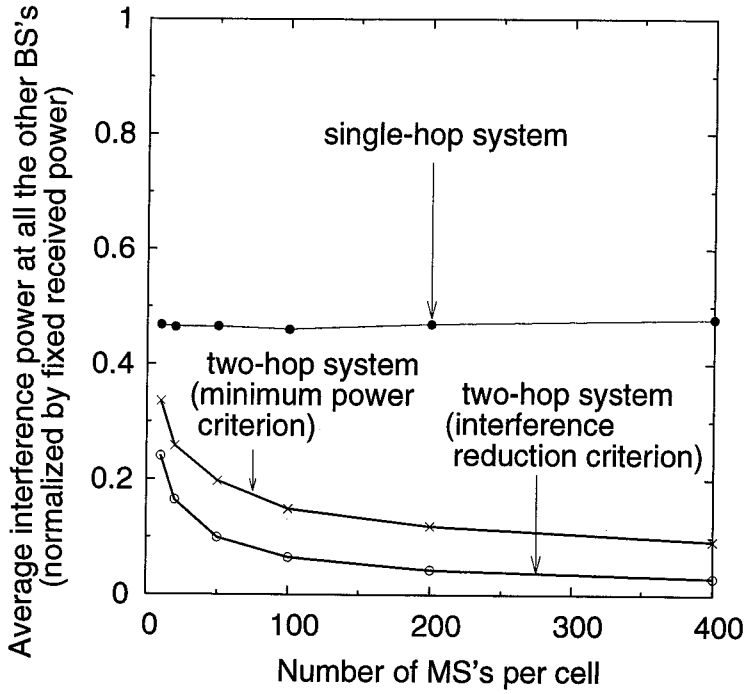

Figure 5.10: Average interference of two route selection criteria as a function of the number of MS's.

The performances of these two-hop systems can be dependent on the number of MS's. Figure 5.10 shows the average total interference power at the other BS's versus the number of MS's for the two route selection criteria. When the number of MS's increases, the number of candidates for RS increases, leading to lower interference in two-hop cellular systems. Consequently, it is shown that the proposed interference reduction criterion is more effective than the conventional minimum power criterion in respect of the amount of interference reduction.

Capacity Evaluation of Two-hop Systems Using the Proposed Routing Algorithm

In this section, we evaluate the system capacity of two-hop cellular systems using the proposed routing algorithm. Figure 5.11 shows the capacity per base station versus the system load for single-hop and two-hop cellular systems. The capacity of single-hop

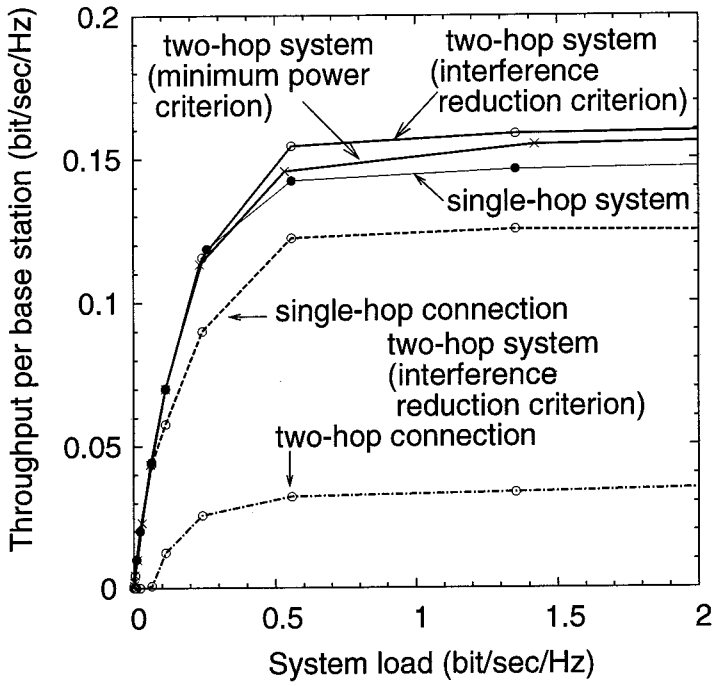

Figure 5.11: Throughput per base station as a function of system load for single-hop and two-hop cellular systems.

cellular systems is independent of the arrangement of MS's. In contrast to this, the capacity of the two-hop systems with the interference reduction criterion is increased by about 10% constantly owing to the change of network topology.

In spite of allowing two-hop relaying, some MS's transmit signals using single-hop transmissions. Therefore, the throughput of data transmitted via single-hop transmissions and that transmitted via two-hop transmissions are also presented in Figure 5.11. Since the end-to-end throughput of single-hop transmissions and that of two-hop transmissions are the same, the number of active MS's is expected to be in proportion to the throughput. Therefore, one-third MS's transmit a signal using two-hop transmissions under heavy traffic load conditions.

Figure 5.12 shows the blocking probability. Though the blocking probability increases along with the increase of traffic load as a result of the call admission control, two-hop

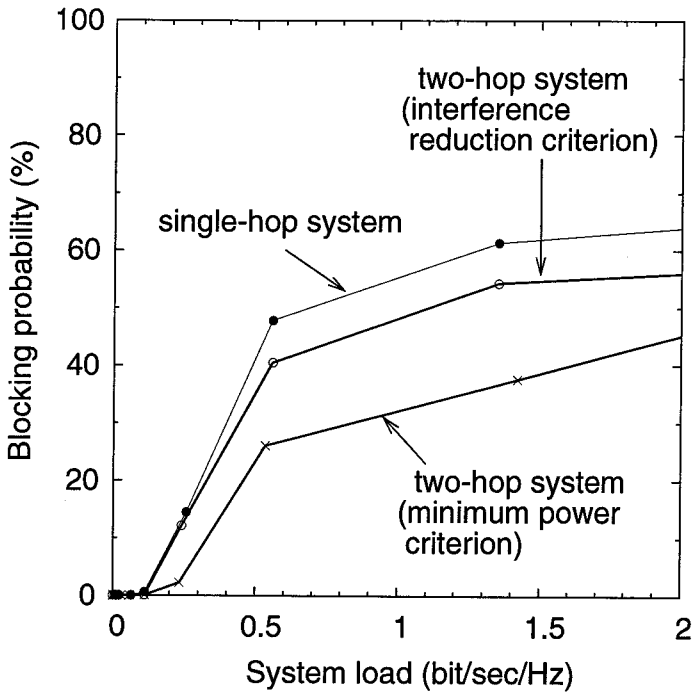

Figure 5.12: Blocking probability as a function of system load for single-hop and two-hop cellular systems.

relaying may mitigate blocking owing to interference reduction.

Figures 5.11 and 5.12 also show the performance with the minimum power criterion as well as that with the interference reduction criterion. The blocking probability with the minimum power criterion is smaller than that with the interference reduction criterion. On the other hand, throughput with the minimum power criterion is smaller. This is because some MS's increase the interference by using two-hop relaying and, consequently, a failure occurs on packet reception. Therefore, under heavy traffic conditions, the proposed interference reduction criterion is more effective to enhance the capacity.

5.5 Summary

In this chapter, we showed that the two-hop relaying might not be helpful for capacity enhancement in the single-cell environment. With the aim of evaluating inter-cell interfer-

ence, the downlink geometry was introduced. Based on these analysis, we then proposed a new route selection criterion that maximizes the amount of interference reduction. Simulation results demonstrate that the proposed criterion outperform the conventional criterion minimizing the total transmit power. In order to enhance the capacity as a result of this interference reduction, we also proposed a new routing algorithm. In this algorithm, when a call request is blocked as a result of the call admission control, BS's in the adjacent cells ask to switch MS's from a single-hop transmission to a two-hop transmission. Simulation results reveal that the capacity of CDMA cellular systems can be increased by 10% owing to the proposed routing algorithm.

Chapter 6

Game-Theoretic Analysis for Decentralized Adaptive Route Selections

In ad hoc networks, the decentralization and distribution of control mean that such networks are inherently scalable. However, the conflict among multiple nodes due to selfishness cannot always achieve throughput near the capacity estimated in previous papers [20, 26] and Chapter 3.

In this chapter, we consider a scenario where there are multiple source-destination pairs. In contrast to the previous chapters, each source node is selfish and attempts to select a route to the destination so as to enhance own throughput. We attack this decentralized adaptive route selection (DARS) problem. This problem is similar to that defined by Eidenbenz et al. [47]. However, the focus here is not connectivity but the capacity of bandwidth-constrained wireless networks.

We first define this problem as a DARS game in which the set of possible routes is a set of strategies and the resultant throughput is a payoff. We apply equilibrium analysis to the DARS game. Using the concept of Nash equilibria, we classify the many possible node arrangements according to the number of equilibria: none, a unique equilibrium, and multiple equilibria. We show that even with perfect information such as path gain

Table 6.1: Parameters used in evaluations.

Parameters	Values
System area	$20\,\mathrm{m} \times 20\,\mathrm{m}$
Bandwidth W	$1\,\mathrm{MHz}$
Noise power spectral density ν	$10^{-15}\,\mathrm{W/Hz}$
Carrier frequency	$2\,\mathrm{GHz}$
Antenna gain	$0\,\mathrm{dBi}$
Path loss	Free space

between every two nodes except for knowledge of the other nodes' routes, each source node cannot determine the best route in terms of the achievable end-to-end throughput. We then compare the capacity with centralized control and the achievable throughput with decentralized control. Next, we consider a scenario where each source node attempts to select transmit power as well as a route.

The remainder of this chapter is organized as follows: In Section 6.1, we discuss a system model. In Section 6.2, we introduce the normal form game and define the DARS game. In Section 6.3–6.4, we investigate the Nash equilibria of the DARS game. We also analyze the achievable throughput of a network under DARS and compare it to the capacity region [26]. Finally, in Section 6.5 we give some final remarks.

6.1 Wireless Ad Hoc Network Model

Table 6.1 summarizes the parameters we used in our evaluation. M nodes are uniformly and independently distributed in a two-dimensional square area and are stationary throughout the evaluation. We assume that each node can only be transmitting or receiving at a given time and can serve as a repeater for only one other source node. Free space path loss is assumed between any two nodes. The effects of shadowing and multipath fading are not considered for the sake of simplicity, as has been done in [7]. Omnidirectional antennas are used for the nodes. Under these assumptions, the power

gain between nodes i and j is given by

$$G_{ij} = \left(\frac{\lambda}{4\pi d_{ij}}\right)^2, \tag{6.1}$$

where λ represents the wavelength and d_{ij} represents the distance between nodes i and j.

6.1.1 Rate Adaptation and Resulting Physical Layer Bit Rate

Let P_i denote the transmit power of node i, so that node j receives a signal with power $G_{ij}P_i$. Let $\mathcal{T}$ be the subset of nodes simultaneously transmitting at any given time. When node j ($\notin \mathcal{T}$) is receiving a signal from node i ($\in \mathcal{T}$), the received carrier-to-interference plus noise ratio (CINR) at node j is

$$\gamma_{ij} = \frac{G_{ij}P_i}{\nu_j W + \sum_{k\in\mathcal{T}, k\neq i} G_{kj}P_k}, \tag{6.2}$$

where ν_j represents the noise power spectral density at receiving node j and W represents the bandwidth. All interference signals are assumed to be equivalent to additive white Gaussian noise over the signal bandwidth.

We assume that transmitting node i adjusts transmission rate r_{ij} based on the received CINR γ_{ij}, and that the signal can be received with a negligible probability of error at receiving node j. Shannon capacity is used as the specific dependence of r_{ij} on γ_{ij} as used in [26]:

$$r_{ij} = W \log_2(1 + \gamma_{ij}). \tag{6.3}$$

6.1.2 Time and Packet Scheduling

The achievable throughput at the MAC layer in wireless networks with only single-hop transmission depends on the physical layer bit rate, the efficiency of the MAC layer, the size of the packets, and the number of nodes in the network [64, 65]. Since the

main purpose of this chapter is to investigate the performance of the DARS game, no coordinated time and packet scheduling among nodes is assumed.

In order to evaluate the throughput of wireless networks with multihop transmission, we use the average end-to-end throughput assuming that the data size of every packet is equal and that as soon as the destination node receives a packet, the source node transmits the next packet. We refer to this throughput as the capacity of the network for the given packet scheduling.

6.2 Game-Theoretic Framework

6.2.1 Normal Form Game

A game in normal form has three aspects. First, there is a set of players, $\mathcal{I}$, which we take to be the finite set $\{1, 2, \ldots, I\}$. Second, there is a set of pure strategies, S_i ($i \in \mathcal{I}$), available to each player. Finally, there is a set of payoff functions, u_i. Each player has a preference for an outcome. The payoff function represents the player's preference and maps the player's anticipated outcome given his or her selected strategy to a real number. In the game, each player's objective is to select a strategy, $s_i \in S_i$, so as to maximize his or her own payoff function. A mixed strategy for player i is a probability distribution over pure strategies S_i. In this chapter, unless otherwise noted, we assume pure strategies since mixed strategies do not seem reasonable in studies of stability (similar arguments are presented in [47, 66]).

A fundamental solution concept in game theory is a Nash equilibrium, which is a point where neither player gains by changing his or her strategy unilaterally, so that neither player has an incentive to deviate [31]. A pure strategy profile, $\boldsymbol{s}^* = ({s_1}^*, \ldots, {s_I}^*)$, is a Nash equilibrium if, for all players i,

$$u_i(\boldsymbol{s}^*) \geq u_i\left({s_1}^*, \ldots, {s_{i-1}}^*, s_i, {s_{i+1}}^*, \ldots, {s_I}^*\right) \qquad \forall s_i \in S_i. \tag{6.4}$$

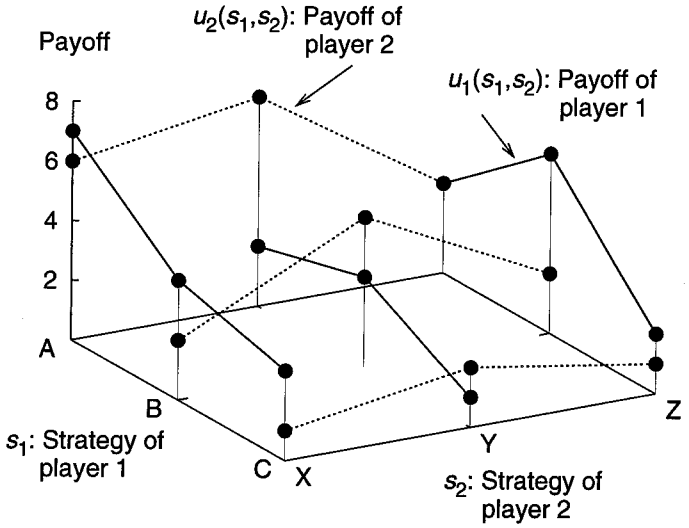

Figure 6.1: Example of a two-player game.

In particular, for a two-player game, a pure strategy profile is a Nash equilibrium if

$$\begin{aligned} u_1\left(s_1{}^*, s_2{}^*\right) &\geq u_1\left(s_1, s_2{}^*\right) && \forall s_1 \in S_1 \\ u_2\left(s_1{}^*, s_2{}^*\right) &\geq u_2\left(s_1{}^*, s_2\right) && \forall s_2 \in S_2. \end{aligned} \tag{6.5}$$

A two player game in normal form can be depicted as Figure 6.1. Players 1 and 2 have three strategies each: A, B, C and X, Y, Z, respectively. Solid lines in Figure 6.1 represent player 1's payoff for the corresponding strategy profile; dashed lines represent player 2's payoff. For example, if player 1 selects strategy A and player 2 selects strategy X, payoff of players 1 and 2 become 7 and 6, respectively. However, player 2 will not select X because Y gives a higher payoff to player 2 than X or Z. Furthermore, when player 1 knows that player 2 will select Y, B is better than A or C. At this strategy profile (B, Y), neither player gains by changing his or her strategy unilaterally. Therefore, this profile is a Nash equilibrium. This example suggests that the global optimal profile is not always selected.

6.2.2 Decentralized Adaptive Route Selection Game

Let us assume source nodes are players in a game. We define a DARS game in which each source node has to select a route to the destination node so that the maximum end-to-end throughput is achieved. Therefore, the set of all possible single-hop and multihop routes is a set of strategies.

We assume that the source nodes have perfect knowledge of the power gain between each transmitting and receiving node pair, the transmit power of each transmitting node, and the noise power spectral density at each receiving node. This assumption is necessary for comparing the achievable throughput under decentralized scheduling and the capacity under centralized scheduling with perfect knowledge. Under this assumption, each source node can estimate the end-to-end throughput of all source nodes as a consequence of their route selections.

6.3 Behavior of DARS Game and Resulting Throughput

In this section, we will demonstrate that it is useful to classify the network topologies based on the number of pure strategy Nash equilibria. The transmit power and power spectral density of every node is assumed to be equal to P and ν, respectively. The first three subsections describe how the DARS game behaves in a network topology with a unique equilibrium, without equilibria, and with multiple equilibria. We estimate network throughput under equilibrium conditions (hereinafter referred to as "equilibrium throughput"). This equilibrium throughput is a reasonable payoff as a result of the DARS game. We then compare the equilibrium throughput and capacity under the given packet scheduling.

For the sake of simplicity, we consider the case where there are only two source-destination pairs and the number of hops is limited to two. This is a reasonable assumption because the purpose of this chapter is to evaluate the impact of the DARS

game among multiple decision-making entities in wireless ad hoc networks. Under this assumption, Nash equilibria can be found using Eq. (6.5). Since we are interested in the maximum throughput, the control overhead associated with route selection is not taken into account.

6.3.1 Network Topology with a Unique Equilibrium

Figure 6.2(a) shows an example network in which the DARS game has a unique equilibrium. In this network, there are two communication pairs: source node 1 to destination node 2 and source node 3 to destination node 4. The number of equilibria depends on the transmit power of the nodes as well as on their spatial arrangements. We will discuss the transmit power dependence of the number of equilibria later in this section.

For given source node N_S and destination node N_D, let $(N_S \rightarrow N_R \rightarrow N_D)$ represent multihop transmission using node N_R as a relaying node. Figure 6.2(a) shows that source node 1's equilibrium route is $(1 \rightarrow 13 \rightarrow 2)$ and source node 3's equilibrium route is $(3 \rightarrow 14 \rightarrow 4)$.

Every point in Figure 6.2(b) represents a possible combination of the throughput of source node 1 and that of source node 3. Particularly, each point on the axes corresponds to the throughput of individual source-destination pairs. Each curve represents a two-dimensional slice of the capacity region [26] for the following three particular strategies.

- Single-hop transmission without spatial reuse
- Multihop transmission without spatial reuse
- Multihop transmission with spatial reuse

The capacity region is a multidimensional region that contains all achievable combinations of throughput between the nodes in the network. If centralized time scheduling can be used, changing the time devoted to the respective route profiles enables different

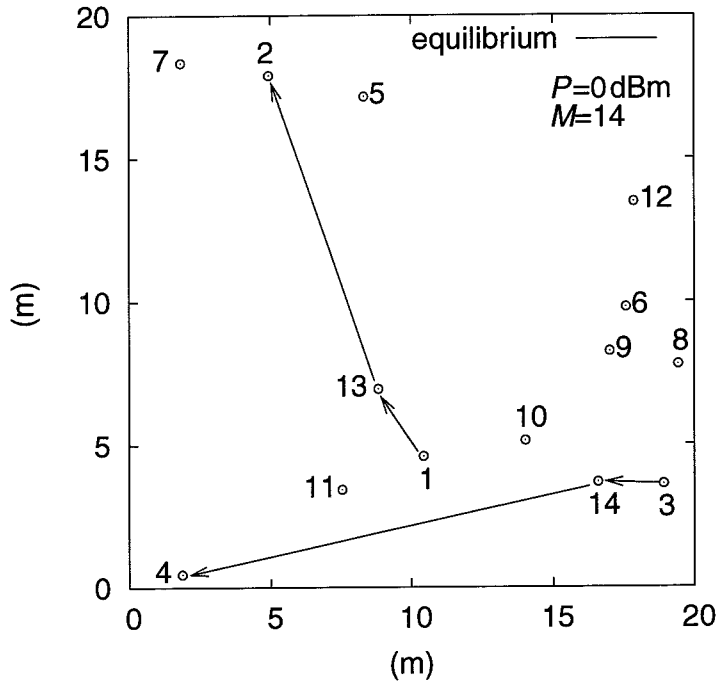

(a) Network topology.

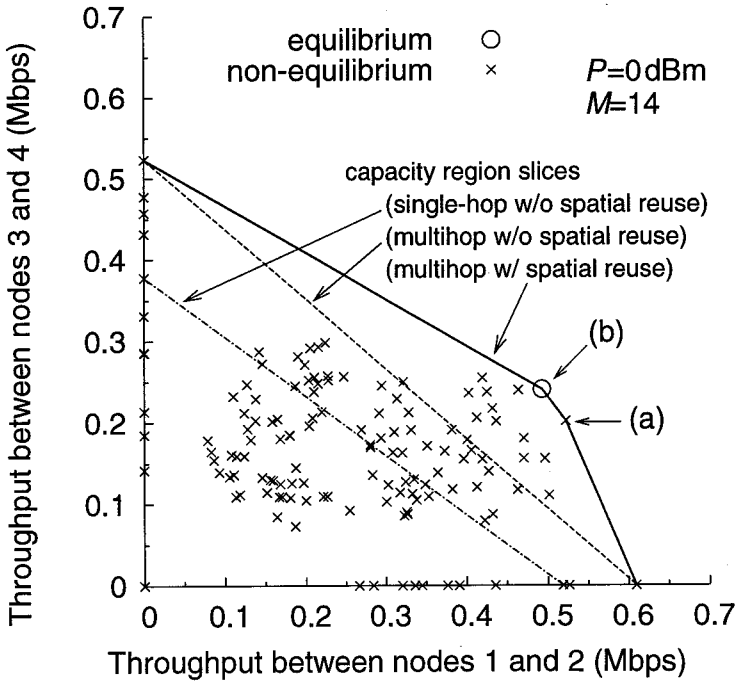

(b) Capacity region and equilibrium throughput.

Figure 6.2: Example network in which DARS game has a unique equilibrium.

points on the line segment defined by two arbitrary points to be achieved. These different points compose the capacity region (explained in more detail in [26]). A slice through the capacity region under the assumption of single-hop transmission without spatial reuse is a straight line. With the introduction of multihop transmission and spatial reuse, the size of the capacity region increases. Hereafter, the capacity region slice under multihop transmission with spatial reuse is treated.

Figure 6.2(b) indicates that two points (a) and (b) are on the capacity region slice except for the points on the axes. These two points correspond to the following route profiles.

(a) $(1 \rightarrow 13 \rightarrow 2)$, $(3 \rightarrow 4)$

(b) $(1 \rightarrow 13 \rightarrow 2)$, $(3 \rightarrow 14 \rightarrow 4)$

Route profile (a), in which source node 3 selects single-hop transmission, is not an equilibrium. Route profile (b) is an equilibrium such that source node 1 selects $(1 \rightarrow 13 \rightarrow 2)$ in both profiles, so the selection of these two route profiles depends only on the preference of source node 3.

6.3.2 Network Topology with No Equilibria

The DARS game does not always have Nash equilibria in all networks. Figure 6.3(a) shows an example network in which the DARS game has no equilibria. In this case, for all strategy pairs, at least one source node has an incentive to deviate. Consider the following four route profiles.

(a) $(1 \rightarrow 2)$, $(3 \rightarrow 12 \rightarrow 4)$

(b) $(1 \rightarrow 10 \rightarrow 2)$, $(3 \rightarrow 12 \rightarrow 4)$

(c) $(1 \rightarrow 10 \rightarrow 2)$, $(3 \rightarrow 6 \rightarrow 4)$

(d) $(1 \rightarrow 2)$, $(3 \rightarrow 6 \rightarrow 4)$

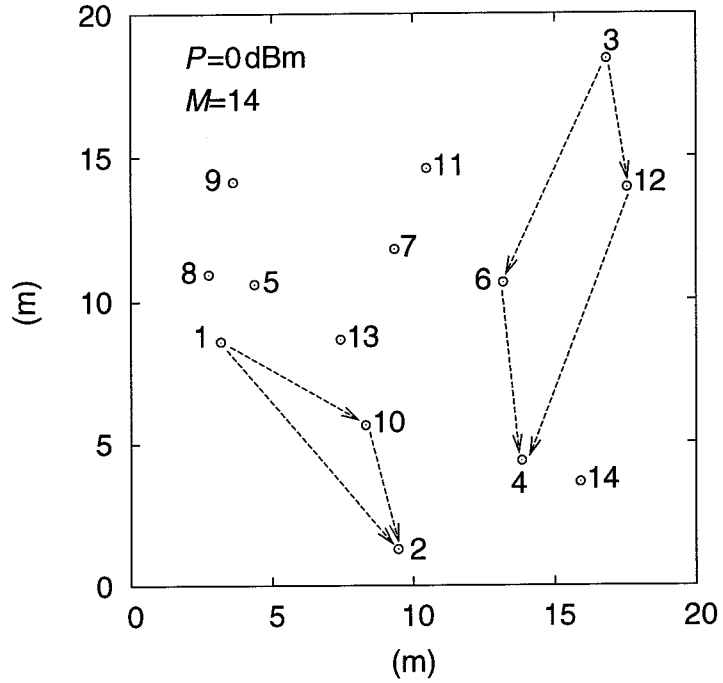

(a) Network topology.

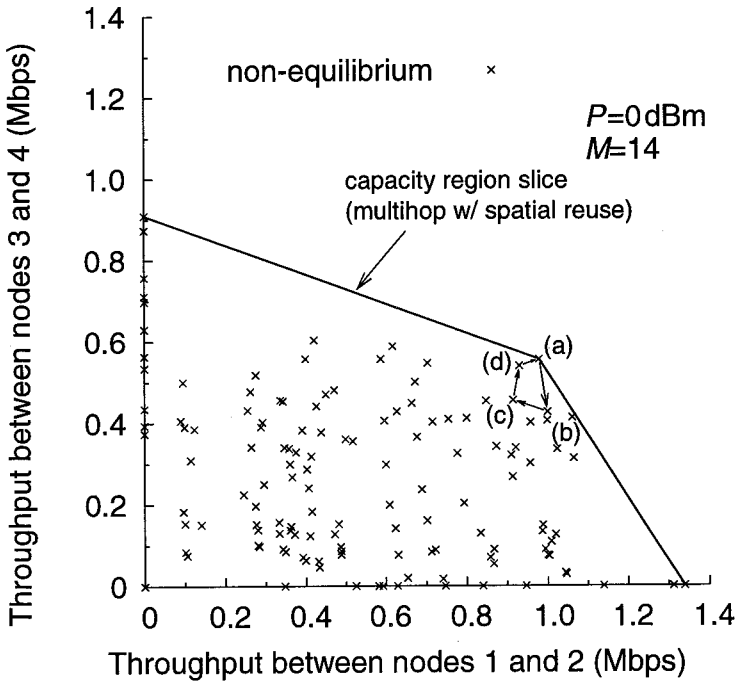

(b) Capacity region and equilibrium throughput.

Figure 6.3: Example network in which DARS game has no equilibria.

Figure 6.3(b) shows the capacity region slice and the combination of throughput for each strategy pair. The four points connected with arrows correspond to the four route profiles above.

The non-existence of equilibria has the following technical aspect. If the DARS game starts at point (a), source node 1 switches to $(1 \rightarrow 10 \rightarrow 2)$, resulting in point (b), and then source node 3 switches to $(3 \rightarrow 6 \rightarrow 4)$, resulting in point (c). The cycle (d), (a), (b), (c) will simply repeat and never converge. Therefore, the non-existence of pure strategy Nash equilibria can be used for analyzing the instability of the route selection.

Consequently, in some cases, even with perfect information except for knowledge of the other nodes' decisions, each rational node cannot determine a unique route. In these cases, the best strategy is determined based on a probability distribution.

6.3.3 Network Topology with Multiple Equilibria

In some networks, the DARS game has multiple Nash equilibria, as shown by the example in Figure 6.4(a). In this network, the following two route profiles are both Nash equilibria.

(a) $(1 \rightarrow 8 \rightarrow 2)$, $(3 \rightarrow 14 \rightarrow 4)$

(b) $(1 \rightarrow 14 \rightarrow 2)$, $(3 \rightarrow 4)$

Source nodes 1 and 3 both try to use the same node, 14.

Figure 6.4(b), which shows the capacity region slice and the combination of throughput for each strategy pair, reveals that these equilibria are not Pareto optimal. A Pareto optimal outcome is one that cannot be improved without reducing the payoff of at least one player. This is because if a route profile on the capacity region is selected, at least one source node has an incentive to deviate. Therefore, the other source node does not select strategies corresponding to this route profile. To reach capacity in these cases, centralized control may be required.

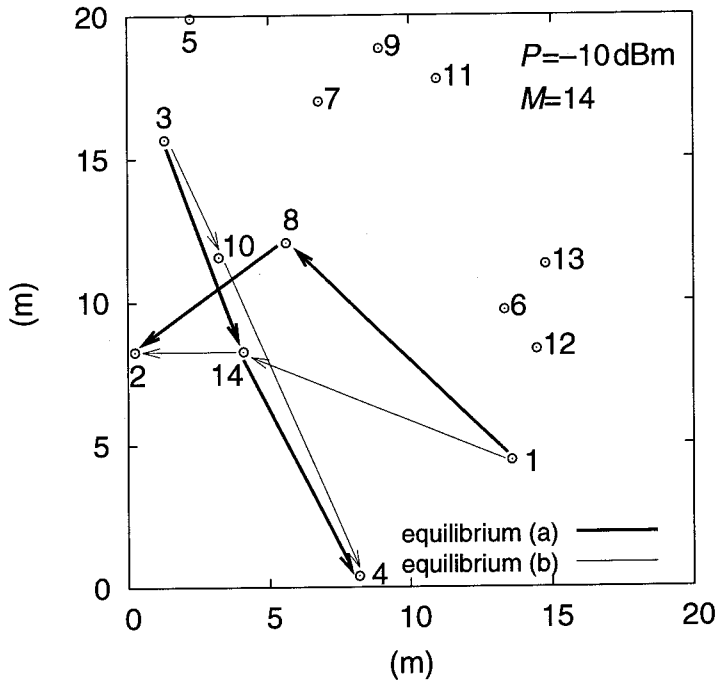

(a) Network topology.

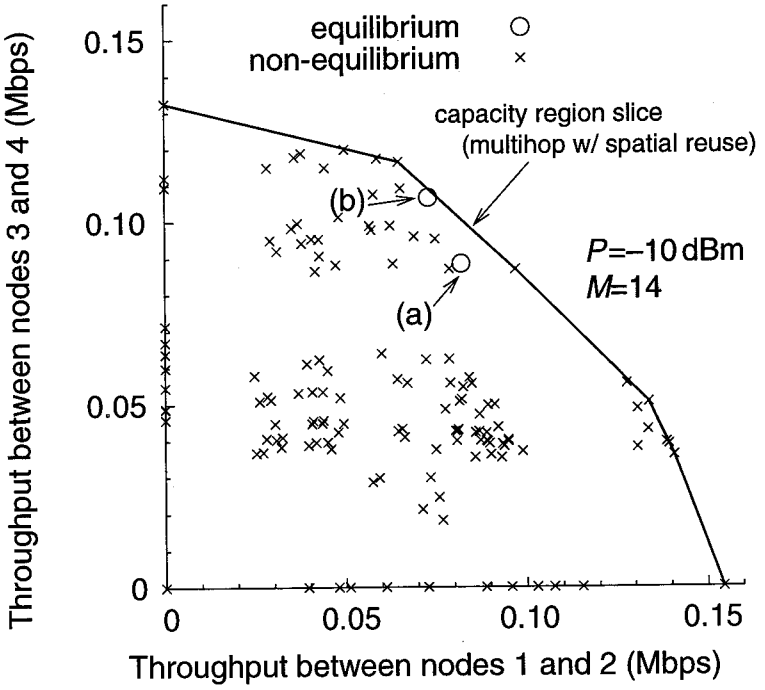

(b) Capacity region and equilibrium throughput.

Figure 6.4: Example network in which DARS game has multiple equilibria.

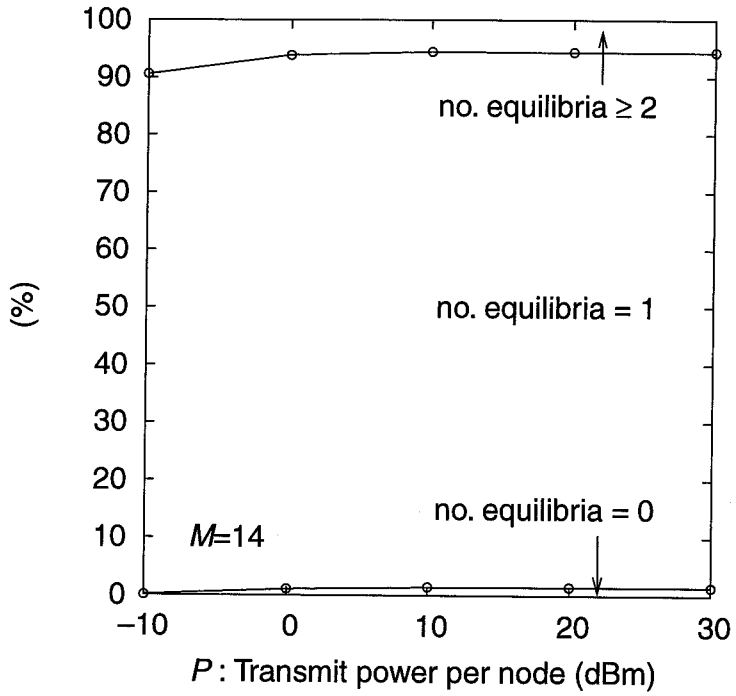

Figure 6.5: Percentage of three categories based on number of equilibria as function of transmit power per node.

6.3.4 Average Capacity

As mentioned above, the behavior of the DARS game varies depending on the spatial arrangements of the nodes and can be classified based on the number of equilibria: none, a unique equilibrium, and multiple equilibria. In this subsection, to evaluate the performance of the DARS game for various node arrangements, we classify the many possible node arrangements into these three categories.

Figure 6.5 shows the percentage of node arrangements in each category as a function of the transmit power per node. The DARS game has a unique equilibrium in 90% or more of the arrangements. The percentage of networks in which there are no Nash equilibria increases with the transmit power per node. This means that with low power levels, the interference between two source-destination pairs is negligible, so route selection can be determined without considering other source nodes.

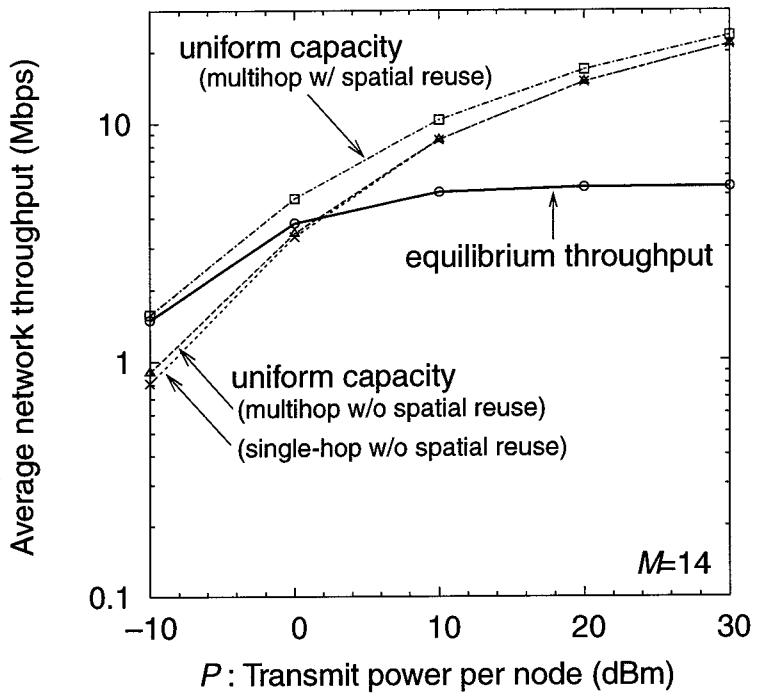

Figure 6.6: Power dependence of average network throughput.

Figure 6.6 shows the transmit power dependence of the average network throughput for the networks with at least one Nash equilibrium. The dashed and dotted lines represent the uniform capacity, which is defined as the total capacity under the assumption that all source nodes have the same end-to-end throughput. It thus corresponds to the boundary of the capacity region (explained in detail in [7,26]). The introduction of multihop transmission increases the uniform capacity under the condition that the transmit power is low. This result can be explained by the finding that multihop transmission is effective under low CNR conditions, as presented in Section 3.2.

The introduction of spatial reuse in addition to multihop transmission increases the uniform capacity, especially when the transmit power is low. This is because the capacity of wireless ad hoc networks with spatial reuse is constrained by the interference of concurrent transmissions and large transmit power leads to large interference to other nodes. This result is also consistent with the finding presented in Section 3.3.

The solid line in Figure 6.6 represents the average equilibrium throughput. If the DARS game has multiple equilibria, we use the average throughput of multiple route profiles under equilibrium conditions. With low transmit power, the DARS game attains the average throughput near the uniform capacity. With high transmit power, the equilibrium throughput is saturated because in the DARS game each source node tends to use spatial reuse, which is not effective under high power conditions.

Figure 6.7 shows the node density dependence of the average network throughput. The equilibrium throughput as well as the uniform capacity increases with the number of nodes. However, at the same time, a large number of nodes can lead to instability of adaptive control, as shown in Figure 6.8, which shows the percentage of each category as a function of the number of nodes under the condition that all nodes transmit at the same power level ($P = 0\,\mathrm{dBm}$).

6.4 Joint Effect of DARS and Transmit Power Control

In this section, we evaluate the equilibrium throughput achieved by the DARS and power control.

6.4.1 Discrete-Rate Transmission

Up to now, we assumed continuous-rate adaptation as defined by Eq. (6.3). In addition to continuous-rate transmission, we evaluate the performance of the DARS game with discrete-rate transmission. In our evaluation, a step function that is bounded above by the function $f(\gamma)$ in Eq. (6.3) is used as a discrete-rate restriction, where the difference in sensitivity between adjacent rates is set to 3 dB, 5 dB, or 10 dB.

Each curve in Figure 6.9 represents a two-dimensional slice of the capacity region and corresponds to a different parameter of variable-rate transmissions of the network shown in Figure 6.2(a). Each point in Figure 6.9 represents the equilibrium throughput.

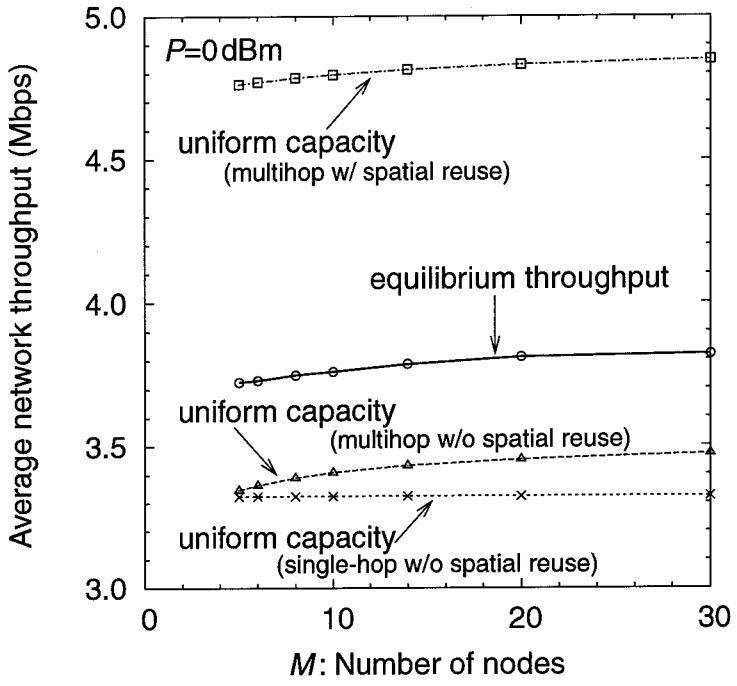

Figure 6.7: Node density dependence of average network throughput.

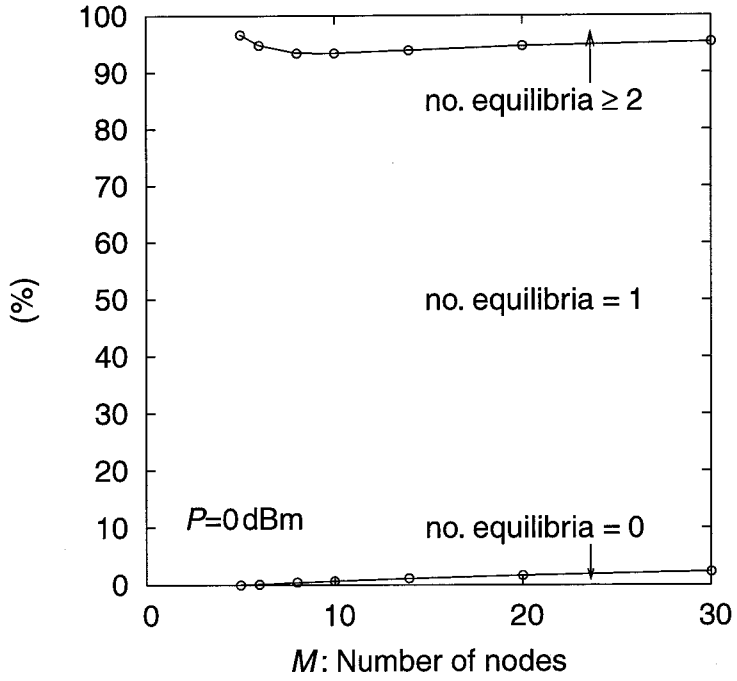

Figure 6.8: Percentage of three categories based on number of equilibria as function of number of nodes.

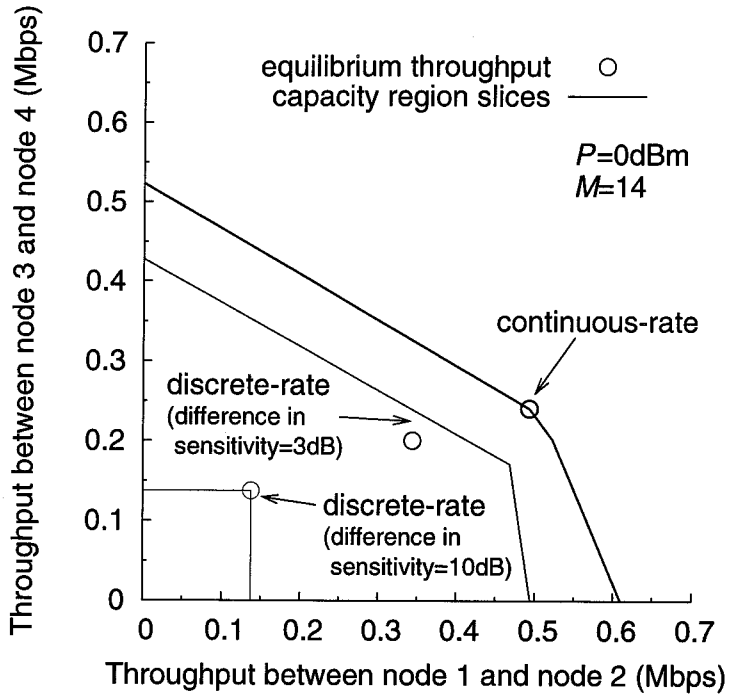

Figure 6.9: Capacity region and equilibrium throughput of Figure 6.2(a) assuming discrete-rate transmission.

Decreasing difference in sensitivity increases the equilibrium throughput as well as the capacity region slice.

6.4.2 Power Control and Discrete-Rate Transmission

Next, we evaluate the performance of the DARS game with power control in addition to discrete-rate transmission. Up to this time, each transmitting node transmits at its maximum power. In case we take power control into consideration, the number of strategies of each source node is increased. In the following, node i selects one of L power levels such that $P_i/2^{l-1}$ $(l = 1, 2, \cdots, L)$.

Figure 6.10(a) shows an example network topology in which power control significantly enhances the capacity. In this case, we assume four-level power control ($L = 4$) and difference in sensitivity is set to 10 dB. When each node transmits with the maximum power, the DARS game has a unique equilibrium corresponding to the following

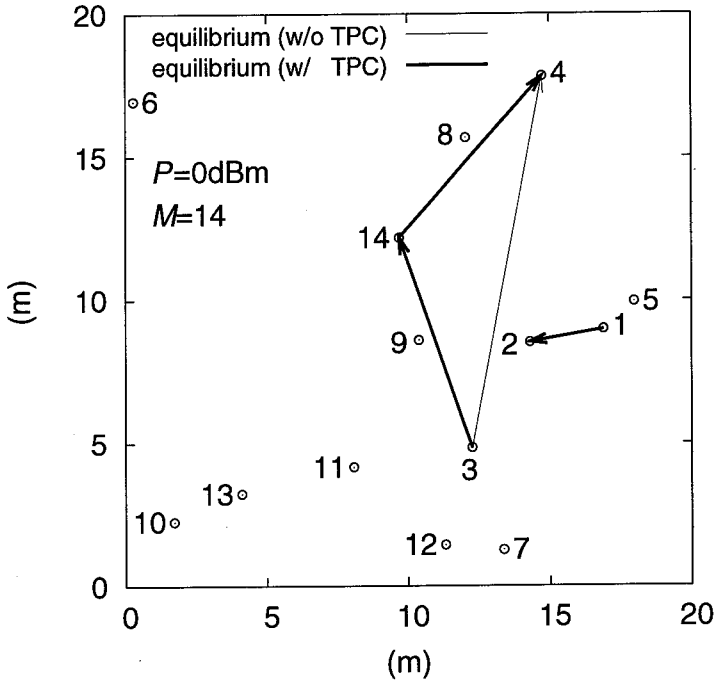

(a) Network topology.

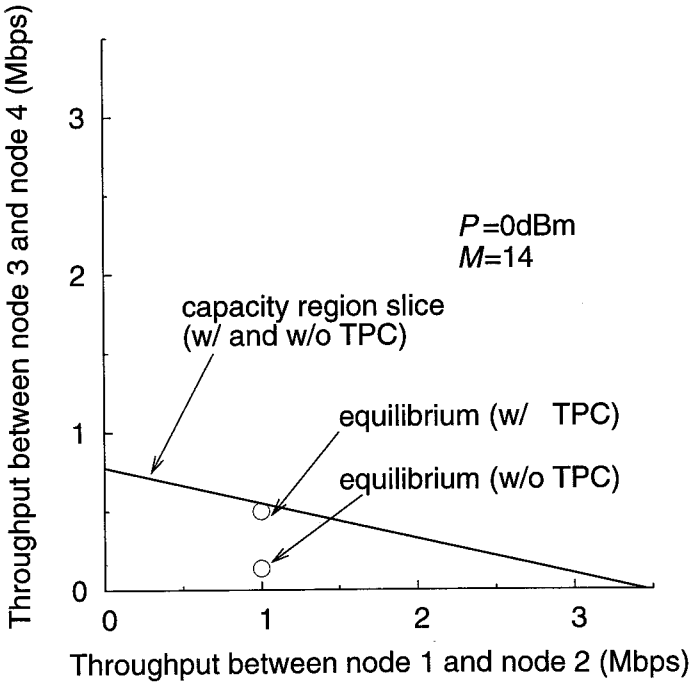

(b) Capacity region and equilibrium throughput.

Figure 6.10: Example network in which power control and discrete-rate transmission (difference in sensitivity is 10 dB) are assumed. Source node 1 selects single-hop transmission in both case with power control and that without power control.

route profile.

(a) $(1 \rightarrow 2)$, $(3 \rightarrow 4)$

When each node is able to use power control, the DARS game also has a unique equilibrium corresponding to the following route profile.

(b) $(1 \rightarrow 2)$, $(3 \rightarrow 14 \rightarrow 4)$

Figure 6.10(b) shows the capacity region slices and the equilibrium throughput with and without power control. The capacity region slice with power control does not change from that without power control. The reason is the following. Both capacity region slices consist of two points on the axes, and these points correspond to transmit strategies without spatial reuse. In case spatial reuse is not used, this type of transmit power control does not enhance the throughput. Because in case of an independent transmission, by reducing transmit power while maintaining the CINR requirements at the receiver, an improvement in energy saving can be achieved, however, the received CINR is not increased, and consequently, the transmission rate is not enhanced.

In contrast to the capacity region, the equilibrium throughput is increased by adopting power control. This can be understood in the following way. In case source node 1 reduces transmit power while maintaining the CINR requirements at node 2, the interference power at node 14 may be decreased, and consequently, source node 3 has an incentive to use the route $(3 \rightarrow 14 \rightarrow 4)$.

6.4.3 Average Capacity

Until now, we have shown the performance of the DARS game in some example network topologies with a unique equilibrium. In this subsection, the performances of the DARS game in arbitrary topologies are evaluated by applying a Monte-Carlo simulation under various arrangements of nodes.

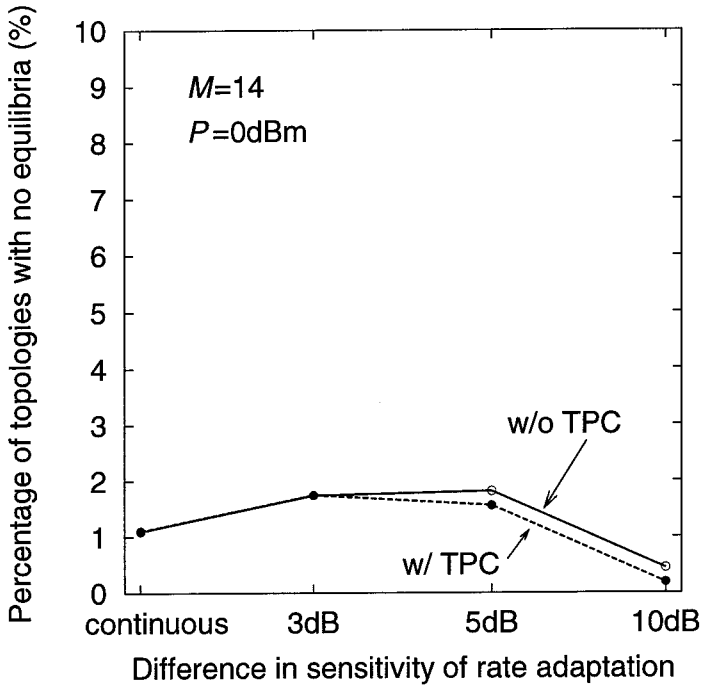

Figure 6.11: Percentage of network topologies with no equilibria.

Some network topologies have no pure strategy Nash equilibria. In these topologies, at least one source node has an incentive to deviate and autonomous route selection scheme may not converge. Figure 6.11 shows the percentage of network topologies without equilibria. Introduction of power control would increase the number of strategies, however, this may not increase instability of DARS game.

One solution to this problem is that two nodes cooperate with each other to enhance the network performance. In this case, the next problem will be how to provide incentive to nodes, knowing that they will have to decease their throughput. Another solution is using the history of decision-making. In this case, each node holds its history of route selection and determines the route depending on the history. These situations can be analyzed using repeated games [31].

Figure 6.12 shows the average equilibrium throughput and the capacity assuming centralized control. Increasing difference in sensitivity decreases the capacity. On the

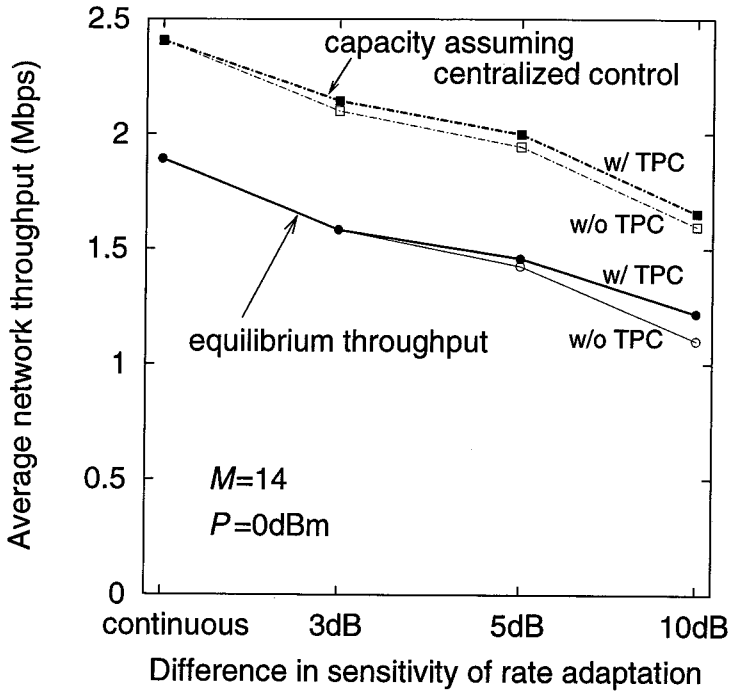

Figure 6.12: Average network throughput assuming discrete rate control.

other hand, when continuous-rate transmission is not used, transmit power control is more effective to increase the capacity. This capacity enhancement with power control and discrete-rate transmission has been studied [26]. What we want to emphasize is that the equilibrium throughput is also increased by using power control in case of discrete-rate transmission. Therefore, it is revealed that power control in addition to DARS with discrete-rate transmission may increase the throughput.

6.5 Summary

We have addressed the problem of decentralized adaptive route selection in wireless ad hoc networks. We investigated the decentralized adaptive route selection problem in which each source node wants to maximize its own throughput at the same time. We defined this problem as a DARS game. Numerical results show that the existence of Nash equilibria is not guaranteed in some cases even under the assumption that nodes have

perfect information except for the knowledge of the other nodes' actual route selections. They also show that the percentage of networks in which there are no pure strategy Nash equilibria depends on the transmit power per node as well as on the spatial arrangement of the nodes.

We also evaluated network throughput under equilibrium conditions as the achievable throughput of the DARS game. Numerical results show that the DARS game attains average throughput near the capacity under centralized scheduling when transmit power is low. This is because each node in the DARS game actively reuses the same bandwidth at spatially separated locations.

We would like to emphasize that the purpose of this chapter was to present a means to evaluate decentralized and adaptive route selections. Further research is required to develop stable and highly efficient adaptive route selection algorithms for wireless ad hoc networks.

Chapter 7

Conclusions and Future Work

This thesis has investigated some types of spectral efficiency for multihop radio networks and multihop cellular systems. We also studied the achievable throughput under decentralized adaptive route selections and compared it with the capacity under centralized scheduling in wireless ad hoc networks. Through these investigations, we obtained valuable insight into the configuration of multihop radio networks.

We first examined the bandwidth efficiency of a single isolated multihop route, which is defined as the maximum end-to-end bit rate through multiple hops per unit bandwidth. We found that instead of spending some bandwidth efficiency, we can extend the end-to-end communication range by controlling symbol rate or using multihop transmission. We also found that when spatial channel reuse is not allowed, transmission at the maximum power is effective in terms of the bandwidth efficiency. We also studied the benefit of spatial channel reuse and found that energy efficiency can be increased by reducing the transmit power per node at the cost of a slight decrease in the bandwidth efficiency.

We then established a tradeoff between the bandwidth efficiency and the area spectral efficiency, which is defined as the maximum end-to-end bit rate through multiple hops per unit bandwidth per unit area. In particular, we assumed that every communication pair has nearly the same performance in multihop radio networks. We found that the control of symbol rate can decrease the area spectral efficiency, however, the use of multihop

transmission, which has the same effects of symbol rate control on bandwidth efficiency, can increase the area spectral efficiency.

Next, we applied the insight gained from the above simple analysis to the performance evaluation of multihop TDMA cellular systems under single-cell environment where mobile stations are distributed randomly in a cell. We also considered the shadowing effects as well as the path loss. By using the similar methodology for the formulation of rate-adaptive cellular systems, we formulated the cell-radius dependence of spectral efficiency and outage probability of multihop cellular systems. We found that introduction of multihop relaying is superior to rate adaptation in terms of both coverage and spectral efficiency.

Under single-cell environment, the decision of strategy based upon one's own throughput may result in high spectral efficiency. In contrast to this, under interference-limited situation such as multi-cell cellular systems, introduction of two-hop relaying might cause excessive interference due to uncoordinated frequency reuse. Thus, it is interesting to see what kinds of route selection technique will achieve high spectral efficiency under interference-limited situation.

Therefore, we studied the performance of multihop CDMA cellular systems under multi-cell environment, in which accurate power control is essential to overcome the well-known near-far problem and promote the quality and efficiency of service. We found that the geometry, which was used to represent location-dependent interference in downlink, was valuable to evaluate the interference power in uplink. We proposed a new route selection criterion maximizing the amount of interference reduction and revealed that the proposed criterion is superior to the conventional minimum power criterion in respect of the amount of interference reduction. We also proposed an efficient routing algorithm and indicated that the proposed routing algorithm can increase the system capacity by 10% even under heavy traffic conditions.

Note that the absolute value of this capacity enhancement due to two-hop relaying is sensitive to lots of factors. For example, too small interference margin may lead to excessive packet loss, whereas too large interference margin results in lower spectral efficiency. In addition, capacity enhancement can be also achieved by packet scheduling or diversity handover as well as multihop transmission. These are the subjects of future work.

As we have seen, if there is centralized control or scheduling, rejections of new calls from mobile stations located near the cell edge will increase the spectral efficiency. On the other hand, in a decentralized controlled system such as wireless ad hoc networks, centralized admission control cannot be utilized. Thus, we studied the situation where there are multiple source-destination pair and each source node selfishly attempts to increase own throughput. We defined a decentralized adaptive route selection (DARS) game and revealed that even with perfect information except for the knowledge of the other nodes' actual selections, in some cases each source node cannot determine a unique route. We then compared the capacity under centralized scheduling and the throughput with equilibrium route selections. Numerical results reveal that the DARS game attains average throughput near the capacity when transmit power is low.

In these studies, we assumed the perfect information about the path loss between the transmitter and receiver, however, this assumption is unrealistic in a large network. In addition, it would be interesting to consider what payoff function instead of end-to-end throughput may result in higher network throughput. These are the subjects of future work.

Bibliography

[1] J. Weatherall and A. Jones, "Ubiquitous networks and their applications," IEEE Wireless Commun. Mag., vol.9, no.1, pp.18–29, Feb. 2002.

[2] R. Ramanathan and J. Redi, "A brief overview of ad hoc networks: Challenges and directions," IEEE Commun. Mag., vol.40, no.5, pp.20–22, May 2002.

[3] A.J. Goldsmith and S.B. Wicker, "Design challenges for energy-constrained ad hoc wireless networks," IEEE Wireless Commun. Mag., vol.9, no.4, pp.8–27, Aug. 2002.

[4] S. Ramanathan and M. Steenstrup, "A survey of routing techniques for mobile communications networks," ACM/Baltzer Mobile Networks and Applications, vol.1, no.2, pp.89–104, 1996.

[5] J. Broch, D.A. Maltz, D.B. Johnson, Y.C. Hu, and J. Jetcheva, "A performance comparison of multi-hop wireless ad hoc network routing protocols," Proc. Fourth Annual ACM/IEEE International Conf. on Mobile Computing and Networking (MOBICOM'98), Dallas, TX, pp.85–97, Oct. 1998.

[6] E.M. Royer and C.K. Toh, "A review of current routing protocols for ad hoc mobile wireless networks," IEEE Pers. Commun. Mag., vol.6, no.2, pp.46–55, April 1999.

[7] S. Toumpis and A.J. Goldsmith, "Performance, optimization, and cross-layer design of media access protocols for wireless ad hoc networks," Proc. IEEE ICC '03, pp.2234–2240, May 2003.

[8] S. Shakkottai, T.S. Rappaport, and P.C. Karlsson, "Cross-layer design for wireless networks," IEEE Commun. Mag., vol.41, no.10, pp.74–80, Oct. 2003.

[9] K. Mase, M. Sengoku, and S. Shinoda, "A perspective on next-generation ad hoc networks — a proposal for an open community network —," IEICE Trans. Fundamentals, vol.E84-A, no.1, pp.98–106, Jan. 2001.

[10] R. Haas and J.C. Belfiore, "Spectrum efficiency limits in mobile cellular systems," IEEE Trans. Veh. Technol., vol.45, no.1, pp.33–40, Feb. 1996.

[11] M.S. Alouini and A.J. Goldsmith, "Area spectral efficiency of cellular mobile radio systems," IEEE Trans. Veh. Technol., vol.48, no.4, pp.1047–1066, July 1999.

[12] K.J. Hole and G.E. Øien, "Spectral efficiency of adaptive coded modulation urban microcellular networks," IEEE Trans. Veh. Technol., vol.50, no.1, pp.205–222, Jan. 2001.

[13] T. Mukai, H. Murata, and S. Yoshida, "Study on channel selection algorithm and number of established routes of multi-hop autonomous distributed radio networks," IEICE Trans. Commun. (Japanese Edition), vol.J85-B, no.12, pp.2080–2086, Dec. 2002.

[14] J. Jun and M.L. Sichitiu, "Fairness and QoS in multihop wireless networks," Proc. IEEE VTC 2003-Fall, pp.6–9, Oct. 2003.

[15] H. Kwak and S. Yoshida, "Tradeoff between fairness and throughput in multi-hop wireless LAN," IEICE Trans. Fundamentals, vol.E87-A, no.7, pp.1733–1741, July 2004.

[16] V. Gambiroza, B. Sadeghi, and E.W. Knightly, "End-to-end performance and fairness in multihop wireless backhaul networks," Proc. MOBICOM 2004, pp.287–301, Sep.–Oct. 2004.

[17] M. Grossglauser and D.N.C. Tse, "Mobility increases the capacity of ad hoc wireless networks," IEEE/ACM Trans. Netw., vol.10, no.4, pp.477–486, Aug. 2002.

[18] K. Yamamoto and S. Yoshida, "Analysis of distributed route selection scheme in wireless ad hoc networks," Proc. the 15th IEEE International Symposium on Personal, Indoor and Mobile Radio Communications (PIMRC 2004), Sept. 2004.

[19] K. Yamamoto and S. Yoshida, "Game-theoretic approach to capacity and stability evaluations of decentralized adaptive route selections in wireless ad hoc networks," IEICE Trans. Commun., vol.E88-B, no.3, pp.1009–1016, March 2005.

[20] P. Gupta and P.R. Kumar, "The capacity of wireless networks," IEEE Trans. Inf. Theory, vol.46, no.2, pp.388–404, March 2000.

[21] G.N. Aggélou and R. Tafazolli, "On the relaying capability of next-generation GSM cellular networks," IEEE Pers. Commun. Mag., vol.8, no.1, pp.40–47, Feb. 2001.

[22] H. Wu, C. Qiao, S. De, and O. Tonguz, "Integrated cellular and ad hoc relaying systems: iCAR," IEEE J. Select. Areas Commun., vol.19, no.10, pp.2105–2115, Oct. 2001.

[23] T. Rouse, I. Band, and S. McLaughlin, "Capacity and power investigation of opportunity driven multiple access (ODMA)," Proc. IEEE ICC '02, vol.5, pp.3202–3206, April 2002.

[24] A.N. Zadeh and B. Jabbari, "Performance analysis of multihop packet CDMA cellular networks," Proc. IEEE GLOBECOM '01, pp.2875–2879, Nov. 2001.

[25] A. Fujiwara, S. Takeda, H. Yoshino, and T. Otsu, "Capacity improvement with a multi-hop access scheme in broadband CDMA cellular systems," IEICE Trans. Commun., vol.J85-B, no.12, pp.2073–2079, Dec. 2002.

[26] S. Toumpis and A.J. Goldsmith, "Capacity regions for wireless ad hoc networks," IEEE Trans. Wireless Commun., vol.2, no.4, pp.736–748, July 2003.

[27] N. Bambos, "Toward power-sensitive network architecture in wireless communications: Concepts, issues, and design aspects," IEEE Pers. Commun. Mag., pp.50–59, June 1998.

[28] D. Goodman and N. Mandayam, "Power control for wireless data," IEEE Pers. Commun. Mag., vol.7, no.2, pp.231–235, April 2000.

[29] D. Goodman and N. Mandayam, "Network assisted power control for wireless data," Mobile Networks and Applications, vol.6, no.5, pp.409–418, Sept. 2001.

[30] A.B. MacKenzie and S.B. Wicker, "Game theory and the design of self-configuring, adaptive wireless networks," IEEE Commun. Mag., vol.39, pp.126–131, Nov. 2001.

[31] D. Fudenberg and J. Tirole, Game Theory, MIT Press, 1991.

[32] A.B. MacKenzie and S.B. Wicker, "Selfish users in Aloha: A game-theoretic approach," Proc. IEEE VTC 2001-Fall, pp.1354–1357, Oct. 2001.

[33] A.B. MacKenzie and S.B. Wicker, "Stability of multipacket slotted Aloha with selfish users and perfect information," Proc. IEEE Infocom '03, April 2003.

[34] Z. Fu, H. Luo, P. Zerfos, S. Lu, L. Zhang, and M. Gerla, "The impact of multihop wireless channel on TCP performance," IEEE Trans. Mobile Comput., vol.4, no.2, pp.209–221, March/Apr. 2005.

[35] J.N. Laneman and G.W. Wornell, "Energy-efficient antenna sharing and relaying for wireless networks," Proc. IEEE WCNC '00, Sept. 2000.

[36] J.N. Laneman and G.W. Wornell, "Distributed space-time coded protocols for exploiting cooperative diversity in wireless networks," IEEE Trans. Inf. Theory, vol.49, no.10, pp.2415–2525, Oct. 2003.

[37] J.N. Laneman, D.N.C. Tse, and G.W. Wornell, "Cooperative diversity in wireless networks: Efficient protocols and outage behavior," IEEE Trans. Inf. Theory, vol.50, no.12, pp.3062–3080, Dec. 2004.

[38] A. Sendonaris, E. Erkip, and B. Aazhang, "User cooperation diversity-part I: System description," IEEE Trans. Commun., vol.51, no.11, pp.1927–1938, Nov. 2003.

[39] A. Sendonaris, E. Erkip, and B. Aazhang, "User cooperation diversity-part II: Implementation aspects and performance analysis," IEEE Trans. Commun., vol.51, no.11, pp.1939–1948, Nov. 2003.

[40] J. Boyer, D.D. Falconer, and H. Yanikomeroglu, "Multihop diversity in wireless relaying channels," IEEE Trans. Commun., vol.52, no.10, pp.1820–1830, Oct. 2004.

[41] S. Sampei, Applications of Digital Wireless Technologies to Global Wireless Communications, Prentice-Hall, 1997.

[42] A.A.N.A. Kusuma and L.L.H. Andrew, "Minimum power routing for multihop cellular networks," Proc. IEEE GLOBECOM '02, pp.37–41, Nov. 2002.

[43] F. Adachi, M. Sawahashi, and H. Suda, "Wideband DS-CDMA for next-generation mobile communications systems," IEEE Commun. Mag., vol.36, no.9, pp.56–69, Sept. 1998.

[44] K. Tachikawa, W-CDMA Mobile Communications System, John Wiley, 2002.

[45] TIA TR45.5, "The cdma2000 ITU-R RTT Candidate Submission," IMT-2000 Radio Transmission Technology (RTT) Proposals (8–2), June 1998.

[46] V. Srinivasan, P. Nuggehalli, C.F. Chiasserini, and R.R. Rao, "Cooperation in wireless ad hoc networks," Proc. IEEE Infocom '03, no.1, pp.808–817, March 2003.

[47] S. Eidenbenz, V.A. Kumar, and S. Zust, "Equilibria in topology control games for ad hoc networks," Proc. DialM-POMC '03, pp.2–11, Sept. 2003.

[48] H.H. Xia, "A simplified analytical model for predicting path loss in urban and suburban environments," IEEE Trans. Veh. Technol., vol.46, no.4, pp.1040–1046, Nov. 1997.

[49] ETSI TR 101 112 (v3.2.0), "Universal mobile telecommunications system (UMTS); selection procedures for the choice of radio transmission technologies of the UMTS (UMTS 30.03)," April 1998.

[50] 3GPP, TR25.942 (v6.4.0), "Radio frequency (RF) system scenarios," March 2005.

[51] L.B. Milstein, D.L. Schilling, R.L. Pickholtz, V. Erceg, M. Kullback, E.G. Kanterakis, D.S. Fishman, and W.H. Biederman, "On the feasibility of a CDMA overlay for personal communications networks," IEEE J. Select. Areas Commun., vol.10, no.4, pp.655–668, May 1992.

[52] A. Goldsmith, Wireless Communications, Cambridge University Press, Aug. 2005.

[53] W.C.Y. Lee, Mobile Communications Design Fundamentals, John Wiley & Sons, 1993.

[54] M. Sikora, J.N. Laneman, M. Haenggi, D.J. Costello, and T. Fuja, "On the optimum number of hops in linear wireless networks," IEEE Information Theory Workshop, Oct. 2004.

[55] M. Haenggi, "Twelve reasons not to route over many short hops," Proc. IEEE VTC 2004-Fall, Sept. 2004.

[56] A.J. Goldsmith and S.G. Chua, "Variable-rate variable-power MQAM for fading channels," IEEE Trans. Commun., vol.45, no.10, pp.1218–1230, Oct. 1997.

[57] T. Ue, S. Sampei, and N. Morinaga, "Symbol rate controlled adaptive modulation/TDMA/TDD for wireless personal communication systems," IEICE Trans. Commun., vol.E78-B, no.8, pp.1117–1124, Aug. 1995.

[58] P. Jung, P.W. Baier, and A. Steil, "Advantages of CDMA and spread spectrum techniques over FDMA and TDMA in cellular mobile radio applications," IEEE Trans. Veh. Technol., vol.42, no.3, pp.357–364, Aug. 1993.

[59] N. Morinaga, M. Yokoyama, and S. Sampei, "Intelligent radio communication techniques for advanced wireless communications systems," IEICE Trans. Commun., vol.E79-B, no.3, pp.214–221, March 1996.

[60] M.G. Jansen and R. Prasad, "Capacity, throughput, and delay analysis of a cellular DS CDMA system with imperfect power control and imperfect sectorization," IEEE Trans. Veh. Technol., vol.44, no.1, pp.67–75, Feb. 1995.

[61] A. Abrardo and D. Sennati, "On the analytical evaluation of closed-loop power-control error statistics in ds-cdma cellular systems," IEEE Trans. Veh. Technol., vol.49, no.6, pp.2071–2080, Nov. 2000.

[62] A.M. Viterbi and A.J. Viterbi, "Erlang capacity of a power controlled CDMA system," IEEE J. Select. Areas Commun., vol.11, no.6, pp.892–900, Aug. 1993.

[63] Y. Ishikawa and N. Umeda, "Capacity design and performance of call admission control in cellular CDMA systems," IEEE J. Select. Areas Commun., vol.15, no.8, pp.1627–1635, Oct. 1997.

[64] J. Jun, P. Peddabachagari, and M. Sichitiu, "Theoretical maximum throughput of IEEE 802.11 and its applications," Proc. 2nd IEEE International Symposium on Network Computing and Applications, pp.249–256, April 2003.

[65] J. Jun and M.L. Sichitiu, "The nominal capacity of wireless mesh networks," IEEE Wireless Commun. Mag., vol.10, no.5, pp.8–14, Oct. 2003.

[66] E. Anshelevich, A. Dasgupta, E. Tardos, and T. Wexler, "Near-optimal network design with selfish agents," Proc. Thirty-Fifth Annual ACM Symposium on Theory of Computing, pp.511–520, 2003.

Author's Publication List

Journal Papers

1. K. Yamamoto and S. Yoshida, "Analysis of reverse link capacity enhancement for CDMA cellular systems using two-hop relaying," IEICE Trans. Fundamentals, vol.E87-A, no.7, pp.1712–1719, July 2004.
2. K. Yamamoto and S. Yoshida, "Game-theoretic approach to capacity and stability evaluations of decentralized adaptive route selections in wireless ad hoc networks," IEICE Trans. Commun., vol.E88-B, no.3, pp.1009–1016, March 2005.
3. K. Yamamoto and S. Yoshida, "Tradeoff between area spectral efficiency and end-to-end throughput in rate-adaptive multihop radio networks," to appear in IEICE Trans. Commun., vol.E88-B, no.9, Sept. 2005.

International Conference Papers

1. K. Yamamoto, H. Murata, S. Yoshida, A. Fujiwara, T. Otsu, and Y. Yamao, "Capacity and transmission power estimation of two-hop CDMA cellular system," Proc. the Fifth International Symposium on Wireless Personal Multimedia Communications (WPMC '02), pp.97–101, Honolulu, Hawaii, Oct. 2002.
2. K. Yamamoto and S. Yoshida, "Call admission control suitable for two-hop CDMA cellular systems," Proc. the IEEE Semiannual Vehicular Technology Conference (VTC '03-Fall), vol.3, pp.1913–1917, Orlando, Florida, Oct. 2003.
3. K. Yamamoto and S. Yoshida, "Capacity enhancement of CDMA cellular systems by two-hop relaying," Proc. The Fourth International Conference on Information, Communications & Signal Processing (ICICS 2003), Singapore, Dec. 2003.
4. H. Xu, K. Yamamoto, and S. Yoshida, "Experimental study on capacity enhancement of ad hoc networks with multihop connections," Proc. the First IEEE VTS

Asia Pacific Wireless Communications Symposium (APWCS), pp.81–85, Seoul, Korea, Jan. 2004.

5. K. Yamamoto and S. Yoshida, "Stability of selfish route selections in wireless ad hoc networks," Proc. the Joint Conference of 10th Asia-Pacific Conference on Communications and 5th International Symposium on Multi-Dimensional Mobile Communications (APCC 2004 / MDMC 2004), vol.2, pp.853–857, Beijing, China, Aug.–Sept. 2004.
6. K. Yamamoto and S. Yoshida, "Analysis of distributed route selection scheme in wireless ad hoc networks," Proc. the 15th IEEE International Symposium on Personal, Indoor and Mobile Radio Communications (PIMRC 2004), Barcelona, Spain, Sept. 2004.
7. A. Kusuda, K. Yamamoto, and S. Yoshida, "Performance comparison of multihop relaying and rate adaptation in cellular communication systems," to be presented at the 16th IEEE International Symposium on Personal, Indoor and Mobile Radio Communications (PIMRC 2005), Berlin, Germany, Sept. 2005.

Technical Meeting Papers

1. K. Yamamoto, H. Murata, S. Yoshida, A. Fujiwara, T. Otsu, and Y. Yamao, "Study on applying relay technique to DS-CDMA cellular system," IEICE Technical Report, RCS2002-20, pp.15–20, April 2002.
2. H. Xu, K. Yamamoto, and S. Yoshida, "Experimental study on performance improvement of radio networks with multi-hop connection," Proc. the 5th YRP Symposium on Cooperation between Industry, Academia and Government in Mobile Telecommunications, pp.98–99, July 2003.
3. H. Xu, K. Yamamoto, and S. Yoshida, "Experimental study on throughput enhancement with multihop connections in wireless LAN," IEICE Technical Report, RCS2003-337, pp.25–28, March 2004.
4. K. Yamamoto and S. Yoshida, "Analysis of autonomous route selection scheme in multihop radio networks," IEICE Technical Report, RCS2003-338, pp.29–32, March 2004.
5. K. Ozaki, K. Yamamoto, and S. Yoshida, "Study on upper bound of throughput in multihop radio networks," Proc. the 6th YRP Symposium on Cooperation between

Industry, Academia and Government in Mobile Telecommunications, pp.120–121, July 2004.

6. K. Yamamoto and S. Yoshida, "Joint effect of autonomous route selection scheme and transmit power control in multihop radio networks," IEICE Technical Report, MoMuC2004-34, pp.7–11, July 2004.
7. K. Yamamoto, A. Kusuda, and S. Yoshida, "Tradeoff between capacity of multihop transmission and area spectral efficiency," IEICE 1st Ad Hoc Network Workshop, pp.49–52, Jan. 2005.
8. K. Yamamoto, A. Kusuda, and S. Yoshida, "Performance comparison between rate adaptation and multihop route selection in single-cell cellular systems," IEICE Technical Report, RCS2004-237, pp.7–11, Jan. 2005.
9. H. Xu, K. Yamamoto, and S. Yoshida, "Experimental study on indoor location estimation using propagation loss information," IEICE Technical Report, RCS2004-255, pp.115–120, Jan. 2005.
10. A. Kusuda, K. Yamamoto, and S. Yoshida, "Performance comparison between rate adaptation and multihop route selection in multi-cell cellular systems," IEICE Technical Report, RCS2004-343, pp.113–117, March 2005.
11. M. Fujii, K. Yamamoto, and S. Yoshida, "Performance evaluation of load balancing rerouting between different wireless interfaces for mesh networks," IEICE Technical Report, RCS2005-4, pp.25–30, April 2005.

Local Conference Papers

1. K. Yamamoto, H. Murata, S. Yoshida, A. Fujiwara, T. Otsu, and Y. Yamao, "Fundamental study on applying relay to DS-CDMA cellular uplink," Proc. IEICE Gen. Conf. '02, B-5-145, p.595, March 2002.
2. K. Yamamoto and S. Yoshida, "Fundamental study on multihop connection of high speed terminal in CDMA cellular uplink," Proc. IEICE Commun. Conf. '02, B-5-179, p.476, Sept. 2002.
3. K. Yamamoto and S. Yoshida, "A study on call admission control for CDMA multihop cellular system," Proc. IEICE Gen. Conf. '03, B-5-305, p.564, March 2003.
4. H. Xu, K. Yamamoto, and S. Yoshida, "Experimental study on throughput enhancement of wireless LAN with multihop connection," Proc. IEICE Commun. Conf. '03, B-5-117, p.494, Sept. 2003.

5. K. Yamamoto and S. Yoshida, "Routing algorithm for capacity enhancement of CDMA multihop cellular systems," Proc. IEICE Commun. Conf. '03, B-5-118, p.495, Sept. 2003.
6. K. Yamamoto and S. Yoshida, "Capacity of two-hop CDMA cellular systems," Proc. the First Singapore-Japan International Workshop on Info-Communications Technologies for the Ubiquitous Networked Society, pp.59–61, Singapore, Dec. 2003.
7. K. Ozaki, K. Yamamoto, and S. Yoshida, "Maximization of throughput in multihop radio networks with rate adaptation," Proc. IEICE Gen. Conf. '04, B-5-124, p.611, March 2004.
8. K. Yamamoto and S. Yoshida, "Study on coverage enhancement using rate adaptation and multihop connections," Proc. IEICE Gen. Conf. '04, B-5-126, p.613, March 2004.
9. A. Kusuda, K. Yamamoto, and S. Yoshida, "Effect of adaptive modulation on multihop transmission over Rayleigh fading channels," Proc. IEICE Commun. Conf.'04, B-5-69, p.403, Sept. 2004.
10. K. Yamamoto, A. Kusuda, and S. Yoshida, "Capacity evaluation of multihop transmission assuming end-to-end error rate," Proc. IEICE Commun. Conf.'04, B-5-70, p.404, Sept. 2004.
11. H. Xu, K. Yamamoto, and S. Yoshida, "Experimental study on throughput of adhoc network with coexisting different rate links," Proc. IEICE Commun. Conf.'04, B-5-120, p.454, Sept. 2004.
12. K. Yamamoto and S. Yoshida, "Study on area spectral efficiency of multihop radio networks assuming rate adaptation," Proc. IEICE Gen. Conf. '05, B-5-132, p.581, March 2005.
13. M. Fujii, H. Xu, K. Yamamoto, and S. Yoshida, "Study on load balance of mesh networks with different wireless interfaces," Proc. IEICE Gen. Conf. '05, B-5-161, p.610, March 2005.
14. L. Xu, K. Ozaki, K. Yamamoto, and S. Yoshida, "An analysis of retransmission schemes for multihop radio transmission," Proc. IEICE Gen. Conf. '05, B-5-229, p.678, March 2005.

Awards

- PIMRC 2004 Best Student Paper Award: Koji Yamamoto, Susumu Yoshida, "Analysis of distributed route selection scheme in wireless ad hoc networks," Proc. PIMRC '04, Sept. 2004.
- IEEE VTS Japan 2003 Young Researcher's Encouragement Award: Koji Yamamoto, Susumu Yoshida, "Call admission control suitable for two-hop CDMA cellular systems," Proc. VTC' 03-Fall, Oct. 2003.

Scholarships and Financial Support

- NTT DoCoMo Scholarship: 2002–2004.
- Research Fellowships of the Japan Society for the Promotion of Science for Young Scientists: 2004–2005.
- Research Assistant for the 21st Century Center of Excellence Program: 2004–2005.